Mechanisms by which the IKK-related kinases affect energy expenditure

by

Jonathan Mowers

A dissertation submitted in partial fulfillment
of the requirements for the degree of
Doctor of Philosophy
(Molecular and Integrative Physiology)
in the University of Michigan
2014

Doctoral Committee:

Professor Alan R Saltiel, Chair
Associate Professor Jiandie Lin
Assistant Professor Carey N. Lumeng
Professor Ormond A. Macdougald
Associate Professor Liangyou Rui

2014

Dedication

This is dedicated to my family and my wife, whose love sustains me

Acknowledgements

I would like to thank members of the Saltiel Lab for their support, and especially my advisor Alan, whose support I am forever grateful for. Alan has a unique ability to see big picture questions and the path to address those questions. Working under his direction has developed me into the scientist I am today and prepared me in my pursuit of becoming an academic researcher. I am sad to leave the lab, but I will carry with me the lessons I have learned from Alan in lab meetings, dissertation committee meetings, and at the bench during informal brainstorming sessions.

Specific thanks go to Louise Chang for her assistance as a co-worker and lab manager. I would also like to thank Dr. Erika Dickson, Dr. David Bridges, Dr. David Buchner, Dr. Shannon Reilly, and Maeran Uhm for suggestions in the revision of this thesis.

Michele Boggs, Ellen Elkin, and Jaime Yost all have my extreme gratitude. So much goes into the planning and organization of graduate student lives, and each of these individuals are essential to making things work within their respective departments.

I would also like to thank my dissertation committee members for their helpful insight and time. I hope these researchers know how much they have meant in my development as a scientist. I had the pleasure of working with Dr. Carey Lumeng for several months as I was beginning my time in the Saltiel lab and he was transitioning into an assistant professorship. His mentorship during that time together was one of the main reasons I stayed on in the Saltiel lab, and I continued to benefit from good mentorship by senior lab members throughout my graduate school years.

Dr. Liangyou Rui was the first graduate teacher I had; he oversaw a seminar series on insulin signaling that I was enrolled in. His positive energy and professionalism were apparent from the first class we had and remained throughout the year, and it was his knowledge in metabolism and enthusiasm that compelled me to put him on my dissertation committee.

Dr. Jiandie Lin conducts his research down the hall from our lab, and I can always count on his scientific counsel. He allowed me to perform oxygen consumption studies early in my graduate school years and was always very hospitable. Through interacting with his lab members and witnessing his diligence at the bench, I have come to appreciate how dedicated Dr. Lin is to his profession and his students. It is a great example that I hope to exemplify going forward.

Dr. Ormond Macdougald was our graduate department chair for the majority of the time I was with the MIP. We served on the graduate committee together during the first several years of the graduate education fund, a fund that Ormond played a huge role in starting that will

provide MIP students support in professional pursuits. His dedication to our education as graduate students and his personal investment in us throughout our years was a great source of inspiration.

Finally, I would like to thank Ron Koenig who has been a great MSTP director. He was the primary reason I came to Michigan 8 years ago.

Table of Contents

List of Figures

Abstract

Numerous studies have implicated an inflammatory link between obesity and type 2 diabetes. While inflammation is highly correlated with increases in adiposity, the role played by inflammation in the manifestations of obesity remains unclear. We applied a multidisciplinary approach spanning from *in vivo* animal physiology to *in vitro* cell culture and biochemistry to address the role of obesity-related inflammation in adipose tissue.

The inhibitor of κB kinase β (IKKβ) has previously been linked to insulin resistance. High-fat diet dramatically increased protein and kinase activity levels of the two noncanonical IKK family members, IKKε and TBK1, in adipose tissue. Genetic ablation of IKKε or pharmacologic inhibition of IKKε and TBK1, using the selective protein kinase inhibitor amlexanox, resulted in many metabolic improvements, including reduced weight gain in mice on a high fat diet. The improvements in IKKε knockout and amlexanox-treated mice on a high fat diet were correlated with increased energy expenditure, core body temperature, adipogenesis, and the proton uncoupling protein, UCP1 protein levels in adipose tissue.

Inhibitors of IKKε and TBK1 that are structurally unrelated to amlexanox substituted for the general cAMP phosphodiesterase inhibitor IBMX, to promote lipid

accumulation and adipocyte proliferation in 3T3-L1 adipocytes. Increased adipogenesis in response to IKKε and TBK1 inhibitors paralleled the adipocyte hyperplasia seen in the IKKε knockout mouse. *Ex vivo* stimulation of white adipose tissue from IKKε knockout mice with the adenylyl cyclase activator forskolin, resulted in increased glycerol release and lipolytic signaling compared to white adipose tissue from wild type mice. Moreover, treating 3T3-L1 adipocytes with amlexanox increased lipolysis in a dose-dependent manner and increased oxygen consumption to the same degree that forskolin does. These studies suggested that IKKε and TBK1 attenuate cAMP-dependent processes in adipocytes to regulate energy expenditure.

Further studies with 3T3-L1 adipocytes elucidated the mechanism by which IKKε and TBK1 regulate cAMP and β-adrenergic signaling in 3T3-L1 adipocytes. Expression of IKKε in 3T3-L1 adipocytes decreased UCP1 expression in response to β-adrenergic stimulation. The rate of lipolysis, levels of cAMP, and phosphorylation of PKA substrates such as hormone sensitive lipase (HSL) were also diminished in response to isoproterenol or forskolin by overexpression of IKKε or TBK1 in 3T3-L1 adipocytes. IKKε and TBK1 are induced by inflammatory stimuli, such as tumor necrosis α (TNFα) and Poly(I:C), and blockade of these kinases reversed the diminution of β-adrenergic signaling, cAMP, and lipolysis. The reduction of cAMP levels in 3T3-L1 adipocytes expressing IKKε or TBK1 was reversed by the phosphodiesterase 3B inhibitor, zardaverine. IKKε and TBK1 were found to bind to and phosphorylate PDE3B at serine 318, resulting in its activation and 14-3-3β binding. These studies suggest that reduced cAMP production through phosphorylation and activation of PDE3B by IKKε and TBK1 is responsible for mediating the effects of IKKε and TBK1 in adipocytes.

Chapter I:
Introduction

Obesity Epidemiology

Obesity is a central feature of a vast array of diseases including type 2 diabetes, atherosclerosis, asthma, and cancer (1), and its increasing prevalence has defined a new epidemic in human history (2). Whereas “overweight” technically refers to excess body weight and “obese” refers to excess body fat, these terms have been adapted into body mass index (BMI) categories, for which there are mathematical definitions. BMI is measured as body weight (in kg) divided by height squared (in meters^2). The World Health Organization and National Heart, Lung, and Blood Institute define overweight as a BMI greater than 25, but less than 30, while obesity is defined as a BMI of greater than 30 kg/m^2 (3). While the worldwide prevalence of obesity is 12% (2), the United States has the highest rate of obesity for developed countries with 35.6% of the population in 2010 (4). Given its prevalence and health implications, understanding the pathogenesis of obesity is critical to improve human health.

The factors that contribute to adult obesity can occur at any age, and environmental contributions to obesity exist throughout life. Prenatal contributions to obesity may include maternal smoking (5) as well as maternal type 2 diabetes and obesity (6). Preventative factors exist also, as increased breastfeeding was linked to

reduced risk of childhood (7) and adult (8) obesity. While adiposity very early in childhood is not a good predictor of adult obesity, adiposity from age 5 onwards is a significant risk factor for obesity (9). Therefore, early negative influences disadvantage children by increasing the likelihood of obesity and its comorbidities later in life.

Beyond childhood, overnutrition and a sedentary lifestyle are the main contributing factors to obesity, and fluctuations in these factors result in weight changes through life (10). Increased food supplies and food consumption may be partly responsible for the rising prevalence of obesity (11). It has been reported in western society that reduced energy expenditure contributes more heavily to modern obesity than overnutrition (10). The contribution of decreased energy expenditure to obesity is important to highlight, because many of the studies performed in this thesis address defects in energy expenditure and potential therapeutic targets to alter energy expenditure and prevent obesity.

Energy Expenditure in Obesity

In its simplest form, weight gain results from an imbalance between energy intake and energy expenditure. Total energy expenditure can be broken into obligatory energy expenditure (OEE), energy expenditure due to physical activity, and adaptive thermogenesis (12). OEE can be summarized as the energy required for the performance of cellular and organ functions. Variations of this term converge on a measure of energy expenditure during an unstressed, resting state of an animal. Physical activity-related energy expenditure is inherently variable and it depends mostly on the type and intensity of activity. Adaptive thermogenesis is also variable but, similar to OEE and in contrast to physical activity, it is regulated by the autonomic nervous

system. Perturbations in any of these components of energy expenditure can therefore affect body weight, but “with few exceptions, most rodent models of obesity have defects in adaptive thermogenesis” (12).

Adaptive thermogenesis is a homeostatic process regulated by the hypothalamus, which increases brown adipose tissue (BAT) thermogenic activity in response to decreased temperature as well as in response to diet (13). In cold-induced thermogenesis, hypothalamic integration of low temperature signals leads acutely to heat generated through shivering. In addition to shivering, chronic cold exposure recruits nonshivering thermogenesis by activating BAT to maintain homeothermy. Diet regulates adaptive thermogenesis both immediately after eating as well as chronically through signals from energy reserves. A single meal leads to a significant, transient increase in metabolism in BAT due to elevated plasma insulin and glucose uptake, known as “postprandial thermogenesis” (14). Increases in the ability to generate heat due to excess energy reserves over time are known as “diet-induced thermogenesis.” This effect is mediated mostly by leptin, secreted from white adipose depots, which acts at the hypothalamus to indicate energy excess and then signal BAT to increase activity, which balances energy homeostasis (15).

Both cold-induced and dietary thermogenesis are homeostatic mechanisms in BAT to maintain different set points, but through a similar mechanism of uncoupling the electron transport chain from ATP synthesis. Uncoupling protein 1 (UCP1), also known as thermogenin, is found on the inner mitochondrial membrane where it dissipates the mitochondrial proton gradient to generate heat, which is largely responsible for adaptive thermogenesis (13). Norepinephrine, generated by the hypothalamus through the

sympathetic chain, activates β-adrenergic receptors in BAT to initiate a cascade of events through protein kinase A (PKA) culminating in the transcriptional up-regulation of UCP1 as well as post-transcriptional UCP1 activation by liberated free fatty acids (16). Brown fat, therefore, plays a prominent role in adaptive thermogenesis using UCP1. Since thermogenic capacity is almost entirely attributed to UCP1, any reference to BAT thermogenic function is a reference to UCP1 activity, even when that thermogenic activity is found outside of traditional BAT depots.

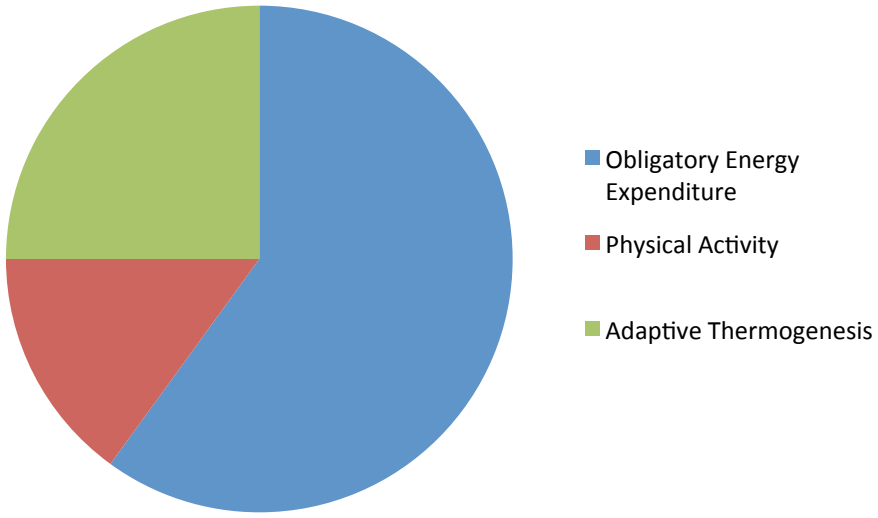

Figure 1.1: Schematic of Energy Expenditure: OEE, physical activity, and adaptive thermogenesis. Whereas obligatory energy expenditure is constant, physical activity and adaptive thermogenesis are variable. Adaptive thermogenesis depends on temperature and dietary inputs.

Lipolytic Pathway in Adipose Tissue

Lipolysis is the liberation of free fatty acids from triglycerides in adipose tissue and occurs through several different mechanisms. Lipolysis may occur extracellularly in vascular beds mediated by lipoprotein lipase (LPL) (17). Intracellular lipolysis is increased through the action of the mitogen-activated protein kinase (MAPK) signaling pathways or through the cyclic nucleotides, cAMP and cGMP (18, 19). Other forms of intracellular lipolysis depend on breakdown of lipid droplet-forming machinery, including downregulation of peroxisome proliferator-activated receptor-γ (PPARγ) (20). Hormonal regulation of cyclic nucleotide levels in adipocytes is partly regulated by natriuretic peptides (21), whose receptors have intrinsic guanylyl cyclase catalytic activity; however, cAMP levels are mainly regulated by insulin and catecholamines (13).

Obese subjects have reduced whole-body adrenergic stimulated lipolysis (22-25). Desensitization to catecholamines is seen in both muscle and adipose tissue (23, 24). Adipocytes cultured from obese individuals have a dramatic reduction in isoproterenol- or norepinephrine-induced lipolysis (26, 27). Infusion of epinephrine was able to increase plasma fatty acid flux and oxidation in lean subjects while plasma free fatty acid levels were unchanged in obese subjects (22, 23).

Studies of obese children with impaired responses to adrenergic stimuli suggest catecholamine resistance is a primary defect in obesity (28, 29). Reduced catecholamine-induced lipolysis in adipose tissue does not improve after weight reduction (24). Impaired lipolysis is a characteristic of obesity in childhood (28, 29), and has been observed in adipocytes from first degree relatives of obese subjects (30)

suggesting a role of genetics or early environmental factors in reduced lipolytic responses.

Mouse knockout models of the lipolytic machinery, observations from adipose tissue from obese subjects, and polymorphisms of mediators of lipolysis have allowed the field to further investigate the roles of these proteins in lipolysis and whole body metabolism.

Adrenergic Receptors, Heterotrimeric G-proteins, and Adenylyl Cyclase

Catecholamines bind adrenergic receptors, which are seven α-helix transmembrane receptors, and their functions have been extensively studied (13). These receptors are broken into $\alpha_{1,2}$ and $\beta_{1\text{-}3}$ subtypes that differ in their affinity for catecholamines, tissue distribution, pharmacologic agonists and antagonists, and mechanism of action. Unlike the natriuretic peptide receptor that has guanylyl cyclase activity, α and β adrenergic receptors are coupled to heterotrimeric G-proteins. Heterotrimeric G-proteins are made up of a Gα subunit and a βγ complex. When catecholamines bind to α or β adrenergic receptors, the receptor acts as a guanine nucleotide exchange factor for Gα, promoting GTP to replace GDP, which results in Gα activation and the separation of the βγ complex from Gα. The main role of Gα is to modulate the conversion of ATP to cyclic AMP by adenylyl cyclase.

In adipocytes, Gα can be either stimulatory (G_s) or inhibitory (G_i) toward adenylyl cyclase activity (31). All three β-adrenergic receptors are coupled to G_s to promote lipolysis in adipose tissue. Whereas $\beta_{1,2}$ receptors are mostly responsible for hormonal control of human adipose tissue, rodents utilize the β_3 adrenoreceptor more heavily

(32). In contrast to β-adrenergic receptors, α_2-adrenergic receptors in adipocytes are coupled to G_i subunits which serve to inhibit lipolysis in adipose tissue (33). However the net effect of adrenergic stimuli predominantly is to increase in cAMP in adipocytes.

Adrenergic receptors are coupled to Gα to affect adenylyl cyclase activity in the production of cAMP (13). There are ten known adenylyl cyclase isoforms in mammals. Most isoforms of adenylyl cyclase are activated by G_s, and are pharmacologically stimulated by forskolin, whereas G_i works only on adenylyl cyclase types I, V, and VI (34). Mature adipocytes have significantly higher type V and VI adenylyl cyclase transcript levels than preadipocytes, suggesting that these isoforms may play a significant role in both stimulatory and inhibitory regulation of cAMP in adipocyte function (35).

In obesity, the desensitization of adrenergic stimulation in fat has been partly attributed to decreased levels of β_2-adrenergic receptors (36). Studies of polymorphisms in the lipolytic pathways suggest that obesity and resistance to catecholamine-induced lipolysis are linked. The β_2-adrenergic receptor has several polymorphisms that have aberrant signaling, and these have been correlated with defects in catecholamine-induced signaling both in cell culture (37, 38) and in the context of obesity (39), including blunted *in vivo* lipolysis and fatty acid oxidation (40). The $\beta_{1\text{-}3}$-adrenergic receptor triple knockout mice are obese on a normal diet and are cold intolerant (41), which I will discuss later. Along with decreases in β-adrenergic receptor levels, activation of α_2-receptors in obese adipose tissue after exercise has also been observed (33). Together, these defects provide a mechanism by which cAMP levels are

attenuated in obese adipose tissue. Reduced receptor levels lead to impaired cAMP production, resulting in decreased PKA activity.

Cyclic Adenosine Monophosphate (cAMP)

cAMP was the first “second messenger” discovered, and its action in adipocytes has been studied extensively (13). cAMP is known to stimulate protein kinase A, which subsequently phosphorylates downstream substrates. cAMP also stimulates Epac, a guanine nucleotide exchange factor for the Rap subfamily of small GTPases (42). Both the regulatory subunit of PKA and Epac have regulatory cyclic AMP-binding domains, and PKA and Epac act independently, synergistically, and antagonistically toward each other. Epac activates AMPK to improve adipocyte lipid and energy metabolism in mice (43), and Epac also plays a role in adipocyte differentiation (44). While the role of Epac in adipocyte development and metabolism continues to be elucidated, the role of PKA in adipocyte function has been studied for over 30 years. Co-incubation of adipocytes with the PKA inhibitor H89 results in a near-total ablation of lipolysis induced by isoproterenol (45). Surprisingly, few, if any, polymorphisms in PKA or Epac have been identified in the study of obesity, despite their essential roles in β-adrenergic signaling.

Lipases and Associated Proteins

The hydrolysis of triglycerides into three fatty acids and glycerol is performed by the coordinated action of three lipases: adipose triglyceride lipase (ATGL), hormone sensitive lipase (HSL), and monoglyceride lipase (MGL). Beyond the receptor, catecholamine-induced lipolysis in obesity can be blunted by reducing lipolytic machinery.

Adipose Triglyceride Lipase (ATGL)

Activation of ATGL, a process not directly attributed to PKA (46), facilitates the conversion of triglycerides to diacylglycerides (DAG). A triglyceride hydrolase activator first identified in C. elegans, CGI-58, increases ATGL activity up to 20 fold (47). CGI-58 can reversibly bind the lipid droplet associated protein, perilipin, in a PKA-dependent manner (48, 49). Therefore, a combination of PKA-dependent and independent mechanisms regulate ATGL action.

ATGL knockout mice have increased body weight and fat mass, and decreased catecholamine-induced lipolysis (50). Absence of ATGL results in defective lipolysis and cold adaptation, due to reduced accessibility of fatty acids. Subjects with loss-of-function mutations in ATGL (51) and CGI-58 (47) have lipid storage diseases, which result in adiposity in multiple organs and reduced adipose tissue lipid storage. Furthermore, 12 ATGL polymorphisms have been associated with significant deviations of plasma free fatty acids, triglycerides, glucose, and risk of type 2 diabetes (52). However, studies have not reported reduced catecholamine-induced lipolysis in either ATGL or CGI-58 defective subjects, and the implications of ATGL activity in human physiology are largely unknown.

Hormone Sensitive Lipase (HSL) and Perilipin

Together, ATGL and HSL combine to account for greater than 95% of triglyceride hydrolysis in mouse adipose tissue (53, 54). While ATGL prevails in basal lipolysis, HSL plays a predominant role in catecholamine-stimulated lipolysis. Once cAMP is produced, PKA phosphorylates perilipin, which allows access of lipases to the lipid droplet (55-58). PKA also phosphorylates HSL, which activates its lipolytic activity (59).

HSL phosphorylation promotes the association of HSL with lipid droplets to hydrolyze diacylglycerol (and triacylglycerol at times) (60). Lipotransin is another lipid droplet protein that translocates HSL to lipid droplets (61). While PKA action accounts for a large percentage (80%) of catecholamine-induced lipolysis, MAPK signaling pathways also mediate a minor portion (20%) of lipolysis by phosphorylating HSL (18).

Reduced expression of HSL has been observed in adipose tissue of obese subjects (62, 63), and a catalytically deficient form of HSL has also been observed in obese adipose tissue (64). HSL knockout mice are lean despite the inability to respond to β-adrenergic stimuli. Conflicting reports of insulin sensitivity have been made in HSL knockout mice (65-68). HSL is decreased in both expression and activity of first degree relatives of obese subjects, suggesting heritability or early environmental influences of HSL in obesity (30). A -60C/G polymorphism within the HSL promoter decreases expression of HSL in cell culture by 40% (69) and plays a role in body fat composition (70). Another polymorphism in an intronic region of the HSL gene is associated with obesity and decreased catecholamine-induced lipolysis (71-73).

Polymorphisms in perilipin are associated with obesity-related phenotypes and impaired ability to lose weight (74, 75). One such polymorphism, in intron six of the perilipin gene, is associated with reduced perilipin protein levels as well as increased basal and catecholamine-induced lipolysis from adipocytes from obese subjects (74, 75). Perilipin knockout mice have an inability to maintain lipid stores, as seen through increased basal lipolysis, resulting in decreased fat mass (76, 77). Increased systemic lipid load has been suggested to be responsible for decreased insulin sensitivity in these animals (77). Catecholamine-induced lipolysis is also decreased, due to

diminished HSL translocation, indicating that dyslipidemia may play an important role in adipocyte function.

Monoacylglycerol Lipase

The last lipase involved in lipolysis involves monoacylglycerol lipase (MGL). MGL hydrolyzes the final fatty acid from glycerol in a hormonally unregulated manner (78). MGL is required for lipolysis and the development of diet-induced insulin resistance (79). Due to the ability of MGL to deactivate endocannabinoid 2-arachidonoyl-sn-glycerol (2-AG), a known player in central nervous system-mediated thermogenesis, overexpression of MGL resulted in increased energy expenditure (80). Together, ATGL, HSL, MGL, and their associated proteins combine to break down triglycerides to provide fatty acids to be used by other tissues as energy substrates, and the genetic ablation of these proteins result in defects in energy expenditure.

Routes of Fatty Acid Efflux

Fatty acids that accumulate intracellularly as a result of lipolysis are exported both by diffusion and facilitated transport, using transport proteins, across the adipocyte cell membrane on their way to the bloodstream for use by other tissues (81). Fatty acid translocase (FAT) (82), fatty acid binding protein plasma membrane (FABPpm) (83), fatty acid transport protein (FATP) (84), and caveolin-1 (85) all aid in fatty acid transport across the adipocyte cell membrane. In addition to binding perilipin, HSL interacts with fatty acid binding protein 4 (FABP4) (86-88) to facilitate the release of fatty acids out of adipocytes. Active transport has also been proposed for adipocyte fatty acid efflux, but the identity of this pump remains unknown (89).

Glycerol efflux occurs by facilitated transport primarily using aquaporin 7 in adipocytes (90). Aquaporin 7 knockout mice are obese and also have defects in catecholamine-induced glycerol release (90-92). This transporter is reduced in adipose tissue of obese subjects (93). FABP4 knockout mice have decreased basal and isoproterenol-stimulated lipolysis (88). In sum, not only is the ability to generate free fatty acids associated with obesity, but free fatty acid and glycerol transport out of the adipocyte are also important determinants of obesity.

Adipose Tissue Blood Flow

Fatty acid flux in and out of adipocytes involves coordination with vascular capillary beds. The importance of adipose tissue blood flow for regulating lipolysis has long been appreciated in human subjects. Blood flow increases through adipose tissue during times of lipid storage postprandially (94), as well as during times of lipid mobilization when fatty acids are released for use by other tissues (95, 96). These processes are regulated in part by adrenergic action in smooth muscle vascular cells.

The inability to increase adipose tissue blood flow in obese subjects following exercise further suggests a role for adrenergic desensitization in obese adipose tissue (97, 98). In adipose tissue, response to epinephrine as lipolysis or adipose tissue blood flow were attenuated in obese subjects compared to lean ones (99). Lower fasting adipose tissue blood flow was observed in obese patients (94, 95).

Regional Differences in Lipolysis

Conflicting reports have emerged about regional differences in adipose tissue lipolysis. The consensus is that not all fat depots respond to adrenergic stimuli the same. Several studies reported higher basal and total lipolysis in subcutaneous versus

visceral adipocytes, but visceral adipocytes respond more strongly, as measured in fold change, to adrenergic stimuli (100). Visceral fat depots respond more strongly to catecholamines compared to subcutaneous depots, which has been attributed to differences in β-adrenergic receptor levels (101), lipase levels (102), as well as levels of FABP4 (103). Finally, adipose depots also respond differentially to insulin; visceral adipose tissue does not respond as strongly to insulin as does subcutaneous tissue, which has been attributed to differences in insulin receptor levels (104), phosphorylation of insulin receptor and insulin receptor substrate-1 (IRS-1) (105), and tyrosine phosphatase activity on the insulin receptor (106).

Attenuation of Lipolysis by Insulin

Several molecules are known to negatively regulate lipolysis. Prostaglandins (107), nicotinic acid (108), adenosine (109), neuropeptide Y and peptide YY (110, 111), activate G_i and thereby inhibit adenylyl cyclase activity. Also, isoproterenol causes adipocytes to secrete adrenomedulin which generates autocrine negative feedback through a nitric oxide-dependent mechanism (112). However, insulin is the most well-known suppressor of lipolysis.

Insulin is the most powerful anabolic hormone (113). Insulin stimulates adipocyte differentiation and adipose tissue expansion. Insulin's effects on adipose tissue expansion are attributed to its ability to inhibit lipolysis, stimulate the uptake of free fatty acids and glucose, and initiate *de novo* fatty acid synthesis. While skeletal muscle is the main tissue for insulin-stimulated glucose uptake, genetic ablation in adipose tissue of insulin-stimulated glucose transporter, GLUT4, produces defects in glucose homeostasis (114), and adipose-specific transgenic expression of GLUT4 reverses

defective glucose homeostasis in muscle-specific GLUT4 knockout mice (115). While the fat-specific insulin receptor knockout mouse has normal whole body glucose metabolism, these mice have reduced adipose tissue mass and extended lifespan (116).

Insulin decreases lipolysis through a variety of targets. Insulin attenuates β-adrenergic pathways by sequestering β-adrenergic receptors intracellularly (117), decreasing adenylyl cyclase activity (118), preventing localization of PKA to β-adrenergic receptors (119), activating protein phosphatases to dephosphorylate HSL (120), and activating the phosphodiesterase 3B (PDE3B) (121). Whereas the activation of adenylyl cyclase produces cAMP, phosphodiesterases are responsible for cleaving cAMP to AMP to terminate PKA-dependent signaling. Therefore, the activation of phosphodiesterases by hormonal cues, such as insulin, promotes anabolic processes and decreases catabolic processes in adipose tissue.

Phosphodiesterase 3B

Phosphodiesterases comprise an eleven member superfamily in mammals (PDE1-11) with different catalytic specificities to cleave cAMP and cGMP that act in different cellular contexts (122). Although other phosphodiesterases have recently been implicated in adipocyte biology (123), PDE3B and PDE4 are the main phosphodiesterases that regulate cAMP in adipocytes (124). The PDE3 family is composed of two members with similar structural organization, PDE3A and PDE3B (125). PDE3A and PDE3B are encoded by separate genes and perform distinct functions. Both members act in vascular smooth muscle, kidney, and gametes (121).

However, PDE3A acts in cardiomyocytes and platelets, while PDE3B acts in white blood cells and in metabolic tissues, such as adipose tissue and liver.

The PDE3B protein contains an N-terminal membrane-targeting domain that allows PDE3B to be retained on membranes, followed by a regulatory domain that is phosphorylated to alter function (125). Near the carboxy terminus is the catalytic domain and a distal, hydrophillic region. The catalytic domain of PDE3B has a K_m value that has been measured to be between 100nM to 800nM for cAMP and has a 4-10 fold higher affinity and velocity for cAMP than cGMP.

PDE3B is regulated by binding proteins, intracellular localization, and phosphorylation. PDE3B localizes to the plasma membrane, including lipid rafts and caveolae, and the endoplasmic reticulum through its N-terminal membrane-targeting domain (121, 126, 127). Caveolae are involutions of plasma membrane constructed of cholesterol and lipids stabilized by caveolin (128). These structures are concentrated in adipocytes to organize intracellular signaling events. Since PDE3B localizes to caveolin, PDE3B may be regulated by signaling processes occurring in this compartment.

Interestingly, PDE3B is phosphorylated and activated in adipocytes and hepatocytes in response to both insulin and elevated cAMP levels. This is somewhat surprising; insulin and intracellular cAMP have antagonistic effects to each other. Insulin stimulates the phosphorylation and activation of PDE3B, which reduces cAMP to prevent lipolysis (129) (130). Insulin-stimulated reduction in cAMP also prevents activation of AMPK resulting in retention of fatty acids and decreased fatty acid oxidation (45, 131). However, cAMP activates PKA which then phosphorylates and

activates PDE3B to act as negative feedback for cAMP-dependent signals (121). This is not exclusive to PDE3B function, as PDE4D3 can also be phosphorylated and activated by PKA to negatively regulate cAMP levels (132)

Several serine residues in the regulatory domain of PDE3B are phosphorylated in response to insulin or cAMP in hepatocytes and adipocytes (125, 133-135). No phosphorylation site on PDE3B has been better characterized than serine 318 (human), which is a presumed consensus site for both Akt and PKA phosphorylation as well as a consensus 14-3-3 binding motif (133). In fact, PDE3B is thought to be activated by phosphorylation at human serine 318 in response to both insulin and cAMP (136), and 14-3-3β binding protects this site from phosphatase-catalyzed dephosphorylation and inactivation (137). Several other phosphorylation sites that respond to insulin and forskolin have been identified, but they are less well characterized (133).

Phosphorylation of PDE3B also depends on intracellular location and associated protein complexes, providing additional layers of complexity to PDE3B regulation. Insulin phosphorylates and activates PDE3B that is localized to the endoplasmic reticulum (135), while PKA-dependent phosphorylation of PDE3B occurs at the plasma membrane (135). Insulin-stimulated PDE3B has been reported to form complexes with IRS1 and other insulin signaling intermediates, whereas PKA dependent PDE3B complexes contain the β-adrenergic receptor and hormone sensitive lipase (134, 135). Therefore, the co-localization of these two groups of molecules may be necessary for the specific, coordinated action of PDE3B with either insulin or β-adrenergic-stimulated complexes.

PDE3B serves important functions in obesity as well. While some studies suggest a reduction of PDE3B in obesity, much of our understanding of the role of PDE3B *in vivo* for obesity is gleaned from the Pde3B knockout mice (138). Importantly, PDE3B was essential for reduced white adipose tissue and increased lean mass, which were attributed to increases in lipolysis in Pde3B knockout mice. Knockout mice revealed a role for PDE3B in expanding adipose tissue depots and promoting weight gain while on a high-fat diet, (121). Livers from these mice failed to reduce glucose output in response to insulin, which was correlated with upregulated gluconeogenic genes (138, 139). Several studies reported decreased PDE3B activity in adipose tissue of obese subjects (140-143), which may contribute to insulin resistance. These studies demonstrate the role of PDE3B in anabolism and its potential contribution to macronutrient storage.

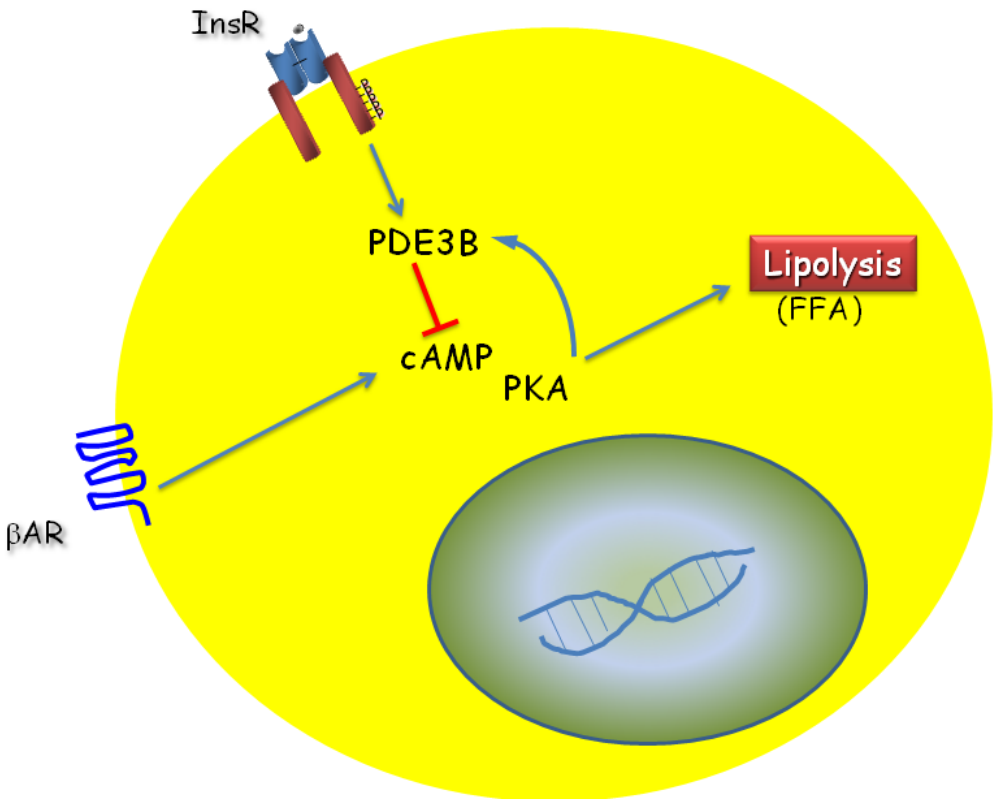

Figure 1.2: Model of Lipolysis and Insulin Action in Adipocytes

Activation of UCP1

Adaptive thermogenesis is due in part to the activation of UCP1 by free fatty acids from lipolysis (13). Thermogenic responses in brown-fat cells are fully UCP1-dependent for adrenergic or fatty-acid induced thermogenesis (144). This suggests that the induction of thermogenesis from lipolysis is inextricable; thermogenesis does not occur without hormonally-induced lipolysis-dependent free fatty acids. This process is dependent on PKA, since UCP1 gene expression and thermogenesis is inhibited by the PKA inhibitor H89 (145). The current model that exists for UCP1 activation is that fatty acids serve as thermogenic substrates for UCP1, and GDP effectively competes with free fatty acids to prevent UCP1 action (13). The proton gradient that UCP1 dissipates to achieve thermogenesis is derived from fatty acids undergoing β-oxidation or carbohydrates undergoing glycolysis. Metabolized energy substrates therefore provide the proton gradient, through glycolytic and TCA cycles, and free fatty acids directly activate UCP1 activity. UCP1 in adipose tissue is not only controlled by free fatty acids, but UCP1 is also regulated on a transcriptional level, which is also partly due to β-adrenergic signaling (13). Therefore, transcriptional control of thermogenic programs in adipocytes warrant further discussion.

Adipocyte Development and Differentiation

To understand the thermogenic potential of adipocytes, we must first understand how brown and white adipocytes develop. Fat is of mesenchymal origin. It is currently thought that brown and white adipocytes diverge early in mesenchymal stem cell differentiation (146).

White Adipocyte Development and Differentiation

Adipogenesis has been studied extensively in 3T3-L1 adipocytes (147). Some of the first transcription factors known to initiate adipogenesis were the CCAAT/enhancer binding proteins (c/EBPs) (148, 149). c/EBPβ and δ mRNA and protein levels increase early in the differentiation process, but taper off later in the adipogenic program. c/EBPα is induced later in the differentiation process, and precedes maximal insulin-stimulated glucose uptake in adipocytes. Early experiments with c/EBPα showed that ectopic expression of c/EBPα promotes adipogenic program (150), and c/EBPα loss-of-function blocks adipogenesis (151).

PPARγ is the master regulator of adipogenesis (147). Early experiments in adipocyte differentiation demonstrated that PPARγ expression is sufficient to induce the adipogenic program (152). Also, c/EBPα was able to cooperate with PPARγ to stimulate the adipocyte program dramatically. Together, PPARγ and c/EBPα drive adipogenesis.

Factors that increase cAMP strongly accelerate the initiation of the adipogenic differentiation program by suppressing Wnt10b and promoting c/EBPβ (153). cAMP stimulates CREB early in adipocyte differentiation to result in c/EBPβ expression (154). Wnt signaling inhibits adipocyte differentiation in 3T3-L1 cells by suppressing PPARγ and c/EBPα expression (147). cAMP results in methylation of the Wnt10b, preventing Wnt10b expression and promoting adipogenesis (155). Therefore, the ability of cAMP to promote c/EBPβ expression and downregulate Wnt10b are partly responsible for the initiation of adipogenesis.

Brown Adipocyte Development and Differentiation

Brown fat is surprisingly more closely related developmentally to muscle than it is to white fat (156). Brown adipocytes and muscle both descend from dermomyotome precursors that express Engrailed-1 (157). Interscapular BAT is present in rodents and newborns, but this depot disappears postnatally in humans. White adipose tissue develops later and continues to expand after birth (158). In mice, cells that express myf5, a marker of skeletal muscle precursors, were found in brown, but not white, adipose depots (156). Expression of PR domain containing-16 (PRDM16) in skeletal myoblasts promoted differentiation toward a brown adipocyte fate (156, 159). PRDM16 was found in complex with PPARγ and c/EBPβ (156, 159). PRDM16 can bind to either the PPARγ-PPARα transcriptional complex or c/EBPβ to coactivate their transcriptional effects and drive brown adipogenic differentiation.

Functions of Brown and White Adipose Tissue

The main function of brown adipose tissue is to transfer energy into heat using its extraordinarily high concentration of mitochondria and UCP1 (13). While white adipose tissue has been established as a dynamic tissue involved in neurohormonal control, one of its main functions is as an energy reservoir to flexibly release or store fatty acids depending on the energy needs of an animal, including during adaptive thermogenesis (160). In this sense, brown and white adipocytes have functionally opposite, but complementary, roles in energy consumption and storage.

Brown Adipocytes in White Adipose Depots

It has been reported in mice that brown adipocytes can emerge in white adipose depots, but from a separate developmental origin than normal brown adipocytes (161,

162). Brown adipocyte recruitment into white depots is thought to have evolved to protect the body from hypothermia, serving as an extension of the normal role of brown adipocytes in BAT. The upregulation of UCP1 through brown adipocyte recruitment to white adipose depots is mediated by many of the same players that control UCP1 expression in BAT (13). Just like in BAT, adaptive thermogenic sympathetic outflow from cold exposure and dietary sources results in neural stimulation of WAT (163). In fact, there are common neurons in sympathetic nervous system outflow circuits to WAT and BAT that are traced back to the hypothalamus (164).

Brown adipocytes emerge in white adipose tissue in response to cold exposure or a β_3-specific adrenergic agonist, CL-316243 (165). These cells were initially proposed to result from a transdifferentiation of white adipocytes to brown adipocytes (166), but whether brown adipocytes in white adipose depots are due to transdifferentiation or differentiation of brown-like preadipocyte precursors in white adipose tissue remains unclear (162).

Recruited brown adipocytes from mice treated with the β-3 adrenergic agonist CL-316243 are derived from a non-myf5 expressing lineage, suggesting a separate progenitor cell from brown adipose depots and skeletal myocytes (156). Chronic PPARγ activation of epididymally-derived white adipocyte cultures revealed a population of thermogenically competent, UCP1-containing adipocytes which are distinct from classic brown adipocytes (167). These cells were named “beige” adipocytes for their shared brown and white adipocyte characteristics. Other groups have also isolated beige preadipocytes from white adipose tissue (162). Unlike white adipocytes, differentiated beige adipocytes have highly inducible UCP1 expression and cellular respiration, but

also do not descend from a myf-5 lineage. Interestingly, the brown fat in adult humans has more beige molecular characteristics that brown adipose cells. In agreement with lineage studies, the loci responsible for controlling cold-induced brown adipocytes in white adipose depots vary from those that control interscapular brown fat (168). These studies suggest an adipocyte precursor, not of brown lineage, differentiate into an adipocyte that responds more strongly to adrenergic stimulation and PPARγ agonists than white adipocytes to develop thermogenic capacity. Regardless of what color we assign it, when white adipose tissue serves as an adaptive thermogenic organ, it will likely be through the induction of UCP1 transcription and its sympathetic stimulation in adipocytes.

Transcriptional Control of UCP1

The thermogenic function of brown adipose tissue can be traced back to its utilization of UCP1. Any adipocyte that has significant amounts of UCP1 can contribute to thermogenesis and increase energy expenditure. Therefore, to understand the thermogenic role of brown adipocytes in any adipose depot, it is important to understand the transcriptional control of UCP1.

PKA

Integration of thermogenic cues in the hypothalamus results in stimulation of the sympathetic chain, thereby releasing norepinephrine locally in brown adipose tissue (13). Activation of G-protein coupled β-adrenergic receptors on brown adipocytes allows G_s to activate adenylyl cyclase to produce cAMP that activates PKA. PKA activity alone is sufficient to induce UCP1 and other thermogenic gene expression, resulting in elevations in metabolic rate and body temperature (169). Inhibition of UCP1 gene

expression and thermogenesis by H89 indicates protein kinase A mediation of β3-adrenergic signaling is required for adipocyte thermogenic function (145). Therefore, PKA is a central mediator of UCP1 transcription and thermogenesis.

PKA expression is regulated by the FoxC2 transcription factor. FoxC2 induces the expression of PKA regulatory subunit to enhance β-adrenergic and thermogenic signaling, and FoxC2 also enhances angiogenesis (170). Transgenic expression of FoxC2 in adipocytes showed this transcription factor is sufficient to downregulate obesity and metabolic disease (171). pRb suppresses FoxC2 expression, and functional inactivation of pRb results in increased PKA subunit RIα and UCP1 transcription (172).

PKA Targets: CREB and p38

One of the first traditional PKA targets established to affect UCP1 transcription was cAMP response element binding protein (CREB) (173). PKA phosphorylates and activates CREB, which functions as a transcription factor in a variety of processes (174). cAMP response elements are found in a 220 base pair region of the UCP1 promoter that were essential for induction of UCP1 by norepinephrine (173).

The MAPK pathway plays a role in UCP1 transcription (175). In adipocytes, upregulation of UCP1 transcription by β-adrenergic stimulation is controlled by p38 via PKA (175). PKA activates p38α through MAP kinase kinase 3 and is responsible for the induction of UCP1 in response to β-adrenergic stimuli (176). p38 controls UCP1 transcription by phosphorylating both activating transcription factor 2 and PGC-1α (177). Phosphorylation of p38 was also increased early in response to cold exposure in the

obesity resistant A/J strain compared to C57BL/6 (178). Together, these studies suggest an important role of p38 in UCP1 upregulation.

c/EBPs

PPARγ and members of the CCAAT/enhancer-binding protein (c/EBP) family of transcription factors are important transcriptional regulators of both white and brown adipocyte differentiation (147, 153). However the expression of c/EBPβ is higher in brown adipocytes versus white adipocytes. When c/EBPβ is absent, thermoregulation and lipid metabolism is compromised (179). When c/EBPβ is enriched in white adipocytes, they acquire more of a brown adipocyte pattern of gene expression (180). Additionally, c/EBPβ promotes conversion of myoblasts to brown adipocytes (159). Binding sites for c/EBPα and c/EBPβ are present in the proximal UCP1 promoter (181).

The c/EBPβ knockout mice have defective thermoregulation and impaired lipid metabolism (179). One study of white, northern European families found 11 allelic variants in c/EBPα and 12 variants of c/EBPβ that could potentially influence abdominal obesity and related metabolic abnormalities associated with type 2 diabetes and cardiovascular disease, such as leptin and adiponectin levels (182). In sum, regulation of UCP1 transcription by the c/EBP family of proteins is important for thermogenesis.

Thyroid Hormone

UCP1 transcription in BAT is also regulated by thyroid hormone, which is converted to its active form by deiodinase d2, the thyroid hormone converting enzyme, locally in adipose tissue (183). Thyroid hormone action in adipocytes increases UCP1 gene expression via thyroid hormone nuclear receptors, which enhance the thermogenic potential of brown adipocytes (184). The active form of thyroid hormone

acts synergistically with norepinephrine to induce expression of UCP1 in adipocytes (185). Two thyroid responsive elements are found 27 bp apart between −2·33 kb and −2·39 kb in the UCP1 promoter (186). The synergism between cAMP and thyroid hormone seems to reside in a 39 bp sequence downstream (−2·28/−2·32 kb). Thyroid hormone, therefore, potentiates UCP1 expression to facilitate adaptive thermogenesis in adipose tissue.

Peroxisome proliferator-activated receptors (PPARs)

In brown adipocyte development, PPARs have important functions. Studies have demonstrated that PPARγ agonists cause white adipose depots to take on brown adipocyte characteristics (167). These adipocytes are smaller, have greater insulin sensitivity, and animals show overall improvements in metabolic health (187). White adipocytes have increased mitochondrial remodeling and biogenesis (188, 189), as well as blunting of proinflammatory cytokine production and inflammatory transcriptional profiles in response to PPARγ agonists (190, 191). PPARγ agonists are also able to increase transcription of UCP1 (192), PGC-1α (193) and Cidea (194) in white adipocytes.

PPARα has also been strongly linked to UCP1 transcription (178) as well as pathways involved in lipid oxidation and energy expenditure in brown adipocytes (195), suggesting PPARα is important for adaptive thermogenesis. PPARα and PPARγ bind the UCP1 promoter in the −2485/−2458 base pair region to stimulate UCP1 expression (195). Surprisingly, PPARα-knockout mice do not have impaired BAT function, and it is thought that other PPAR family members compensate in its absence (146).

PPARγ coactivator-1α

PPARγ coactivator-1α (PGC-1α) is a coactivator of many transcription factors, including PPARs, driving UCP1 transcription. Overexpression of PGC-1α in white adipocytes results in brown thermogenic expression, including UCP1 and deiodinase d2 (161, 196). Sympathetic stimulation fails to induce UCP1 in brown adipocytes isolated from PGC-1α knockout mice (197). PGC-1β can compensate for the loss of PGC-1α in brown adipocyte differentiation and mitochondrial biogenesis. PGC-1α knockout mice have a variety of metabolic derangements (198), they are unable to defend core body temperature during cold exposure due to defective adaptive thermogenesis (199). In humans, polymorphisms in the PGC-1α gene, especially Gly482Ser, have been associated with diabetes and its complications (200).

Repressors of PGC-1α

In addition to transcriptional activators of brown adipocyte features, genetic deletion mouse models reveal contributions of multiple factors to downregulate the brown phenotypic program. Several of these factors are proposed to act through PGC-1α. pRb binds and represses the PGC-1α promoter (201). RIP140 binds PGC-1α to inhibit its coactivation of thermogenic transcription factors (201, 202). RIP140 knockout mice have decreased fat accumulation (203) along with increased oxidative metabolism and mitochondrial biogenesis (204). Similarly, twist-1, another transcriptional repressor, binds PGC-1α to provide negative feedback on PPAR complex activity (205). The nuclear receptor LXRα behaves as a transcriptional repressor by inhibiting the PGC-1α, PPARγ complex from binding the UCP1 promoter (206). Whether brown and white adipocytes behave differently in response to these repressors remains largely unknown.

PRDM16

One protein that drives brown adipocyte cell fate is the PR domain containing-16 (PRDM16) zinc finger transcription factor (207). Expression of PRDM16 in fibroblasts or white preadipocytes promotes brown adipocyte differentiation. Transgenic expression of PRDM16 in white adipocytes results in resistance to obesity and the emergence of brown adipocytes in white adipose depots. PRDM16 knockout mice die shortly after birth and show large lipid droplets and impaired thermogenic gene expression, including UCP1 and PGC-1α, in brown adipose depots combined with increased skeletal muscle transcriptional profile. Reduction of PRDM16 transcripts in isolated brown preadipocytes also attenuates brown adipocyte thermogenic gene expression in favor of a skeletal myocyte phenotype (156).

The expression of UCP1 is inextricable from brown adipocyte thermogenic potential. As we have discussed, many factors contribute to brown adipocyte UCP1 expression levels.

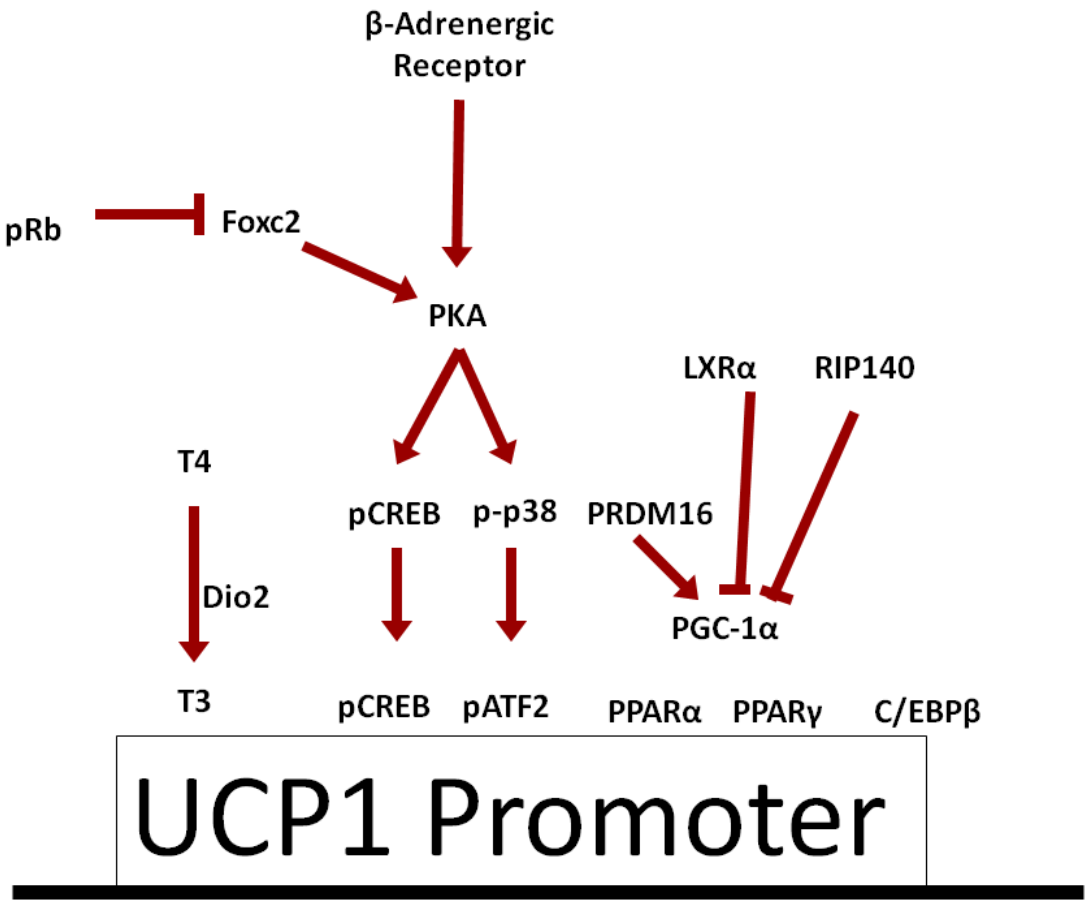

Figure 1.3: Schematic of the UCP1 Promoter

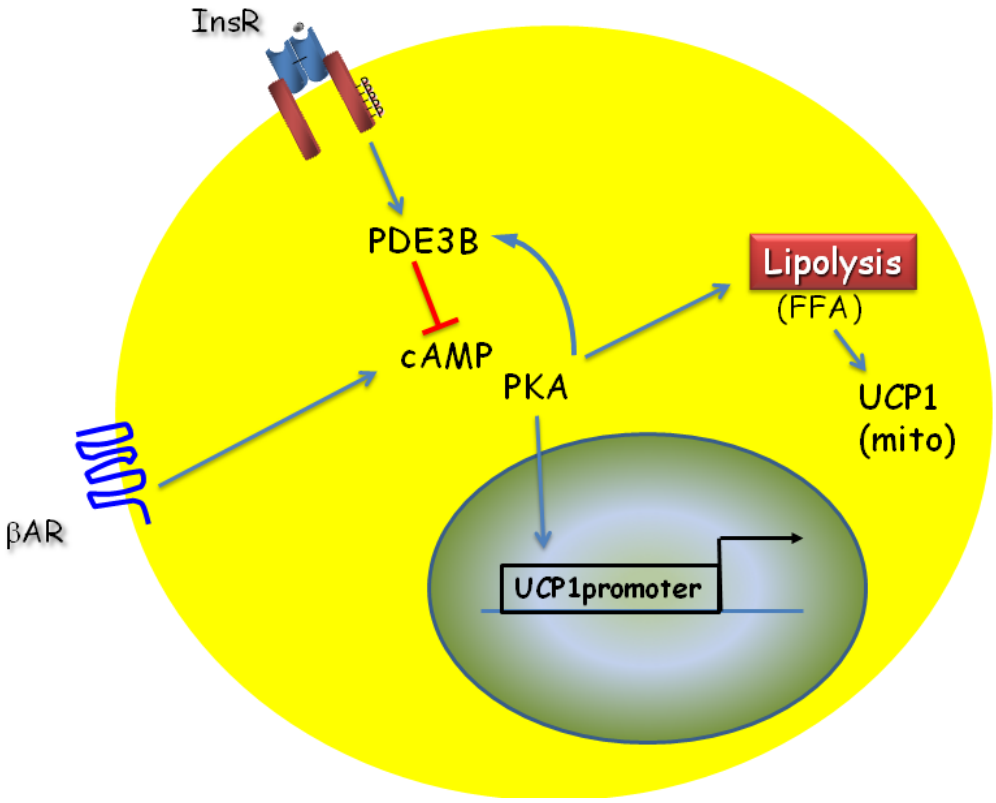

Figure 1.4: Model of UCP1 Transcription and Activation

Thermogenesis and UCP1

Since brown adipocytes have been identified in humans, there is added potential for UCP1 to alleviate obesity and metabolic disease (208-213). Transgenic adipose-specific UCP1 expression is cytotoxic to brown adipose tissue, yet still protects animals from diet-induced obesity by enhancing fatty acid oxidation and decreasing lipogenesis in WAT (214). In the following section, I will review the role of UCP1 on whole animal physiology. A more extensive review by Cannon was done in 2004 (13), but this field has expanded significantly since then.

As an overview, the UCP1 knockout mouse has allowed us to study the physiological significance of UCP1 in the proton uncoupling functions of adipose tissue (215). Reduction in adipose tissue mass from either β-adrenergic agonists or leptin can be largely attributed to UCP1 dependent processes. When brown adipose activity is reduced, animals readily gain weight. The ability of brown adipose tissue to absorb and utilize glucose also is dependent on thermogenesis. However, other thermogenic processes are not dependent on UCP1 activity. The properties of brown adipose tissue, and its recent identification in humans, allows for the possibility that brown adipocytes may play a significant role in energy balance in humans. The consistent theme from this field is that both UCP1 and adrenergic activation are required for a robust nonshivering thermogenic response.

Adaptive Thermogenesis in Adipose Tissue

Cold exposure and adaptation to diet are linked to adaptive adrenergic thermogenesis (215). Both of these processes depend on the presence of UCP1. There is a 10% increase in basal metabolic rate in response to cold exposure, which occurs in

both wild type and UCP1 knockout mice (216), suggesting that this effect is UCP1 independent. However, a 10% change in thermogenesis is not a sufficient response to protect against hypothermia (which requires ~400% increase), so UCP1-independent thermogenesis is not considered to be sufficient for survival in colder temperatures.

UCP1-independent Thermogenic Processes.

Fever is a thermogenic response that is mostly UCP1-independent. The febrile response is recruited as a specific response to pathogens. UCP1 is not necessary for febrile response, although it can be stimulated in a febrile response (215). The body uses all means necessary, but a loss of nonshivering thermogenesis does not prevent fever. Adipokines, such as interleukin-6 , may be released from adipose tissue into circulation to further the febrile response (215). However, the role of brown adipose tissue in fever is limited.

Thermogenic responses to adrenergic stimuli exist outside of brown adipose tissue UCP1 (216-218). The heart increases its metabolism by increasing rhythmicity and contractility of cardiac muscle in response to sympathetic activation, which requires ATP through coupled aerobic respiration (215). This results in increased biochemical reactions that, consequently, give off more heat. Sustained sympathetic stimulation on tissues other than BAT, such as cardiac and skeletal muscle, however, will not adaptively increase thermogenesis over time. In contrast, brown adipose tissue that is recruited for adaptive purposes by sympathetic stimulation will yield a much larger increase in thermogenesis and energy expenditure over time than an unadapted animal (215).

UCP1-independent Cold-induced Thermogenesis

Animals presented with a cold challenge protect body temperature through shivering and nonshivering thermogenesis, and both contribute to maintaining body temperature (215). A mouse acutely exposed to cold depends primarily on shivering thermogenesis to meet its needs until brown adipose tissue is recruited (219, 220). Cold exposure also leads to changes in the acyl-phospholipid composition in the mitochondrial membrane of brown adipocytes (221). Membrane composition is an important determinant of native proton conductance and thermogenesis in mammals compared to other species, and differences in lipid composition of mitochondrial membranes are independent of UCP1 activity. Angiogenesis in brown adipose tissue requires adrenergic stimulation from cold exposure to aid in thermogenesis (222). Adrenergic stimulation results in the release of VEGF in brown adipose tissue, but does not depend on UCP1 as well(222, 223).

UCP1-dependent Thermogenesis

The role of UCP1 in brown adipose thermogenesis has become more accessible with the creation of UCP1 knockout mice (224). UCP1 from brown adipocytes has been reported to be completely necessary for β-adrenergic stimulated non-shivering thermogenesis (144, 225).

Norepinephrine-induced Thermogenesis

At the time that the nonshivering thermogenesis field was in its infancy, it was observed that recruitment of nonshivering thermogenesis was paired with a potentiation of thermogenesis in response to injected catecholamines (215). Many years later, it was discovered that UCP1 was required for enhanced thermogenesis in response to

catecholamines (215). Norepinephrine is responsible for cold-induced adaptive thermogenesis by stimulating both β_3 and α_1 adrenergic receptors in rodents (226-230). Therefore, norepinephrine from the sympathetic chain is essential to nonshivering thermogenesis.

UCP1-dependent Nonshivering Thermogenesis

Non-shivering thermogenesis is a specialized heat producing mechanism in mammals that is elicited by cold exposure. Initially, shivering dramatically increases heat production (219, 220). Gradually, shivering heat production is replaced by nonshivering adaptive thermogenesis (215). Although first thought to occur in muscle, the characterization of the UCP1 knockout mouse demonstrated that brown adipose tissue is responsible for nonshivering thermogenesis, as these mice continue to shiver with prolonged cold exposure (219). Furthermore, no other uncoupling protein or metabolic process can substitute for UCP1 in brown adipose tissue to mediate nonshivering thermogenesis (231). Whereas cold exposure does not normally decrease lifespan (232), UCP1 knockout mice exposed to cold have significantly decreased lifespan (219). Together, these studies suggest a primary role for UCP1 in nonshivering thermogenesis and survival in cold environments.

Diet-induced Thermogenesis

Diet-induced thermogenesis is a difficult-to-define phenomenon that, for the purposes of clarity, will exclude the energy expended in the digestion of nutritional macromolecules. High-fat diet increases norepinephrine-induced thermogenesis, which is dependent on the presence of UCP1 in mice (217). However, the idea that diet-induced thermogenesis may combat obesity is not supported by several researchers

within the field (233). Leptin is released from expanded adipose tissue to act on the hypothalamus to decrease food intake and increase energy expenditure through thermogenesis (234). Early studies showed that leptin-deficient animals have a thermogenic defect (235). Interestingly, UCP1 is required for leptin-stimulated increases in energy expenditure and reductions in white adipose tissue in pair fed mice (236). Therefore, humans would need substantial brown adipose tissue to increase thermogenesis to respond to leptin infusion. It has also reported that brown adipose tissue can respond to a single meal, which may or may not be independent of leptin-induced dietary thermogenesis (237). However, for all intents and purposes, both cold-induced and dietary adaptive thermogenesis are UCP1-dependent.

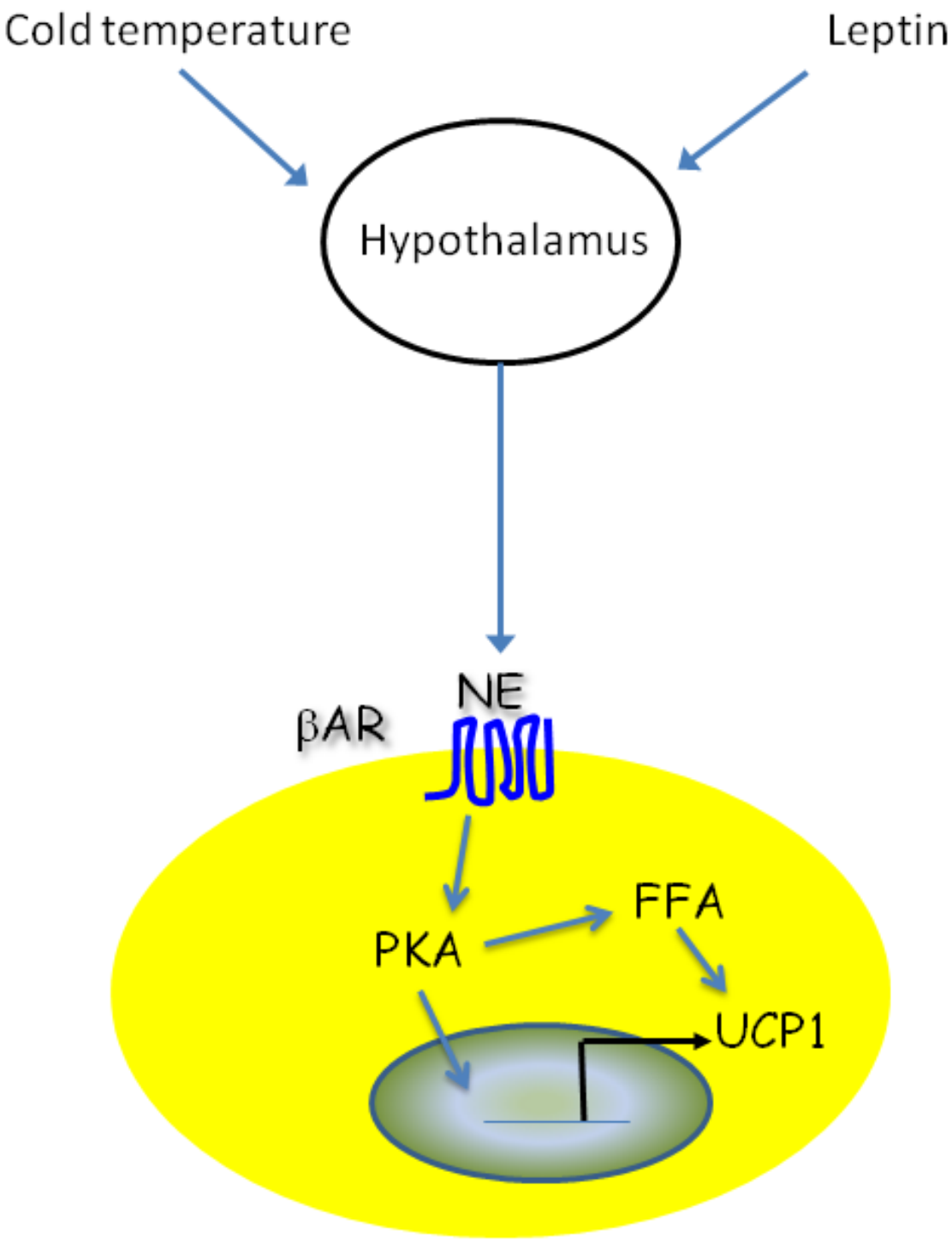

Figure 1.5: Model of UCP1 activation in Adaptive Thermogenesis

UCP1 is Required to Prevent Obesity

Obesity occurs when animals experience a chronic positive energy balance. This is accomplished through either an increase in calorie intake or a decrease in energy expenditure. As mentioned before, “with few exceptions, most rodent models of obesity have defects in adaptive thermogenesis” (12). Researchers have tried for a long time to find a thermogenic defect in obesity, but results have been mixed (233). One possibility is that the thermogenic activity is maintained in obesity, but increases in thermogenic potential are held in check by negative regulators of adaptive thermogenesis. So far, only one polymorphism related to UCP1 expression has been described (238), and the correlation between that polymorphism and obesity has generated mixed results (239, 240). This suggests that defects related to UCP1 are not due to UCP1 variant inaction. Instead, primary defects in obesity and metabolism may be related to the pathophysiologic control of UCP1 activity, such as defects in lipolysis and UCP1 transcription. Regardless of source, the presence of UCP1 in animals has a profound effect on metabolism. Since UCP1 is responsible for adaptive thermogenesis, the UCP1 knockout mouse provides an important model for defective adaptive thermogenesis in obesity.

UCP1-ablated Mice Become Fat in a Thermoneutral Environment

Thermoneutrality, or the temperature at which an organism expends the least amount of energy to maintain homeothermy, varies from animal to animal. Humans prefer a lower ambient temperature than mice because clothes and other environmental modifiers can protect homeothermy. Mouse thermoneutrality is approximately 30°C, and mice select this temperature over others (241). Initial studies of UCP1 knockout mice at

temperatures beneath thermoneutrality paradoxically showed resistance to obesity (224, 242), and no obesogenic effect was observed in UCP1 knockout mice raised just beneath thermoneutrality (242, 243). However, UCP1 is required to maintain lower body weights even on a normal diet under thermoneutral conditions (217), and this phenotype is exacerbated by high-fat feeding. Along with increased susceptibility to obesity with high-fat diet, the obesogenic effect is more prominent with age in UCP1 knockout mice (244). These experiments highlight how important the thermal environment is to altering UCP1-dependent phenotypes.

Effects of β_3 agonists on Weight

β_3 agonists reportedly increase aerobic energy expenditure in mice, even in the absence of UCP1 (218, 245); however, several groups have not seen a UCP1-independent thermogenic response to β_3 agonists (215, 243), making UCP1-independent β_3 thermogenic responses in mice controversial. Perhaps, increased metabolism observed in mice treated with β_3 agonists may be attributed to tissues other than brown adipose tissue because of the known involvement of the β_3 receptor in the metabolism of a variety of tissues, including heart, gall bladder, gastrointestinal tract, prostate, urinary bladder detrusor, brain and near-term myometrium (246). Regardless, weight loss in response to β_3 agonists occurs in the presence of UCP1 (218), suggesting an essential role for brown adipose tissue in this process. Therefore, the weight reducing potential of β_3 agonists may only be effective in animals with substantial amounts of brown fat already. Brown adipocyte proliferation is a β_1 receptor stimulated process (247) and not a β_3 stimulated process (248, 249). Because brown preadipocytes do not have β_3 receptors present (250), it may be important to stimulate

brown adipocyte proliferation before the beneficial effects of β_3 agonists are possible in animals lacking significant numbers of adipocytes with brown features, including humans. Additionally, the thermogenic potential of beige precursor cells in white adipose tissue may require a more thorough understanding of how these cells proliferate (162). Since the presence of sufficient thermogenic cells and adrenergic receptors in human adipose tissue is also controversial, the potential of brown adipose activity in human obesity remains ambiguous (208, 251, 252).

UCP1-dependent Catecholamine-stimulated Glucose Uptake

Although the dogma surrounding the UCP1 field is that lipid is the only important energy substrate for adaptive thermogenesis, respiratory quotient experiments during cold exposure indicate that both glucose and lipid are utilized concurrently, allowing for the possibility that UCP1-laden cells could reduce blood glucose in the context of obesity and type 2 diabetes (215). Uptake of glucose into brown adipose tissue has been observed in rodents exposed to cold (253), and glucose uptake is the how brown adipose tissue was first identified in human patients (208). Additionally, glucose uptake is induced by norepinephrine in wild type mice, but is absent in UCP1 knockout mice (254). Stimulation of isolated brown adipocyte with norepinephrine also results in increased glucose uptake, which further implicates a role for brown adipose tissue glucose uptake in thermogenesis.

Since extra heat during chronic cold exposure comes exclusively from brown adipose tissue, it reasons that brown adipose tissue is either mobilizing stored carbohydrates or absorbing glucose from the blood stream for consumption. Therefore, along with fatty acid activation of UCP1, carbohydrates provide glycolytic products that

will eventually be used to generate a proton gradient to be dissipated by UCP1 in mitochondria. Therefore, humans with less brown adipose tissue do not have this additional mechanism to uptake glucose from the bloodstream and utilize that glucose for thermogenesis, perhaps making these individuals more susceptible to metabolic dysfunction that leads to high blood glucose.

Inflammation in Obesity

Metabolic and immune functions are essential to life, and these systems are highly conserved and integrated. Consequently, dysfunction in either system results in a variety of maladies with both metabolic and immunologic features, including obesity (1). Obesity produces a state of chronic, low-grade inflammation in liver and fat accompanied by macrophage infiltration and the local secretion of inflammatory cytokines and chemokines (1, 255, 256). The resulting increase in TNFα and other cytokines creates a sustained cycle of adipocyte lipolysis and inflammatory crosstalk between adipocytes and recruited macrophages, activating the inhibitor of kappaB kinase β (IKKβ)-nuclear factor κB (NFκB) pathway in both tissue types (255).

Multiple metabolic stressors are thought to work through IKKβ and NFκB. Circulating free fatty acids, interleukin 1, TNFα, advanced glycated end products, glucosamine, and ER stress have all been linked to NFκB in insulin resistance (257). Increased NFκB has also been observed in the hypothalamus of mice fed a high-fat diet. Mice with neural-specific knockout of IKKβ are resistant to diet-induced obesity, which is attributed to decreased food intake (258). Therefore IKKβ-NFκB has been implicated in each stage of the pathogenesis of insulin resistance. However, IKKβ and NFκB are mostly known for their involvement in innate immunity.

NFκB in Immunology

The NFκB family of transcription factors regulates inflammation, along with a variety of stress-oriented cellular responses (259). NFκB activity is an important effector of inflammatory cell surface receptors, such as Toll-like receptors (TLRs) (260), and receptors of proinflammatory cytokines, including TNFα (261). TLRs recognize pathogen-associated molecular patterns, such as lipopolysaccharide (LPS) and double stranded RNA (dsRNA), which trigger inflammatory signals that orchestrate immune cell action to clear microbes from the body (260). Both TLRs and TNFα receptors (TNFRs) initiate inflammatory signaling cascades using protein adaptors and polyubiquitin ligases that colocalize with these receptors (259). TGFβ activated protein kinase (TAK1) is bound by TAK1-binding proteins (TABs), which are phosphorylated in response to inflammatory stimuli, and are necessary for TAK1 stability and activity (262-265). TAK1 activity simultaneously leads to parallel MAPK (p38, JNK) and IKK pathway phosphorylation and activation (266). With respect to IKKs, TLR and TNFα stimulation leads to receptor interacting protein 1 (RIP1) polyubiquitination, which recruits the IKK complex regulatory scaffolding protein NEMO to TAB-TAK1, so that TAK1 phosphorylates and activates the IKKβ (267) (268).

Active IKKβ phosphorylates the inhibitor of κB (IκB), which results in IκB polyubiquitination and subsequent degradation through the 26S proteosome, and activation of NFκB (269). The NFκB family comprises five subunits that act as dimeric transcription factors (259). Family members have a conserved Rel homology domain that is responsible for dimerization, promoter binding, and forming a complex with the inhibitor of kappaB (IκB), which sequesters NFκB proteins to the cytosol. The

degradation of IκB exposes the nuclear translocation sequence of NFκB allowing this transcription factor to translocate to the nucleus and control the expression of inflammatory target genes.

The IKK family of proteins: IKKα, IKKβ, TBK1, and IKKε

The IKK family of proteins is composed of four members: IKKα, IKKβ, IKKε, and TANK-binding kinase (TBK1) (259). Similarities and differences exist in IKK family member function. Whereas IKKα and IKKβ complex with their regulatory subunit NEMO to make the canonical heterotrimeric IKK complex, IKKε and TBK1 complex with their regulatory subunit, TANK, to form the noncanonical IKK-related kinase complex (259). The canonical complex is proposed to exist as a large oligomer with additional adaptor proteins, and the complex is modified by phosphorylation. IKKβ is essential for mediating innate immune responses, including TLR and TNFα signaling, while IKKα is more important for regulating adaptive immunity and lymphoid organogenesis (270). IKKε and TBK1, also known as IKK-related kinases, were initially identified in the thymus, white blood cells, and lymphoid organs (271). IKKε and TBK1 phosphorylate interferon regulatory factors (IRFs), which then translocate to the nucleus to promote the expression of type I interferon genes, such as interferon β, to coordinate antiviral responses (272-274). The transcription of IKKε is induced by NFκB from canonical IKKβ activity (275). Therefore, IKKε is an inducible downstream mediator of NFκB inflammation.

Recent studies have shown that there is cross-talk between canonical IKK and IKK-related kinase signaling pathways facilitated by the binding of NEMO and TANK heterotrimeric scaffold proteins (276). Both TLR3 and TLR4 activate the canonical IKK

pathway, which subsequently phosphorylate the activation loop Ser172 of IKK-related kinases. IKK-related kinases then negatively regulate the canonical IKK complex to dampen NFκB signaling as a feedback mechanism .

Activation of IKKε is rapid, transient, and precedes prolonged TBK1 activation (277). TANK is required for IKKε and TBK1 activation, and the interaction between the IKK canonical complex and the IKK-related kinase complex depends on TANK and NEMO. However, phosphorylation of IRF3 and interferon β production do not require TANK. Therefore, IKKε and TBK1 can mediate the antiviral response through the formation of TANK-independent complexes (278).

The IKK family regulates many facets of immune responses, but kinase activity of IKK family members occurs through a conserved pattern, as phosphorylation of activation loop serine residues is important for IKK family kinase activation. TAK1 phosphorylates IKKβ on activation loop serine 177/181 between kinase subdomains VII and VIII causing a conformational change leading to IKKβ activation (279). Substitution of alanine for serine 177/181 dramatically reduces IKKβ activity, while substitution for phosphomimetic glutamate generates a constituitively active kinase (280, 281). Phosphorylation of serine 172 on TBK1 and IKKε has been associated with increased activity, and this residue is required for activity (282, 283). Therefore, phosphorylation of the activation loop is strongly indicative of IKK family member activity.

Several phosphatases are important for the dephosphorylation of the activation loop to terminate IKK family member activity (284, 285). From the phosphoprotein phosphatase (PPP) family, PP1 and PP2A can block IKKβ activity. From the

phosphoprotein phosphatase M (PPM) family, which require Mn^{2+}/Mg^{2+} metal ions, PPM1A and PPM1B decrease IKKβ activity (284). PPM1B negatively regulates antiviral responses by dephosphorylating serine 172 of TBK1 (285). TAB1 functions as a pseudophosphatase, and it has close structural similarity to PPM family phosphatases (286). In sum, the regulation of IKK family member activation loop phosphorylation by upstream kinases and phosphatases is highly regulated.

Rationale for Project

Since it is well-known that IKKβ affects insulin sensitivity (255), we set out to establish what effects other IKK family members have on energy balance in mice, especially IKKε and TBK1. When I entered the lab, our group was characterizing the IKKε knockout mouse (287) on a high fat diet. Using the IKKε knockout mouse, our lab discovered that IKKε is required for diet-induced weight gain, decreased energy expenditure, decreased insulin sensitivity, increased hepatic steatosis, and systemic inflammation (288). IKKε knockout mice had increased energy expenditure and UCP1 levels in white adipose tissue on a high-fat diet. Furthermore, pharmacologic inhibition of IKKε and TBK1 recapitulated the knockout phenotype (Chiang and Reilly, unpublished). The main objective of my graduate years was to determine the mechanism by which IKKε and TBK1 regulate adipocyte dysfunction and energy expenditure.

Chapter II:
IKKε and TBK1 Promote Obesity by Decreasing Energy Expenditure and UCP1 in Adipose Tissue

Abstract

The IKK family of proteins has been linked to insulin resistance. In this chapter, we explore the effect on IKKε and TBK1 on metabolism, especially in adipose tissue. High fat diet increased IKKε and TBK1 protein levels in adipose tissue. Genetic ablation of IKKε or pharmacologic inhibition of IKKε and TBK1, using the selective inhibitor amlexanox, in mice resulted in many metabolic improvements, including reduced weight gain on a high-fat diet. These improvements were correlated with increased energy expenditure, core body temperature, adipocyte hyperplasia, and UCP1 protein levels in adipose tissue. Inhibitors of IKKε and TBK1 promote lipid accumulation and adipocyte proliferation in 3T3-L1 adipocyte differentiation. Treating 3T3-L1 adipocytes with amlexanox produced a dose-dependent increase in lipolysis and oxygen consumption. These studies suggested that IKKε and TBK1 diminish β-adrenergic/cAMP-dependent processes in adipocytes to regulate energy expenditure.

Introduction

The innate immune system has evolved to combat viral, bacterial, and other infectious challenges. It is also stimulated by noninfectious sources to promote chronic

inflammation, which participates in the pathogenesis of a variety of diseases, including obesity, insulin resistance and type 2 diabetes (1). Obesity is accompanied by a state of low-grade, chronic inflammation in adipose tissue and liver that results in insulin resistance (255, 256). Overnutrition stimulates macrophage infiltration in adipose tissue. The resulting increase in TNF-α and other cytokines creates a sustained cycle of adipocyte lipolysis and inflammatory crosstalk between adipocytes and recruited macrophages (289), activating the IKKβ-NFκB pathway (255, 257). Multiple metabolic stressors are thought to work through IKKβ and NFκB. Circulating free fatty acids, interleukin 1, TNFα, advanced glycated end products, glucosamine, and ER stress have all been linked to NFκB in insulin resistance (257). Increased NFκB has also been observed in the hypothalamus of mice fed a high fat diet. Mice with a neural-specific knockout of IKKβ are resistant to diet-induced obesity, which is attributed to decreased food intake (258). Therefore IKKβ-NFκB has been implicated in each stage of the pathogenesis of insulin resistance.

The IKK family of proteins is composed of four members, IKKα, IKKβ, IKKε, and TBK1 (TANK Binding Kinase 1) (259). While IKKα and IKKβ stimulate the canonical NFκB pathway, the roles of IKKε and TBK1 are less well understood. IKKε was initially thought to phosphorylate the traditional IKK substrate IκB (290), but the list of IKKε substrates has expanded to include other NFκB proteins, interferon regulatory factors (IRFs), and STATs (291). The transcription of IKKε is controlled by NFκB from canonical IKKβ activity (275). Therefore, IKKε is an inducible mediator of NFκB inflammation.

Given the role of IKKβ in generating insulin resistance, our lab set out to determine whether its family members, IKKε and TBK1, also mediated inflammation in

diet-induced obesity. Our lab discovered that a high fat diet induces NFκB activity and the expression of IKKε in white adipose tissue (WAT) of wild type mice (288). Much like IKKβ deficient mice (255), IKKε knockout mice on a high fat diet showed improved insulin resistance compared to wild type mice, as seen through glucose and insulin tolerance tests. Additionally, high fat diet-fed IKKε knockout mice have markedly less hepatic steatosis and circulating markers of systemic inflammation than wild type mice. Interestingly, the targeted deletion of IKKε protects mice against diet-induced obesity, while IKKβ deficient mice are not protected. IKKε knockout mice display decreased weight gain and adipocyte size, despite increased food consumption, compared to wild type mice after 3 months of high fat diet. White adipose tissue from mice had decreased adrenergic signaling *ex vivo*. Pharmacological inhibition of IKKε and TBK1 using the selective inhibitor, amlexanox, recapitulated the IKKε knockout phenotype (Chiang, unpublished). Amlexanox treatment increased oxygen consumption and lipolysis in 3T3-L1 adipocytes as well. Finally, inhibitors of IKKε and TBK1 promoted adipogenesis in 3T3-L1 adipocytes. Together, these studies suggest that IKKε and TBK1 suppress energy expenditure and adipocyte development.

The first figures from this chapter come from a paper published in 2009 (288) and a manuscript recently accepted (292), both of which include me as an author. These figures provide the necessary background to understand the significance of subsequent data later in chapter 2 and chapter 3.

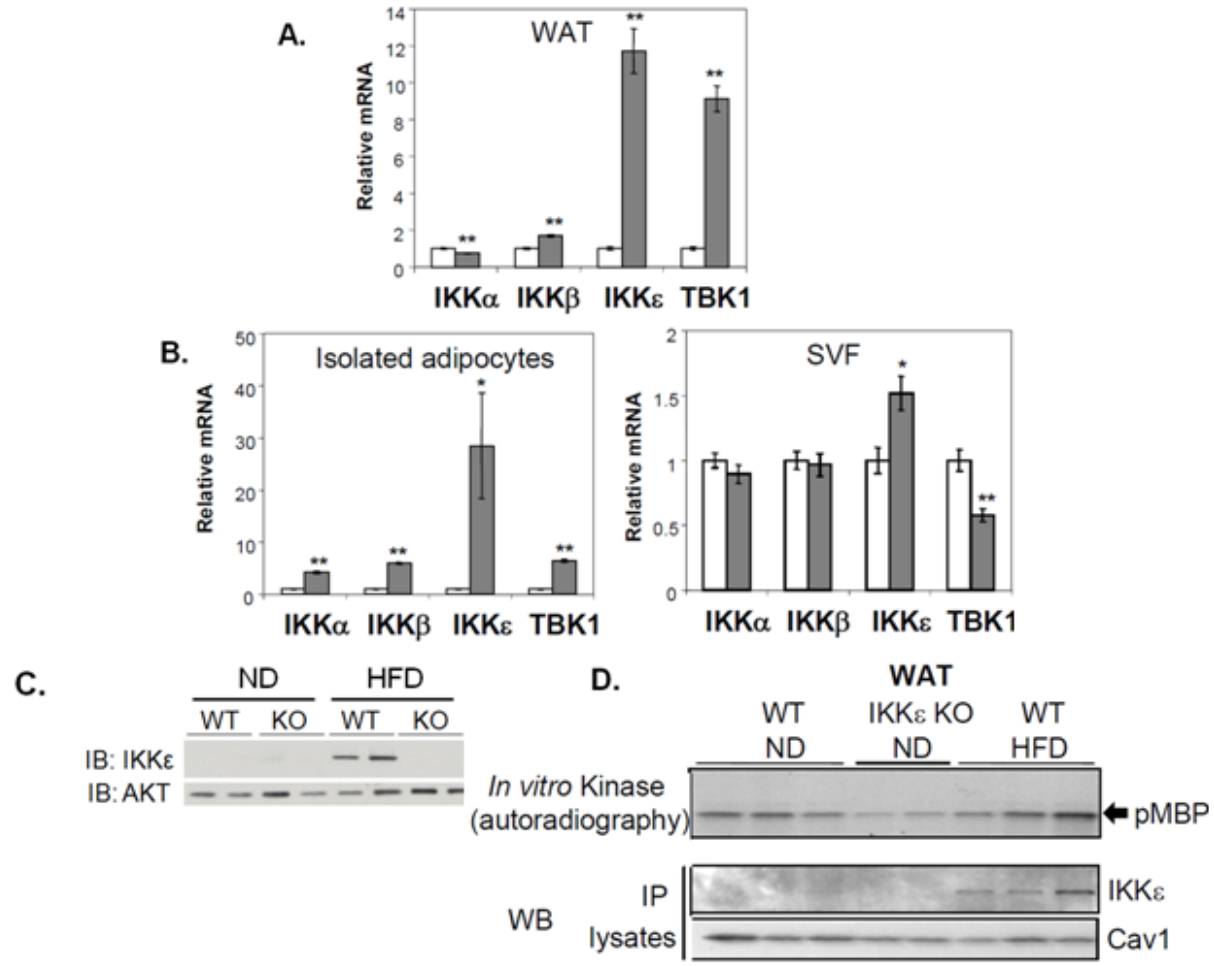

Figure 2.1 HFD Increases IKKε Activity in White Adipose Tissue (A) qPCR analysis on the expression of genes encoding IKK family members in liver and white adipose tissue. White bars, wild-type mice, normal diet (ND) (n = 6); gray bar, wild-type mice, high-fat diet (HFD) for 4 months (n = 6). All data are presented as the average ± SEM normalized to *Rplp0* expression. Average of ND value was set as 1. (B) qPCR analysis on the expression of genes encoding IKK family members in isolated adipocytes and stromal vascular fraction. White bars, ND (n = 6); gray bar, HFD for 4 months (n = 6). (C) Lysates from white adipose tissue (WAT) of wild-type (WT) and IKKε knockout mice (IKKε KO) fed with ND or HFD were blotted with antibody against IKKε as indicated. The expression level of IKKε was determined by immunoblotting with same antibody against IKKε. (D) Lysates from WAT of WT and IKKε KO fed with ND or HFD were immunoprecipitated (IP) with antibody against IKKε and assayed for kinase activity against myelin basic protein (MBP) as substrate. The expression level of IKKε in IP was determined by immunoblotting with same antibody against IKKε. Lysates for IP were immunoblotted against Caveolin 1 as a loading control.

Data were contributed by Dr. Shannon Reilly and Dr. Shian-Huey Chiang (288, 292).

Results

High-Fat Diet Increases IKKε Expression in White Adipose Tissue (288)

Our lab discovered that a high fat diet induces NFκB activity and the expression of IKKε in white adipose tissue (WAT) of wild type mice (288). Using a NFκB responsive promoter luciferase mouse, high fat diet produced a two-fold increase in reporter activity, which was traced back to 5 fold increase in adipose tissue from epididymal and subcutaneous fat depots (data not shown). Macrophage infiltration and adipose "crown-like" structures appeared with long-term high fat diet. Staining for markers of NFκB was enriched in these structures as well. Together, these experiments showed that macrophage infiltration and NFκB activity in adipose tissue is highly correlated with obesity.

Since NFκB is known to control the transcription of IKKε (271), we measured the expression of IKKε in epididymal white adipose tissue by real-time PCR and then compared this to the levels of other IKK family members. HFD produced a small increase in the expression of IKKα, β, and TBK1 in liver, but it produced a 2.6-fold increase in IKKε mRNA (data not shown). In white adipose tissue (WAT), IKKα was reduced, whereas HFD induced IKKβ 1.7-fold, and IKKε and TBK1 by 12- and 9-fold, respectively (Fig 2.1A). To determine which cell types in adipose tissue were responsible for these changes, we collagenase digested WAT and separated adipocytes from the stromal vascular fraction (SVF), and examined expression of IKK family members. HFD produced a 2- to 3-fold increase in expression of IKKα, IKKβ and TBK1 mRNA in adipocytes, whereas IKKε expression was increased 28-fold (Figure 2.1B). However, only IKKε was upregulated in SVF isolated from WAT, although the

number of macrophages in adipose tissue was also significantly increased. Therefore, IKKε and TBK1 are transcriptionally upregulated in liver and adipose tissue. We also monitored IKKε protein levels by western blotting (Figure 2.1C). IKKε expression was low in WAT from wild-type mice on a chow diet, but was markedly increased in after HFD, correlating well with RNA levels. In addition to protein levels, immunoprecipitated *in vitro* IKKε kinase activity in WAT from HFD mice was increased by 1.5-fold compared to normal diet mice (Figure 2.1D).

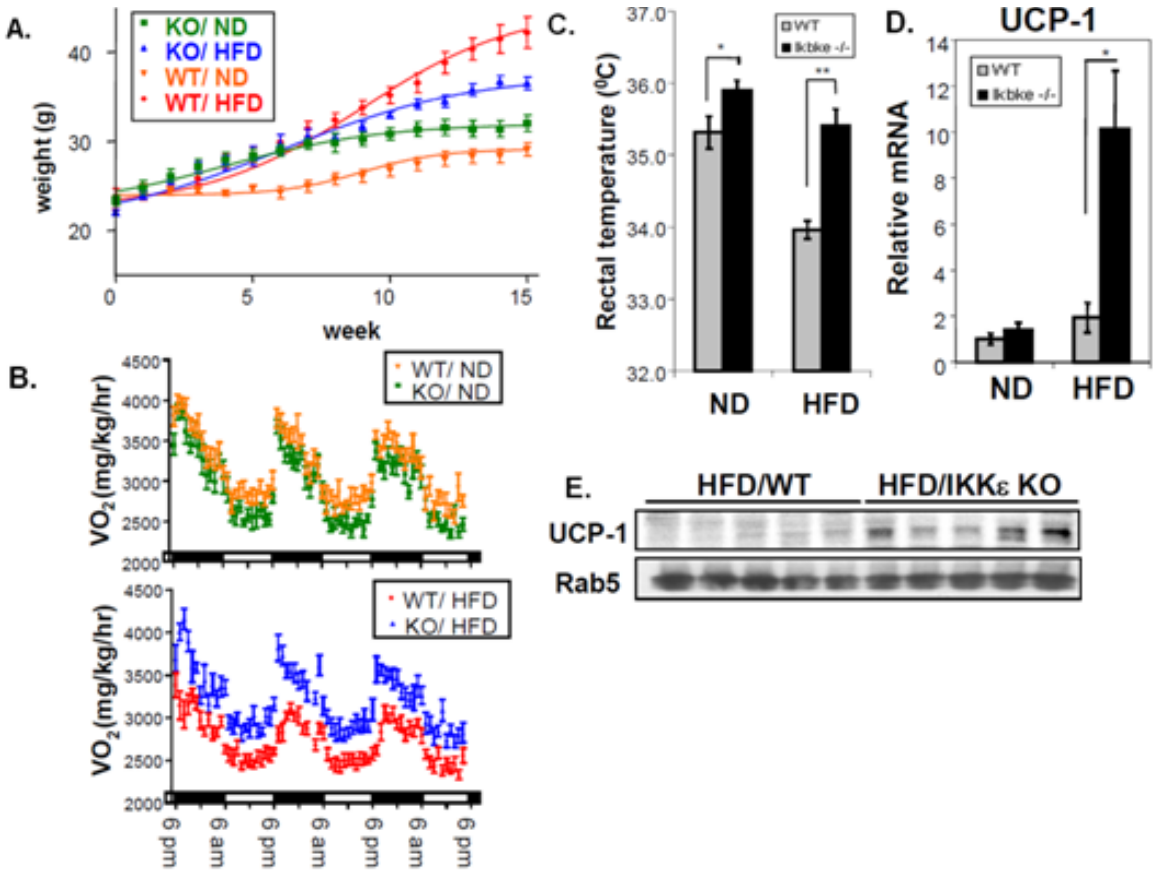

Figure 2.2 IKKε KO Mice Are Protected from Diet-Induced Weight Gain by Increasing Energy Expenditure.(A) Body weight measured for WT, ND (orange); IKKε KO, ND (green); WT, HFD (red) and IKKε KO, HFD (blue) during 15 weeks-period (n=10-12 in each group). (B) Oxygen consumption (VO_2) was measured for WT (orange) and KO (green) mice fed with ND (top) or WT (red) and KO (blue) mice fed with HFD (bottom) for three days as indicated. n = 8 mice per group (C) Rectal temperature measured for WT and KO mice fed with ND (3 months old) or HFD (5 months old with diet for 2 months). n = 10 per group. *p value < 0.05; **, p value < 0.01 (D) qPCR analysis on the expression of genes encoding UCP1 in WAT. Gray bars, wild-type mice (n = 6); black bar, IKKε KO mice (n = 6) fed with ND or HFD as indicated. All data are presented as the average ± SEM normalized to *Rplp0* expression.*, p value < 0.05. Average of WT fed with ND value was set as 1. (E) Protein expression of UCP1 in WAT, measured by immunoblotting with WAT lysates from WT and IKKε KO mice (5 mice in each group) fed with HFD as indicated. Rab5 was used as internal loading control. Data were contributed by Dr. Shian-Huey Chiang and published in (288)

IKKε Knockout Mice Display Decreased Weight Gain and Increased Energy Expenditure on a High-Fat Diet

The increased expression of IKKε in wild type mice on a high fat diet led us to examine if IKKε affects obesity and insulin resistance. We therefore evaluated mice with a targeted deletion in the IKKε gene (287) on a high-fat diet and examined its metabolic phenotype. On normal chow, body weights did not differ significantly between IKKε knockout mice and wild-type mice. However, after 3 months of HFD, wild-type controls gained near 20 g, whereas IKKε knockout mice gained only 12 g (Figure 2.2A).

Body weight represents a balance of food intake and energy expenditure. IKKε knockout mice showed higher daily food intake per body weight compared to wild-type mice, either on chow or HFD (data not shown). Therefore, total caloric consumption between wild type and IKKε knockout mice was not different. Oxygen consumption was similar in both wild-type and IKKε knockout mice on a chow diet (Figure 2.2B). Wild-type mice on HFD showed little change in oxygen consumption, whereas IKKε knockout mice demonstrated a significant increase. This difference was consistent throughout light and dark phases, indicating an increase in energy expenditure.

There were small decreases in respiratory quotient between normal diet and high-fat diet mice, indicative of high-fat diet composition (data not shown). High respiratory quotient, indicating carbohydrate preference, has been correlated with weight gain (293), but no changes in RQ between wild type and IKKε knockout mice were observed. Regardless, differences in weight gain could not be attributed to differences in RQ.

The lack of effect of IKKε knockout on RQ suggested that there was no difference in fuel selection between carbohydrates and lipids, leading us to explore whether the increase in energy expenditure may be due to increased thermogenesis, and we thus evaluated core body temperature (Figure 2.2C). A significant increase in core body temperature was also noted in IKKε knockout mice. IKKε knockout mice were 1.5°C warmer than their wild-type counterparts on HFD, with a smaller 0.5°C increase seen under chow-fed conditions. In chow-fed mice, UCP1 mRNA was low in WAT from wild-type or IKKε knockout mice. HFD produced a 2-fold increase in UCP1 mRNA in wild-type mice, but generated a 10-fold increase in knockout mice (Figure 2.2D). UCP1 protein levels in WAT of knockout mice on HFD were similarly higher (Figure 2.2E), while mitochondrial proteins and UCP1 mRNA and protein levels in brown fat were unchanged (data not shown).

IKKε knockout mice on a high fat diet showed significantly attenuated increases of serum proinflammatory cytokines, such as TNFα, MCP-1, and Rantes compared to wild type mice (data not shown). This attenuation of high fat-induced proinflammatory responses was also evident in white adipose tissue, where IKKε knockout mice on high fat diet had reduced TNFα, Rantes, and MIP1α compared to wild type mice. Decreased hepatic steatosis and insulin resistance were also observed in these mice (data not shown).

IKKε and TBK1 Attenuate β-adrenergic-stimulated Glycerol Release in Obesity

β-adrenergic activation in adipose tissue by either β_3 pharmacologic activation or cold exposure increases the number of multilocular adipocytes and UCP1 in white adipose depots (165). Since we had observed increased UCP1 expression in the

epididymal fat pads of IKKε knockout mice, we wanted to examine the signaling pathways that lead to UCP1 expression and activity. Adrenergic stimuli, such as norepinephrine, activate β-adrenergic receptors in white and brown adipose tissue to initiate a cascade of events through cyclic AMP (cAMP) culminating in the transcriptional upregulation of UCP1, partially through p38, as well as UCP1 activation by HSL-liberated free fatty acids, which results in increased proton leak and energy expenditure (177, 294). Therefore, we stimulated explants of epididymal white adipose tissue with adrenergic stimuli and measured the lipolysis and lipolytic signaling in that tissue.

White adipose tissue from IKKε knockout mice treated with isoproterenol or forskolin have increased glycerol release compared to wild type mice (Figure 2.3A). Phosphorylation of PKA substrates and HSL were increased in white adipose tissue from IKKε knockout mice on a high fat diet as well, indicating increased lipolytic signaling paralleled glycerol release (Figure 2.3B,C). Desensitization to adrenergic stimuli in adipose tissue is correlated with increases in IKKε and TBK1 expression. Studies have shown decreased sensitivity to adrenergic stimuli in adipose tissue as a consequence of decreased β-adrenergic receptors on the surface of adipocytes (36) or increased expression of α_2 adrenergic receptors (295); however, these forskolin studies represent the first time defects beyond the adrenergic receptor account for catecholamine resistance. These experiments suggest IKKε and TBK1 are important for downregulating β-adrenergic signaling beyond the receptor in adipose tissue.

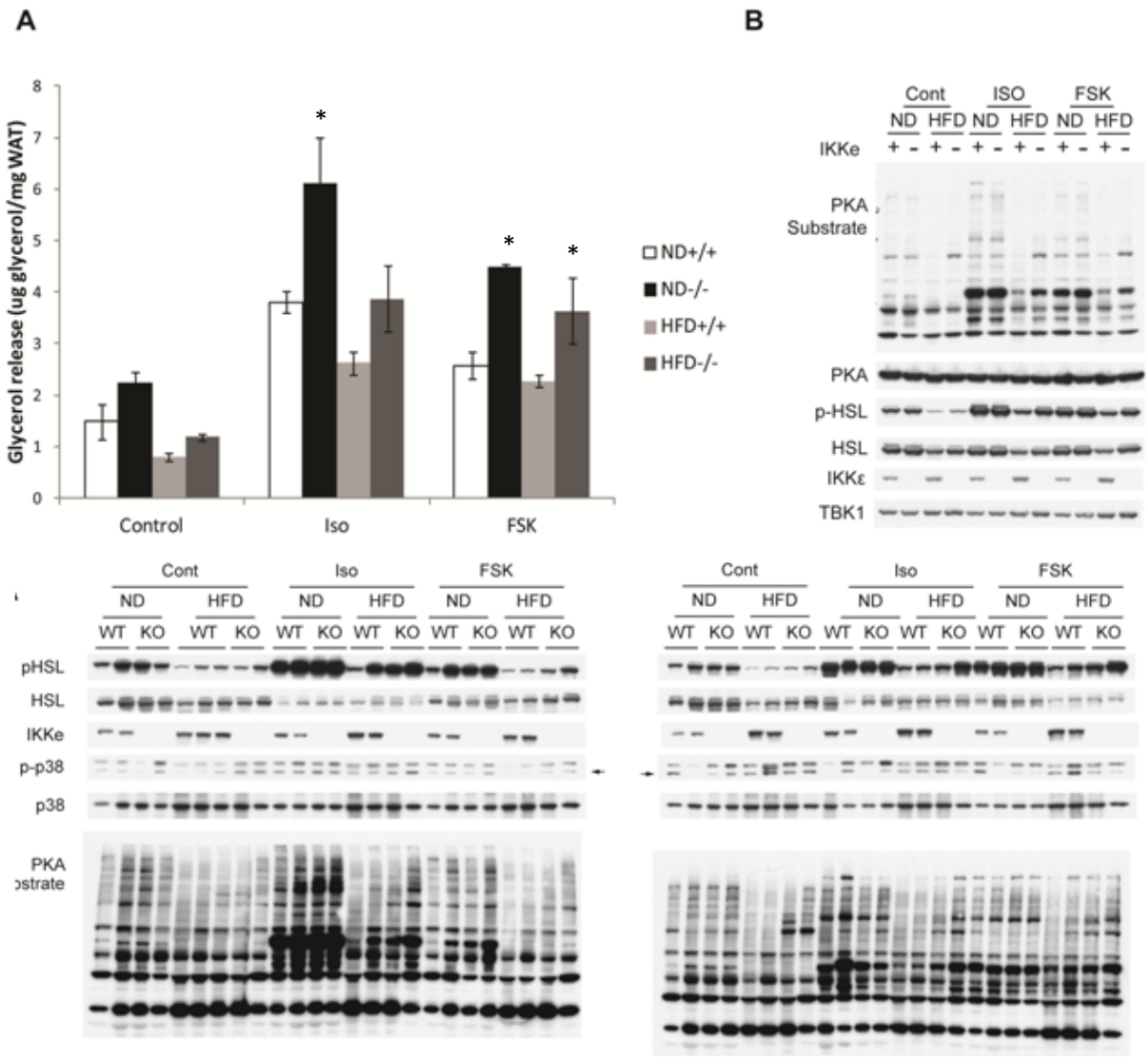

Fig 2.3 IKKε is Required for Decreases in Lipolytic Signaling in White Adipose Tissue (A) Lipolysis from WAT pieces excised from mice fed a high-fat diet treated with isoproterenol or forskolin * p-value <0.05 (B) Western blot from WAT pieces excised from mice fed a high-fat diet treated with isoproterenol or forskolin (Bottom) Western blot from WAT pieces excised from mice fed a high-fat diet treated with isoproterenol or forskolin used for part B.

Mowers J, Unpublished data

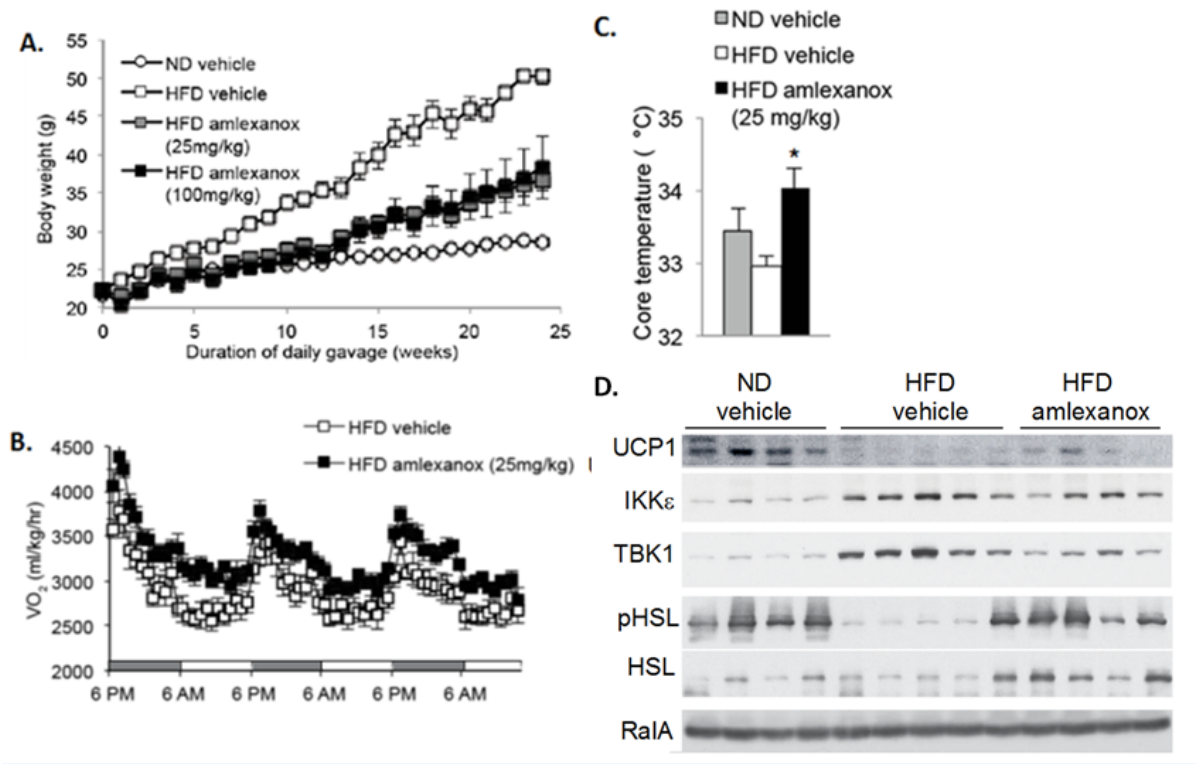

Figure 2.4: Daily Amlexanox Gavage Prevents Diet-induced Obesity. (A) Body weight of preventative group. Mice gavaged with amlexanox at 25 mg/kg (grey squares) or 100 mg/kg (black squares) or vehicle control (white squares = HFD, white circles = ND). Initiation of gavage in the preventative group coincided with high fat diet (HFD) feeding at 8 weeks of age (n=5 per group). (B) Oxygen consumption (VO2) of mice in treatment group; ND (left panel – light grey circles = vehicle, dark grey circles = 25 mg/kg amlexanox) and HFD (right panel – white squares = vehicle, black squares = 25 mg/kg amlexanox). (n=4 for ND groups, n=8 for HFD groups). HFD amlexanox treated mean values are significantly higher than HFD vehicle mean values during all three light and dark cycles, p-value < 0.05. (C) Core body temperature in ND fed mice gavaged with vehicle (grey bar), HFD fed mice gavaged with vehicle (white bar) and HFD fed mice gavaged with 25 mg/kg amlexanox (black bar). * p-value < 0.05 HFD vehicle control versus HFD amlexanox treated or Ob/ob vehicle control versus Ob/ob amlexanox treated. † p-value < 0.05 ND vehicle control versus HFD vehicle control (D) UCP1 protein levels in WAT of preventative and treatment groups. RalA levels are shown as loading controls.

Data published by Dr. Shannon Reilly and Dr. Shian-Huey Chiang (292)

An Inhibitor of TBK1/IKKε Improves Obesity-related Metabolic Dysfunctions

In addition to the IKKε knockout mouse, we described amlexanox, a novel chemical inhibitor of IKKε and TBK1, that reproduces many of the effects observed in the IKKε knockout mouse (292). Much like the IKKε knockout mouse, administration of this compound to mice reduced weight, insulin resistance, inflammation and steatosis in three different obese mouse models. These effects are seen within 3-4 weeks after starting drug therapy, and are reversible. They are likely attributed to increased energy expenditure. Importantly, signaling pathways that modulate these processes are similarly affected *in vitro* by addition of amlexanox or other structurally unrelated IKKε and TBK1 inhibitors to cultured adipocytes.

Amlexanox is a selective inhibitor of IKKε and TBK1

Amlexanox is a selective inhibitor of IKKε and TBK1. Since deletion of the IKKε gene in mice produced partial resistance to the effects of high fat diet (288), our lab screened a library of 150,000 chemical compounds to search for inhibitors of IKKε, using recombinant baculo-viral expressed, purified full length IKKε, with myelin basic protein as substrate, and identified amlexanox as the only verifiable high affinity inhibitor of IKKε within the entire library (data not shown). This previously discovered drug of unknown mechanism is used to treat asthma, allergic rhinitis and aphthous ulcers (296).

Mice Gavaged with Amlexanox Display Decreased Weight Gain and Increased Energy Expenditure on a High-fat Diet

Amlexanox prevents weight gain and causes weight loss when administered to genetic or diet-induced obese mice. Because knockout studies previously showed that deletion of the IKKε gene partially reduces the effects of high fat diet in mice (288), we

assessed the *in vivo* effects of amlexanox of mice on a high-fat diet. C57Bl/6 mice were given a diet of 45% fat, and subject to daily gavage with a vehicle control, 25 or 100 mg/kg amlexanox. Weights of the mice were monitored (figure 2.4A). Normal chow-fed mice on vehicle gavage were used as a lean control. Treatment of animals with either dose of amlexanox prevented the weight gain produced by high fat diet; drug-treated mice maintained weights equivalent to those of control diet mice throughout 12 weeks. Interestingly, there was no effect of the drug on food intake, either at the beginning or end of the study (data not shown).

In addition to preventing obesity, it was important to examine whether amlexanox could be used as a *bona fide* weight loss drug. To determine whether treatment of animals with amlexanox could produce weight loss after obesity had been established, we fed mice a 45% fat diet for 12 weeks, and then treated them with 25 mg/kg amlexanox or vehicle control for 3 weeks (data not shown). Amlexanox produced a 10 gram weight loss after only 4 weeks of treatment, with no further effect thereafter. Moreover, escalation of the dose at this point was without further effect on weight. To determine whether the effects of the drug were reversible, we withdrew the drug after 8 weeks of treatment and then continued mice on vehicle control. Mice quickly regained the weight that had been lost, returning to control weights after 6-8 weeks. Weight loss during the treatment phase was accompanied by more than a 6 gram reduction in overall mass of adipose tissue. Not only did these studies establish that IKKε and TBK1 are required for maintaining adiposity, but they also showed that the beneficial effects of amlexanox were lost when the drug treatment ceased.

Because there was no effect of amlexanox on food intake (data not shown), we reasoned that the weight loss was due to increased energy expenditure. We thus used metabolic cages to monitor energy expenditure in high-fat diet mice treated with or without amlexanox. Four-week treatment with 25 mg/kg amlexanox resulted in significantly increased oxygen consumption as compared to vehicle control, which is consistent with an increase in energy expenditure (Figure 2.4B). The respiratory quotient was similar between mice fed a high-fat diet with or without amlexanox treatment (data not shown). Therefore, differences in adiposity cannot be explained by differences in substrate preference.

These data suggested that amlexanox might induce an increase in thermogenesis. Amlexanox treatment produced an approximate one degree increase in body temperature compared to HFD vehicle-treated mice (Figure 2.4C). The levels of UCP-1 protein were also increased in the adipose tissue of amlexanox-treated mice as compared to HFD vehicle-treated controls in both the treatment and prevention groups of mice (Figure 2.4D). In adipose tissue from HFD-fed mice, hormone sensitive lipase phosphorylation was reduced, consistent with the well-established desensitization of the β-adrenergic pathway in this tissue during obesity. Interestingly, amlexanox treatment prevented the reduction in HSL phosphorylation associated with HFD (Figure 2.4D).

Hyperinsulinemic-euglycemic clamp studies revealed that free fatty acid levels in amlexanox treated animals were higher than untreated animals (data not shown). However, the anti-lipolytic effect of insulin on serum free fatty acid levels was more profound in amlexanox treated animals, suggesting improved insulin sensitivity.

Effects of Amlexanox on 3T3-L1 Adipocytes

The mixed phenotype of increased lipolysis and increased insulin sensitivity led us to examine which of these effects are present in cell culture. Treating 3T3-L1 adipocytes with amlexanox increased lipolysis in a dose dependent manner (data not shown). Interestingly, high doses of amlexanox were able to override the anti-lipolytic effects of insulin. Moreover, amlexanox increased oxygen consumption in 3T3-L1 adipocytes to the same degree that forskolin does (data not shown). By using an inhibitor structurally unrelated to amlexanox, CAY10576 (297), we showed that IKKε and TBK1 were required for insulin stimulated glucose uptake (data not shown). This result was also repeated with amlexanox (Maeran Uhm, unpublished data). Therefore, there is more data to suggest that IKKε and TBK1 are required to suppress lipolysis and promote anabolic pathways, as amlexanox treatment of 3T3-L1 adipocytes demonstrate that amlexanox is a lipolytic agent and not an insulin sensitizer. Therefore, we propose that the *in vivo* administration of amlexanox may lead to reduced weight and adiposity by increasing lipolysis and that the insulin sensitization is likely a secondary effect of increased energy expenditure.

Since inhibitors of IKKε and TBK1 promote lipolysis, we examined 3T3-L1 adipocytes in an IKKε and TBK1 inflammatory context to see if IKKε and TBK1 were required to decrease lipolytic signaling. 3T3-L1 adipocytes treated with TNFα for 24 hours dose dependently increased IKKε expression and TBK1 phosphorylation (Figure 2.5 left). PPARγ levels also decreased in a dose dependent manner, similar to several reports (289). Interestingly, amlexanox rescued isoproterenol-induced phosphorylation

of hormone sensitive lipase in 3T3-L1 adipocytes treated with TNFα for 24 hours to induce IKKε expression and TBK1 activity (Figure 2.5 right).

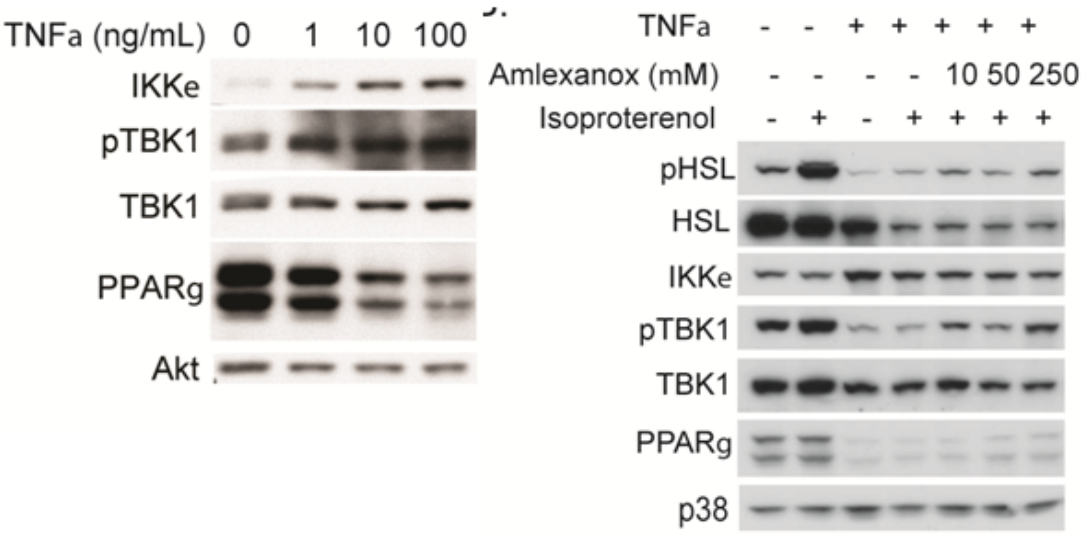

Figure 2.5 IKKε and TBK1 are induced by TNFα and Decrease β-adrenergic signaling (Left) Western blot of 3T3L1 adipocyte treated with different doses of TNFα for 24 hours (Right) Western blot of 3T3L1 adipocyte treated with 50ng/ml of TNFα for 24 hours followed by 1 hour pretreatment of different doses of amlexanox, then 15 minutes with 10μM isoproterenol

Inhibitors of IKKε and TBK1 Promote Adipogenesis in 3T3-L1 Adipocytes

The above studies done in our lab showed that IKKε genetic deletion or pharmacologic inhibition of IKKε and TBK1 using amlexanox resulted in increased energy expenditure, as measured by oxygen consumption. Surprisingly, the IKKε knockout mice have increased adipocyte numbers in their fat pads (288). Adipocyte hyperplasia exists in IKKε knockout mice despite the knockout mice being leaner. The adipocytes from IKKε knockout mouse were smaller than wild-type adipocytes, which agrees with the improved metabolic health of the animals. However, the increased adipocyte number is counterintuitive for a lean mouse, as adipocyte hyperplasia normally occurs in obese animals (298). High fat diet promotes hyperplasia when adipocyte hypertrophy is insufficient to store excess calories from overnutrition. The signals that trigger proliferation of preadipocytes are not fully understood.

Studies in 3T3-L1 adipocytes have emphasized a role for cAMP early in adipocyte differentiation (153). cAMP stimulates CREB early in adipocyte differentiation to result in C/EBPβ expression (154). Wnt signaling inhibits adipocyte differentiation 3T3-L1 cells by suppressing PPARγ and C/EBPα expression (147). cAMP results in methylation of the Wnt10b, preventing Wnt10b expression (155). The ability of cAMP to promote C/EBPβ expression and downregulate Wnt10b are partly responsible for the initiation of adipogenesis.

Since adipogenesis requires cAMP in early stages of adipocyte differentiation, we hypothesized that IKKε may inhibit adipogenesis by downregulating cAMP levels. To address this hypothesis, we treated 3T3-L1 fibroblasts with inhibitors of IKKε and TBK1 substituted for IBMX during the early stage of 3T3-L1 adipocyte differentiation. Inhibitors

of IKKε and TBK1 with different chemical structures were able to increase 3T3-L1 differentiation in a dose dependent manner as shown by oil red O staining (Figure 2.6A) and bright field microscopy (data not shown), whereas these compounds were toxic to cells at doses ten times higher than the optimal differentiation concentration (data not shown). These studies indicate that inhibitors of IKKε and TBK1 may upregulate adipocyte differentiation by increasing cAMP.

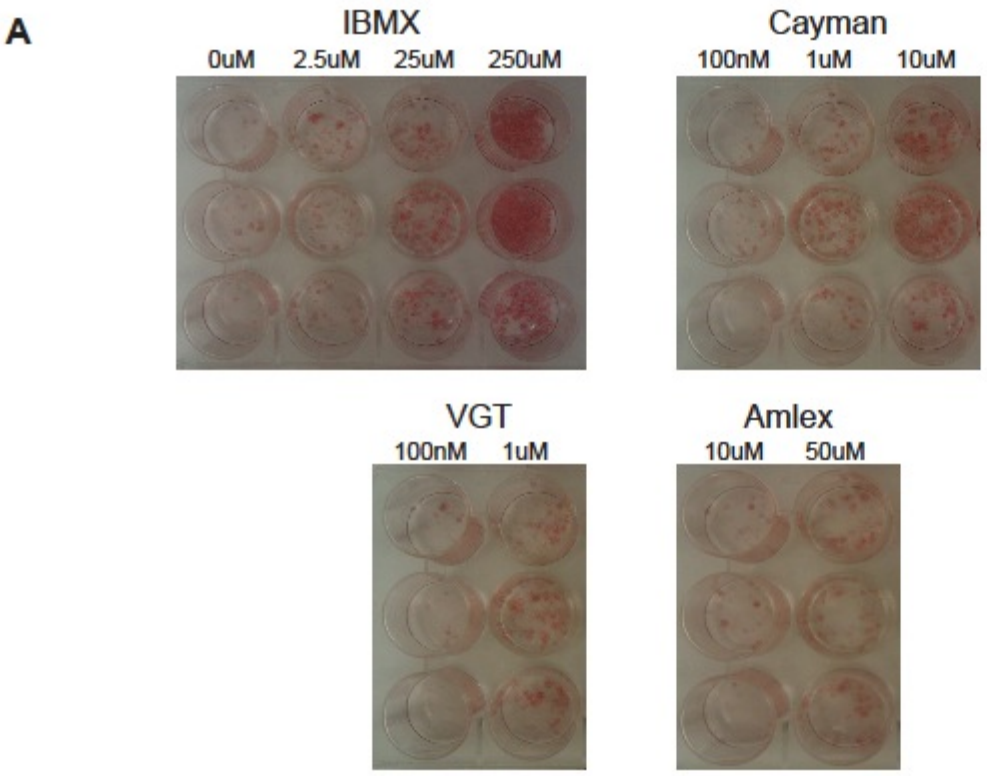

Fig 2.6: Inhibitors of noncanonical IKKs Substitute for IBMX in 3T3-L1 Differentiation (B) Oil red O staining of 3T3-L1 adipocytes differentiated with IBMX or with the TBK1/IKKe inhibitors Cay10576, VGT, or Amlexanox

Discussion

The phenotypes of the IKKε knockout mice and the amlexanox treated mice converge on a similar phenotype. Both the IKKε knockout mouse and the amlexanox treated mice have reduced weight gain, systemic inflammation, hepatic steatosis, and insulin resistance on a high-fat diet compared to wild type or vehicle gavaged mice, respectively. The consistent phenotypes of both genetic ablation and pharmacologic inhibition *in vivo* suggest the same mechanism may govern both phenotypes.

Due to the long time course of obesity development, as well as the many comorbid phenotypes of obesity, it is difficult to establish the definitive cause-and-effect sequence of events that control the development of obesity and insulin sensitivity in the IKKε knockout and amlexanox treated mice. It is possible that the amelioration of systemic inflammation prevents metabolic dysfunction in a variety of tissues. However, it is more likely that the decreases in systemic inflammation in the IKKε knockout and amlexanox-treated mice are secondary to the decreased weight gain. The improvements seen in hepatic steatosis may also be secondary to weight reduction in the IKKε knockout and amlexanox treated mice. Improved insulin sensitivity in the IKKε knockout and amlexanox treated mice is almost certainly not the singular primary effect resulting in weight reduction, because insulin is a powerful anabolic hormone. However, we cannot rule out that improvements in hepatic steatosis, insulin sensitivity, or systemic inflammation may be responsible for weight reduction.

This was the first time IKKε or TBK1 were observed in adipose tissue since the initial study that characterized its expression pattern across many tissues (271). The

increased expression of IKKε and TBK1 in adipose tissue were somewhat expected because NFκB is known to be involved in adipose tissue inflammation (255), and NFκB is known to increase IKKε expression (275). The dramatic increase in IKKε levels in isolated adipocytes over other tissues implies that the phenotype of the knockout may be mediated by adipocytes. This is important because inflammation in adipose tissue due to high fat feeding has been linked with macrophage and liver function as well; however, transcriptional regulation of IKKε in macrophages or liver was not nearly as robust as it was in adipocytes.

In addition to increased transcription of IKKε, protein levels and kinase activity were also increased in adipose tissue on a high fat diet (Fig 2.1C,D). Subsequent studies showed that high fat diet also induced protein levels of TBK1 in adipose tissue (data not shown), and that both IKKε and TBK1 were upregulated in brown adipose tissue on a high fat diet (data not shown). IKK family members are activated by phosphorylation on activation loop serine residues. Whereas high fat diet increases IKKε kinase activity immunoprecipitated from adipose tissue, activation of IKKε kinase activity is not dramatically upregulated when normalized to total immunoprecipitated protein. Instead, IKKε activity correlates with IKKε protein induction. Therefore, IKKε protein levels serve as an indicator of kinase activity in the context of diet-induced obesity in adipose tissue.

Crosstalk between adipose tissue and infiltrating macrophages is an active area of research (299). Interestingly, mice bearing a macrophage-specific knockout of IKKβ are insulin sensitive on a high fat diet, suggesting that insulin resistance in adipose tissue is dependent on IKKβ action in macrophages (300). Since IKKβ is upstream of

many macrophage proinflammatory cytokines, such as TNFα, it is tempting to suggest that macrophages release TNFα, which in turn stimulates the NFκB pathway in adipocytes to upregulate IKKε and TBK1 (275).

What is the role of IKKε and TBK1 in adipose tissue? IKKε and TBK1 were initially characterized as activators of NFκB due to their ability to phosphorylate IκB *in vitro* (290). However, the current model of IKKε and TBK1 action is quite different. Recent studies highlight the crosstalk that exists in IKK family signaling (276). It is now thought that IKKε and TBK1 may be involved in a feedback loop to attenuate NFκB by reducing the activation of IKKβ.

IKKε and TBK1 may influence inflammation in adipose tissue in a manner similar to immunologic tissues. The common perspective in obesity is that inflammation, mediated partly by NFκB, in adipose tissue is detrimental to human health because it promotes insulin resistance, leading to type 2 diabetes and the cardiovascular complications that accompany chronic high blood sugar (255). Since dogma within the field partially attributes insulin resistance to NFκB inflammation in adipose tissue (255), inhibition of IKKε action in adipose tissue could potentially result in greater NFκB activation and, therefore, more insulin resistance. However, that is not the phenotype we observe in the IKKε knockout mouse, which has decreased inflammatory markers both systemically and in adipose tissue with decreased insulin resistance.

Other studies have called into question the role of NFκB in adipose tissue. Constitutive activation of IKKβ in adipose tissue prevents diet-induced obesity in mice (301). Surprisingly, transgenic expression of the NFκB protein p65 in adipose tissue led

to increased insulin sensitivity, which was attributed to improvements in body weight via increased energy expenditure (302). In contrast to the IKKε knockout mouse or inhibitor studies of IKKε and TBK1, constitutive adipose expression of p65 led to a defect in adipogenesis both *in vivo* and *in vitro*. Although these transgenic systems may not represent physiologic activation of the IKKβ—NFκB system, these studies do not support the notion that NFκB promotes obesity. Instead, IKKε and TBK1 may inhibit IKKβ to decrease NFκB and promote obesity.

Interestingly, administration of amlexanox led to weight reduction both before and after the onset of obesity. Amlexanox appears to be a relatively safe drug with long history of use in patients with asthma, allergic rhinitis and aphthous ulcers (303). As such, there might be an interesting opportunity for repurposing this agent for diabetes and obesity. Furthermore, sustained treatment using amlexanox may be necessary to maintain its beneficial effects. While not providing a permanent solution to obesity, treatment with amlexanox may be part of a series of sustained therapeutic interventions to combat obesity. Future clinical studies will be needed to explore this possibility and to validate the hypothesis that these noncanonical IκB kinases contribute to counter-inflammatory actions that sustain metabolic disease.

Although the precise mechanisms by which IKKε and TBK1 promote obesity in rodents remain to be completely elucidated, most of the evidence points to an important role of IKKε and TBK1 in decreasing energy expenditure while increasing fat storage. We propose that IKKε and TBK1 inhibit sympathetic activation of adipose tissue. Decreased sympathetic activation of adipose tissue due to impaired catecholamine activation or sensitivity has been observed in obese patients (26, 36, 99, 304). Obesity

is commonly associated with blunted whole-body catecholamine-induced lipolysis (99). This is thought to occur through a number of mechanisms, including leptin resistance (234), as well as the reduced expression of β (36) or increased expression of α_2 adrenergic receptors (295). White adipose tissue and cultured isolated adipocytes from obese human and mouse models exhibit decreased cAMP-stimulated lipolysis and fat oxidation, due to reduced energy expenditure from decreased mitochondrial uncoupling (294). Desensitization to adrenergic activation is also a feature of childhood onset obesity (28, 29), and has also been observed in adipocytes from first-degree relatives of obese subjects (30).

The IKKε knockout and amlexanox treatment phenocopy traits from mice treated with β-agonists or exposed to cold temperatures (165). Elevated energy expenditure in these mice suggest increased sympathetic activation, as does increased core body temperatures and UCP1 levels in adipose tissue. Interestingly, *ex vivo* forskolin treatment of adipose tissue from mice on a high fat diet suggest that defects in β-adrenergic signaling and PKA activation exist beyond the level of the β-adrenergic receptor.

This series of studies also demonstrates that IKKε and TBK1 inhibit adipocyte differentiation. Increased adipogenesis in 3T3-L1 differentiation correlates well with the adipocyte hyperplasia observed in the IKKε knockout mouse (288). The ability of IKKε and TBK1 inhibitors to substitute for IBMX in adipogenesis suggest that IKKε and TBK1 repress cAMP. One possibility is that induction of IKKε and TBK1 serve to reduce levels of cAMP, which is important for the suppression of Wnts and upregulation of the adipogenic factors PPARγ, C/EBPα, and C/EBPβ (147).

In summary, we demonstrated that IKKε and TBK1 suppress energy expenditure and β-adrenergic signaling both *in vivo* and *in vitro* in adipocytes. We investigate the mechanism by which IKKε and TBK1 suppresses cAMP levels in the following chapter.

Materials and Methods

Reagents. All chemicals were obtained from Sigma-Aldrich unless stated otherwise. Anti-IKKε, anti-TBK1, Phospho-TBK1 (ser172), anti-HSL, phospho-HSL (ser563 or ser660), and anti-PPARγ antibodies were purchased from Cell Signaling. Anti-RalA antibody was obtained from BD Bioscience. Anti-flag antibody was obtained from Sigma. Anti-UCP1 antibody was obtained from Alpha Diagnostics. Enhanced chemiluminescence (ECL) reagents were purchased from NEN, Inc. EDTA-free protease inhibitor tablet was purchased from Roche, Inc. Amlexanox was purchased from Ontario Chemical Inc. (Guelph, Ontario, Canada). TBK1/IKKε inhibitor CAY10576 was purchased from Cayman Chemical (Ann Arbor, MI).

Animals and animal care. Wild type male C57BL/6 mice were fed a high fat diet consisting of 45% of calories from fat (D12451 Research Diets Inc.) starting at 8 weeks of age for 12-24 weeks, while normal diet C57BL/6 controls were maintained on normal chow diet consisting of 4.5% fat (5002 Lab Diet). For the prevention groups, amlexanox (25 mg/kg or 100 mg/kg) administration was begun concurrently with HFD feeding at 8 weeks of age. For the treatment groups, 25 mg/kg amlexanox treatment was begun at 20 weeks of age after 12 weeks of HFD. Animals were housed in a specific pathogen-free facility with a 12-hour light/12-hour dark cycle and given free access to food and water. All animal use was in compliance with the Institute of Laboratory Animal Research Guide for the Care and Use of Laboratory Animals and approved by the University Committee on Use and Care of Animals at the University of Michigan and UCSD.

Energy expenditure and respiratory quotient. C57Bl6 mice in the amlexanox treatment group were placed in metabolic cages. The University of Michigan Animal Metabolic Phenotyping Core measured oxygen consumption (VO2), carbon dioxide production (VCO2) and spontaneous motor activity during 3 consecutive days using the Comprehensive Laboratory Monitoring System (CLAMS, Columbus Instruments), an integrated open-circuit calorimeter equipped with an optical beam activity monitoring system. The respiratory quotient was calculated by dividing carbon dioxide production by oxygen consumption. The mean values for light and dark cycles were used to analyze statistical significance..

Core body temperature. Rectal temperature measurements were performed using a YSI 4600 Precision thermometer (YSI, Inc., Yellow Springs, OH).

Cell culture and transfection. 3T3-L1 fibroblasts (American Type Culture Collection, Manassas, Virginia) were cultured and differentiated as described previously (305). Cells were routinely used within 7 days after completion of the differentiation process; only cultures in which >90% of cells displayed adipocyte morphology were used.

Western analysis. Tissues were homogenized in lysis buffer (50mM Tris, pH7.5, 5mM EDTA, 250mM sucrose, 1% NP40, 2mM DTT, 1mM sodium vanadate, 100mM NaF, 10mM Na4P2O7, and freshly added protease inhibitor tablet), then incubated for one hour at 4 °C (288). Crude lysates were then centrifuged at 14,000 x g for 15 minutes twice and the protein concentration was determined using BioRad Protein Assay Reagent. Samples were diluted in sodium dodecyl sulfate (SDS) sample buffer. Bound proteins were resolved by SDS-polyacrylamide gel electrophoresis and transferred to

nitrocellulose membranes (BioRad). Individual proteins were detected with the specific antibodies and visualized on film using horseradish peroxidase-conjugated secondary antibodies (BioRad) and Western Lightning Enhanced Chemiluminescence (Perkin Elmer Life Sciences).

IKKε and TBK1 immune-complex kinase assay. Liver and White adipose tissues were collected from C57BL/6 mice on normal chow or high fat diet. Tissues were homogenized using Dounce homogenizer with lysis buffer containing 50 mM Tris (pH7.5), 150 mM NaCl, 2 mM EDTA, 5 mM NaF, 25 mM β-glycerophosphate, 1 mM sodium orthovanadate, 10% glycerol, 1% TritonX-100, 1 mM DTT, and 1 mM PMSF in the presence of protease inhibitors (Roche Diagnostics). Tissue cell lysates were incubated for 1 hour at 4˚C and cleared by spinning at 13,000 rpm for 15 minutes at 4˚C in a table-top centrifuge. Each 1 mg of lysate was subjected to immunoprecipitation using 5 µl of rabbit-polyclonal antibody against TBK1 or IKKε for 1.5 hours at 4˚C. Immunocomplexes were harvested by incubation with Protein A beads (Roche Diagnostics) for 2 hours at 4˚C. Immunoprecipitates were extensively washed once with lysis buffer and three times with wash buffer containing 20 mM HEPES (pH 7.4), 50 mM NaCl, 20 mM β-glycerophosphate, 1 mM sodium orthovanadate, 5 mM NaF, 10 mM MgCl2, and 1 mM DTT. An *in vitro* kinase assay using the immunoprecipitated kinases was performed as described above. Relative levels of MBP phosphorylation were detected by autoradiograph and normalized to the levels of IKKε or TBK1 kinase detected in the immunoprecipitate by immunoblotting.

Chapter III:
Inflammation Produces Catecholamine Resistance in Obesity Via Activation of PDE3B by the Protein Kinases IKKε and TBK1

Abstract

Obesity produces a chronic inflammatory state involving the NFκB pathway, resulting in persistent elevation of the noncanonical IκB kinases IKKε and TBK1. In this study, we report that these kinases attenuate β-adrenergic signaling in white adipose tissue. Treatment of 3T3-L1 adipocytes with specific inhibitors of these kinases restored β-adrenergic signaling and lipolysis attenuated by TNFα and Poly (I:C). Conversely, overexpression of the kinases reduced induction of Ucp1, lipolysis, cAMP levels, and phosphorylation of hormone sensitive lipase in response to isoproterenol or forskolin. Noncanonical IKKs reduce catecholamine sensitivity by phosphorylating and activating the major adipocyte phosphodiesterase PDE3B. In vivo inhibition of these kinases by treatment of obese mice with the drug amlexanox reversed obesity-induced catecholamine resistance, and restored PKA signaling in response to injection of a β-3 adrenergic agonist. These studies suggest that by reducing production of cAMP in adipocytes, IKKε and TBK1 may contribute to the repression of energy expenditure during obesity.

Introduction

Obesity generates a state of chronic, low-grade inflammation in liver and adipose tissue accompanied by macrophage infiltration and the local secretion of inflammatory cytokines and chemokines that attenuate insulin action, resulting in insulin resistance and the subsequent development of Type 2 diabetes (1, 255, 256, 299). Numerous studies indicate a strong correlation between inflammation and insulin resistance across several populations (1). Moreover, genetic ablation or pharmacological inhibition of inflammatory pathways can dissociate obesity from insulin resistance (1, 255), suggesting that local inflammation can be a key step in the generation of insulin resistance.

The transcription factor NFκB and its inflammatory program play an important role in the development of insulin resistance in obese liver and adipose tissue (288, 300, 306, 307). NFκB is activated by the IκB kinase (IKK) family, which has four members: IKKα, IKKβ, IKKε, and TBK1. IKKα and IKKβ act with the scaffolding partner NEMO to activate NFκB (259). Although pharmacologic inhibition or genetic ablation of IKKβ defined a role for this kinase in insulin resistance (300, 307), the roles of the noncanonical kinases IKKε and TBK1 are less certain.

We recently reported that both mRNA and protein expression levels of IKKε and TBK1 are increased in adipose tissue from mice fed a high fat diet (288). Both of these kinases are increased as a consequence of the inflammatory program in obesity (292), and contain NFκB regulatory sites in their promoter regions, allowing them to be induced upon NFκB activation (308). Deletion of the IKKε gene rendered mice partially resistant to some of the deleterious effects of high fat feeding, including weight gain,

insulin resistance, hepatic steatosis, and systemic inflammation (288). We report, in this study, that IKKε and TBK1 can desensitize lipolytic signaling in white adipose tissue in response to β-adrenergic agonists by phosphorylating and increasing the activity of PDE3B, in the process decreasing cAMP levels. Thus, induction of these noncanonical IκB kinases might contribute to catecholamine resistance during obesity, and blocking their activity has the potential to increase energy expenditure as an anti-obesity and anti-diabetes therapy.

Results

IKKε and TBK1 Overexpression Decrease Sensitivity to the β-adrenergic/cAMP Pathway in 3T3-L1 Adipocytes

Sympathetic activation of adipose tissue plays a key role in maintaining energy balance by stimulating lipolysis and fat oxidation (27). Activation of β-adrenergic signaling by either β-adrenergic agonists or cold exposure in white and brown adipose tissue initiates a cascade of events through cyclic AMP (cAMP), culminating in the transcriptional upregulation of Ucp1, which results in increased proton leak and energy expenditure (168). Our previous studies revealed that compared to wild-type (WT) controls, IKKε-deficient mice exhibited increased energy expenditure while on a high fat diet (HFD), accompanied by increased expression of Ucp1 in white adipose depots (288). Interestingly, increased energy expenditure in IKKε-deficient mice was only seen in HFD-fed mice (288), suggesting that upon induction of IKKε during obesity, the kinase might repress an increased adaptive thermogenic response to overnutrition. To explore this possibility, we overexpressed IKKε in 3T3-L1 adipocytes and examined Ucp1 gene expression after treatment with the non-selective β-adrenergic agonist, isoproterenol (ISO), or the β3-adrenergic agonist, CL-316,243. Fold difference in Ucp1

gene expression was calculated by normalization of relative Ucp1 mRNA levels in treated relative to control samples. Treatment of empty vector-expressing cells with ISO or CL-316,243 resulted in a 1.6-fold or two-fold increase in Ucp1 mRNA levels, respectively (Figure 3.1A). The induction of Ucp1 gene expression in response to ISO or CL-316,243 was blunted when WT IKKε was overexpressed in these cells. However, expression of the kinase-inactive mutant of IKKε K38A (287) was less effective, but still modestly repressed Ucp1 expression.

In addition to increased Ucp1 expression, IKKε knockout mice also exhibited increased lipolysis and fat oxidation (288), suggesting that decreased lipolysis in adipose tissue from obese mice might result in part from increased expression of IKKε and TBK1 (288). We thus modeled the obesity-dependent increase in the noncanonical IKKs by overexpressing IKKε in 3T3-L1 adipocytes, followed by assay of glycerol release in response to ISO or CL-316,243. Although both isoproterenol and CL-316,243 increased lipolysis in empty vector-expressing cells, overexpression of WT IKKε reduced the lipolytic effects of isoproterenol and CL-316,243 by greater than 40%, and also reduced basal glycerol release (Figure 3.1B). The reduction in lipolysis by IKKε overexpression was accompanied by dramatically reduced phosphorylation of HSL and perilipin in response to ISO or CL-316,243 (Figure 3.1C). Expression of the catalytically inactive kinase was less effective in blocking lipolytic signaling, although the levels of protein achieved by overexpression were lower compared to the WT kinase (Figure 3.1B,C). Overexpression of TBK1 reduced phosphorylation of HSL in response to isoproterenol or the adenylyl cyclase activator, forskolin (Figure 3.1—figure supplement 1B). Identical results were obtained when IKKε was overexpressed in 3T3-L1

adipocytes stimulated with forskolin (Figure 3.1D), as detected by western blotting with an anti-phospho-PKA substrate motif antibody. Overexpression of IKKε also repressed the phosphorylation of p38 (p-p38) in response to forskolin (Figure 3.1D) or isoproterenol (Figure 3.1—figure supplement 1A), whereas overexpression of IKKε K38A was without effect (Figure 3.1—figure supplement 1A). While glycerol release is likely the result of changes in HSL and perilipin phosphorylation, it is important to note that we have not directly assayed whether re-esterification of glycerol intermediates are also affected. Taken together, these data suggest that similar to what is observed in obesity, overexpression of IKKε or TBK1 can repress lipolytic signaling. The partial effectiveness of the kinase-inactive mutants is puzzling, but may reflect their activation of endogenous IKKε or TBK1 kinases due to dimerization (309).

Since PKA signaling is responsible for Ucp1 induction in response to catecholamines (175, 310), we explored the possibility that both IKKε and TBK1 might reduce β-adrenergic sensitivity of adipocytes by decreasing cAMP levels. IKKε overexpression in 3T3-L1 adipocytes reduced by greater than 80% the increase in cAMP levels produced by both isoproterenol and forskolin, whereas overexpression of IKKε K38A did not (Figure 3.1E). Previous studies have shown that decreased sensitivity to adrenergic stimuli in adipose tissue can result from reduced β-adrenergic receptors (36) or increased expression of α2-adrenergic receptors (295). These studies represent the first demonstration that defects distal to the adrenergic receptor may also contribute to catecholamine resistance, and suggest that IKKε and TBK1 can attenuate the β-adrenergic/cAMP pathway in response to β-adrenergic stimuli in adipocytes in a cell-autonomous manner, and further that induction of these kinases during obesity may

account for decreased energy expenditure by reducing sensitivity of adipocytes to β-adrenergic stimulation.

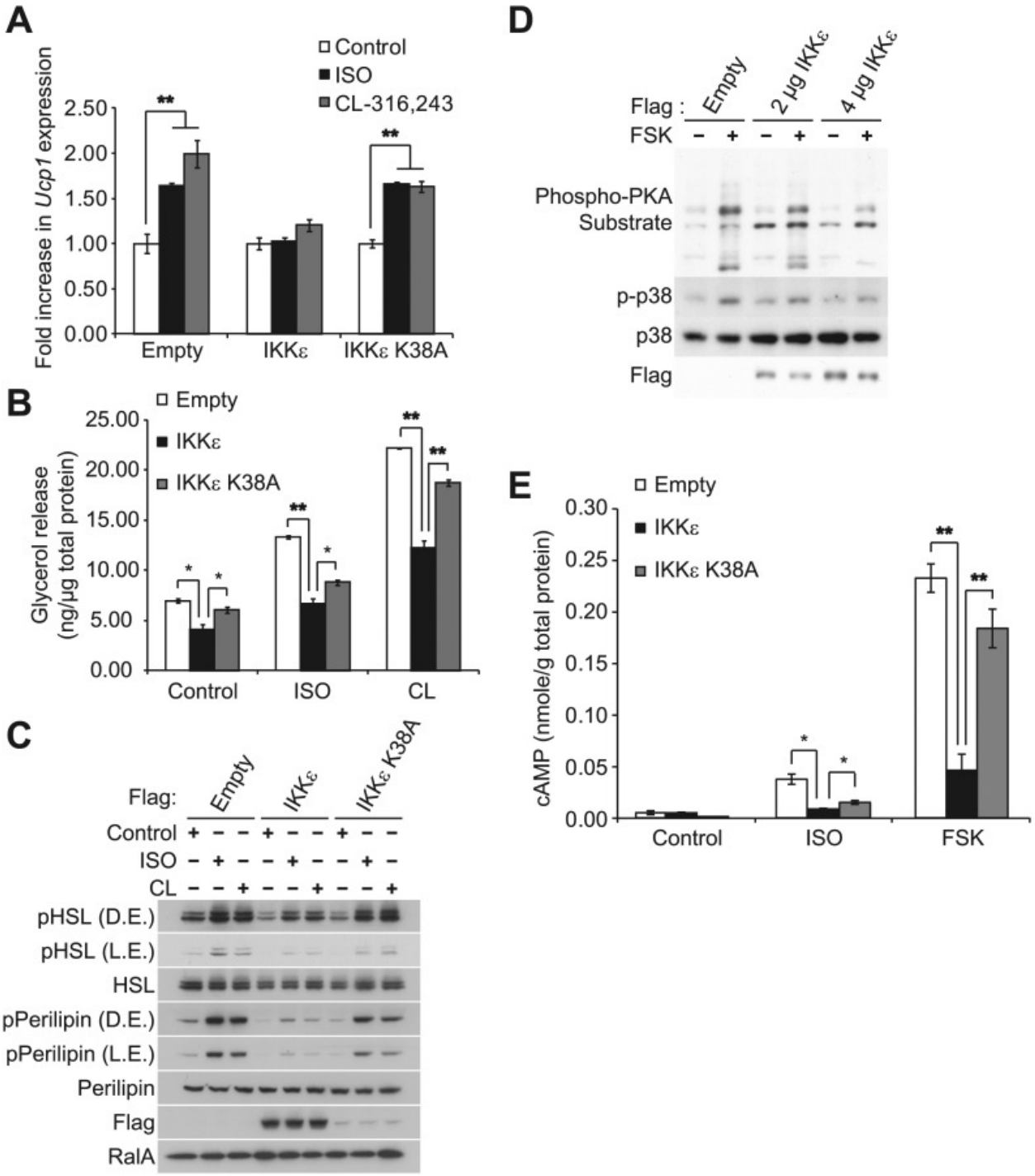

Figure 3.1: IKKε and TBK1 Overexpression Decrease Sensitivity to the β-adrenergic/cAMP pathway in 3T3-L1 adipocytes

(A) Fold increase in Ucp1 expression in 3T3-L1 adipocytes expressing empty vector, Flag-IKKε, or Flag-IKKε K38A following treatment with or without 10 µM ISO (black bars) or 10 µM CL-316,243 (CL, gray bars) for 4 hr. **p<0.01. Performed in triplicate. (B) Glycerol release from 3T3-L1 adipocytes expressing empty vector (white bars),

Flag-IKKε (black bars), or Flag-IKKε K38A (gray bars) treated with or without 10 μM ISO or 10 μM CL. *p<0.05 and **p<0.01. Performed in triplicate. (C) Immunoblots of whole cell lysates from Figure 3.1B. Results were replicated in triplicate. D.E. stands for dark exposure and L.E. stands for light exposure. (D) Immunoblots of whole cell lysates from 3T3-L1 adipocytes expressing empty vector or Flag-IKKε treated with or without 50 μM FSK for 15 min. Results were replicated in multiple experiments. (E) cAMP levels from 3T3-L1 adipocytes expressing empty vector, Flag-IKKε, or Flag-IKKε K38A treated with or without 10 μM ISO or 50 μM FSK for 15 min. **p<0.0001 and *p<0.05. Performed in triplicate.

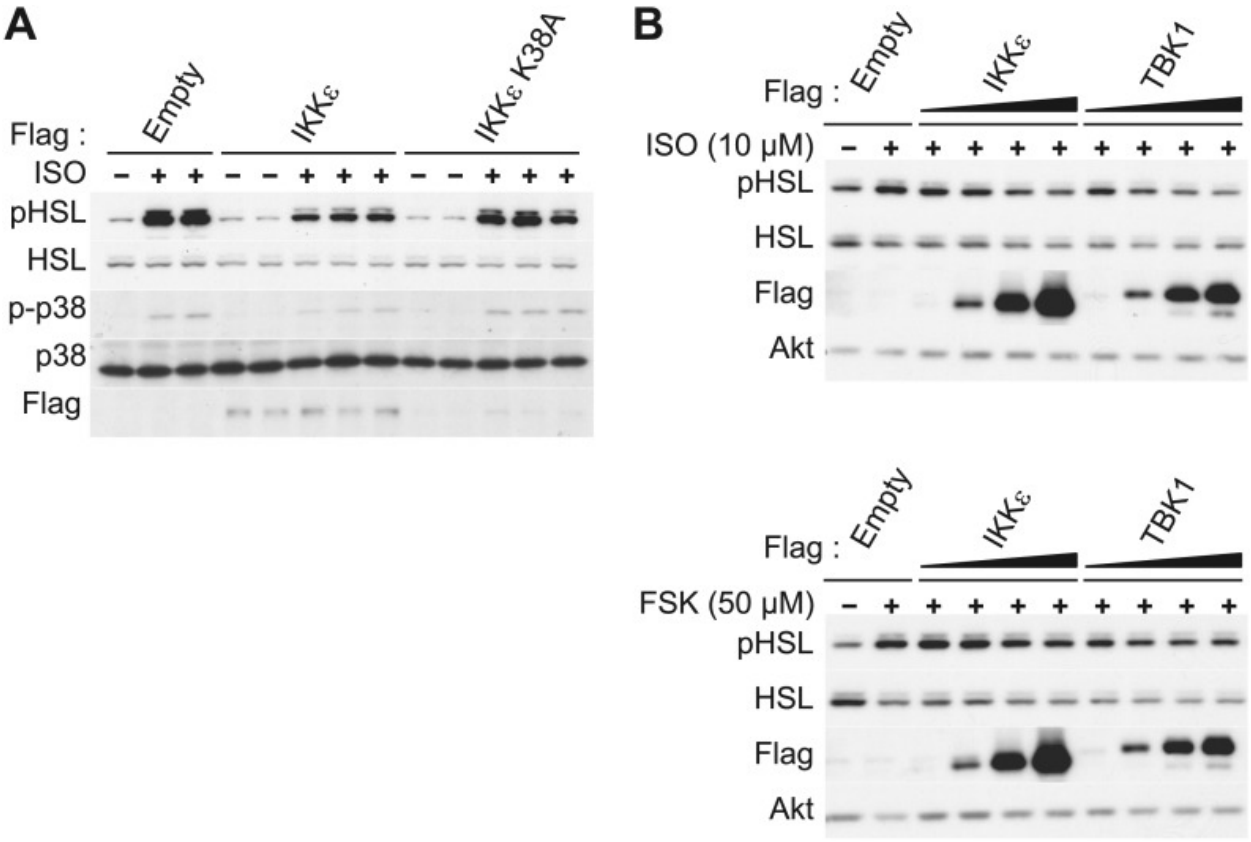

Supplemental Figure 3.1: IKKε and TBK1 Overexpression Decrease Sensitivity to the β-adrenergic/cAMP pathway in 3T3-L1 adipocytes

(A) Immunoblots of whole cell lysates from 3T3-L1 adipocytes expressing empty vector, Flag-IKKε, or Flag-IKKε K38A treated with or without 10 μM ISO for 15 min. Results were replicated in multiple experiments. (B) Immunoblots of whole cell lysates from 3T3-L1 adipocytes expressing increasing amounts of Flag-IKKε or Flag-TBK1 treated with or without 10 μM ISO (top panel) or 50 μM FSK (bottom panel) for 15 min. Results were replicated in multiple experiments.

Prolonged Treatment with TNFα Decreases the Sensitivity of Adipocytes to β-adrenergic Stimulation in a Manner Dependent on the activity of IKKε and TBK1

Obesity is accompanied by infiltration of proinflammatory macrophages into adipose tissue; these cells secrete inflammatory cytokines, such as TNFα, which generate insulin resistance by stimulating catabolic pathways (255, 256). Although TNFα is known to increase lipolysis in adipocytes (311-314), there is also evidence of a counterinflammatory response in obesity that may serve to repress energy expenditure (292, 315-317). We thus used TNFα to model the inflammatory milieu of obese adipose tissue in cell culture to determine whether the cytokine might also regulate β-adrenergic signaling in this context. While short-term treatment with TNFα augmented the increase in cAMP produced by forskolin treatment, this effect declined after 12 hr. After 24 hr of exposure, TNFα inhibited the production of the second messenger produced by forskolin (Figure 3.2—figure supplement 1A). Thus, the catabolic effects of the proinflammatory cytokine TNFα in adipocytes are transient and followed by an inhibitory phase.

Our previous studies revealed that treatment of 3T3-L1 adipocytes with TNFα for 24 hr induced the expression of IKKε and increased TBK1 phosphorylation at the active site in a manner that was dependent on the activity of IKKβ and the NFκB pathway (292). We thus wondered whether the repression of β-adrenergic sensitivity produced by longer-term treatment with TNFα might be due to increased activity of the noncanonical IKKs. Long-term treatment with TNFα repressed the induction of Ucp1 gene expression in response to β-adrenergic stimuli (Figure 3.2—figure supplement

1B), whereas the expression of IKKε mRNA (Ikbke) was upregulated, as previously reported (292). Treatment of 3T3-L1 adipocytes with TNFα for 24 hr decreased glycerol release in response to both isoproterenol and forskolin in a dose-dependent manner (Figure 3.2A). TNFα treatment also decreased isoproterenol- and forskolin-stimulated cAMP production; an effect that was largely rescued by preincubation of cells with the selective, but structurally unrelated inhibitors of IKKε and TBK1, amlexanox (Figure 3.2B) (292) or CAY10576 (Figure 3.2C) (297).

Isoproterenol-stimulated β-adrenergic signaling was also decreased by treatment of cells with TNFα (Figure 3.2D), as manifested by decreased phosphorylation of HSL, perilipin, and other proteins recognized by the PKA substrate motif antibody, whereas IKKε expression was concurrently upregulated and TBK1 phosphorylation was increased by the treatment with TNFα. Pretreatment of 3T3-L1 adipocytes with amlexanox also blocked the inhibitory effect of TNFα on isoproterenol-stimulated β-adrenergic signaling, as determined by western blotting with an anti-phospho-PKA substrate motif antibody, anti-phospho-HSL, and anti-phospho-perilipin antibodies (Figure 3.2E). Interestingly, phosphorylation of p38 in response to isoproterenol was also dramatically augmented by amlexanox in a dose-dependent manner. Previous studies showed that the toll-like receptor 3 (TLR3) agonist, Poly (I:C), results in the direct activation of IKKε and TBK1 (274, 276, 277, 282). Similar to TNFα, treatment of 3T3-L1 adipocytes with Poly (I:C) simultaneously reduced stimulation of cAMP production, lipolysis and phosphorylation in response to β-adrenergic stimulation (Figure 3.2—figure supplement 1C–E), and the inhibitory effects of Poly (I:C) on the sensitivity to isoproterenol stimulation were partially restored by amlexanox pretreatment, but not

to the extent that was observed with TNFα treatment (Figure 3.2E). It is possible that Poly (I:C)-induced desensitization of β-adrenergic pathway engages other pathways that are not directly regulated by IKKε and TBK1. These results suggest that obesity-associated inflammation leads to the activation of IKKε and TBK1, which produces reduced sensitivity of adipocytes to β-adrenergic stimulation.

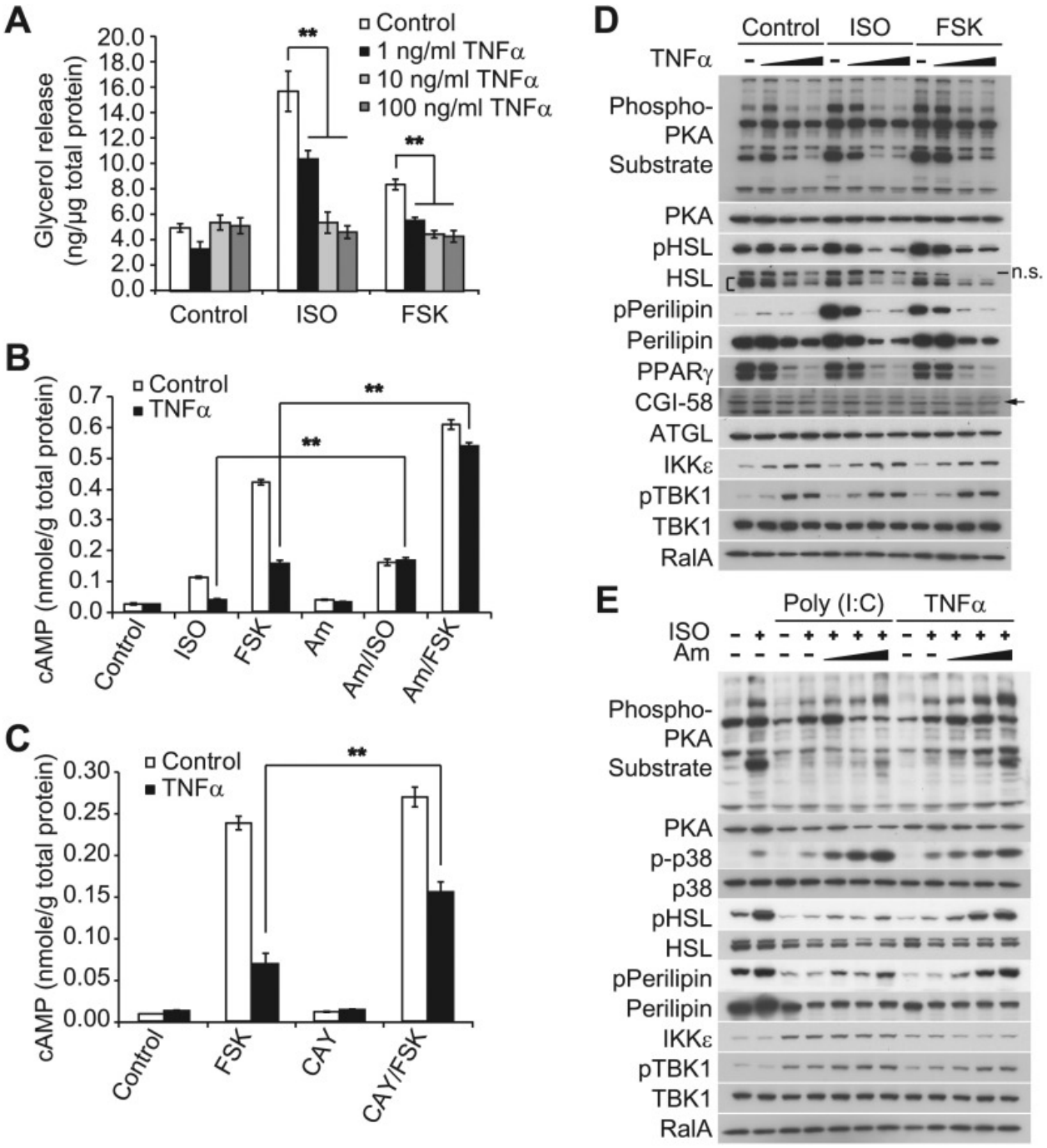

Figure 3.2: Prolonged Treatment with TNFα decreases the sensitivity of adipocytes to β-adrenergic stimulation in a manner dependent on the activity of IKKε and TBK1

(A) Glycerol release from 3T3-L1 adipocytes treated with or without different concentrations of TNFα as indicated for 24 hr followed by treatment with or without 10 µM ISO or 50 µM FSK. **p<0.0001. Performed in quadruplicate. (B) cAMP levels from 3T3-L1 adipocytes treated with or without 100 ng/ml TNFα for 24 hr followed by

treatment with or without 10 μM ISO or 50 μM FSK in the presence or absence of pretreatment of 50 μM Amlexanox (Am). **p<0.0001. Performed in quadruplicate. (C) cAMP levels from 3T3-L1 adipocytes treated with or without 100 ng/ml TNFα for 24 hr followed by treatment with or without 50 μM FSK in the presence or absence of pretreatment of 1 μM CAY10576 (CAY). **p<0.0001. Performed in triplicate. (D) Immunoblots of whole cell lysates from 3T3-L1 adipocytes treated with or without different concentrations of TNFα as same as Figure 3.2A for 24 hr followed by treatment with or without 10 μM ISO or 50 μM FSK. Results were replicated in multiple experiments. '[' indicates total HSL. 'n.s.' represents non-specific band. Arrow indicates CGI-58. (E) Immunoblots of whole cell lysates from 3T3-L1 adipocytes treated with or without 50 ng/ml TNFα or 100 μg/ml poly (I:C) for 24 hr followed by treatment with or without 10 μM ISO for 15 min in the presence or absence of pretreatment with increasing concentrations (0, 10, 50, and 200 μM) of amlexanox for 30 min. Results were replicated in multiple experiments.

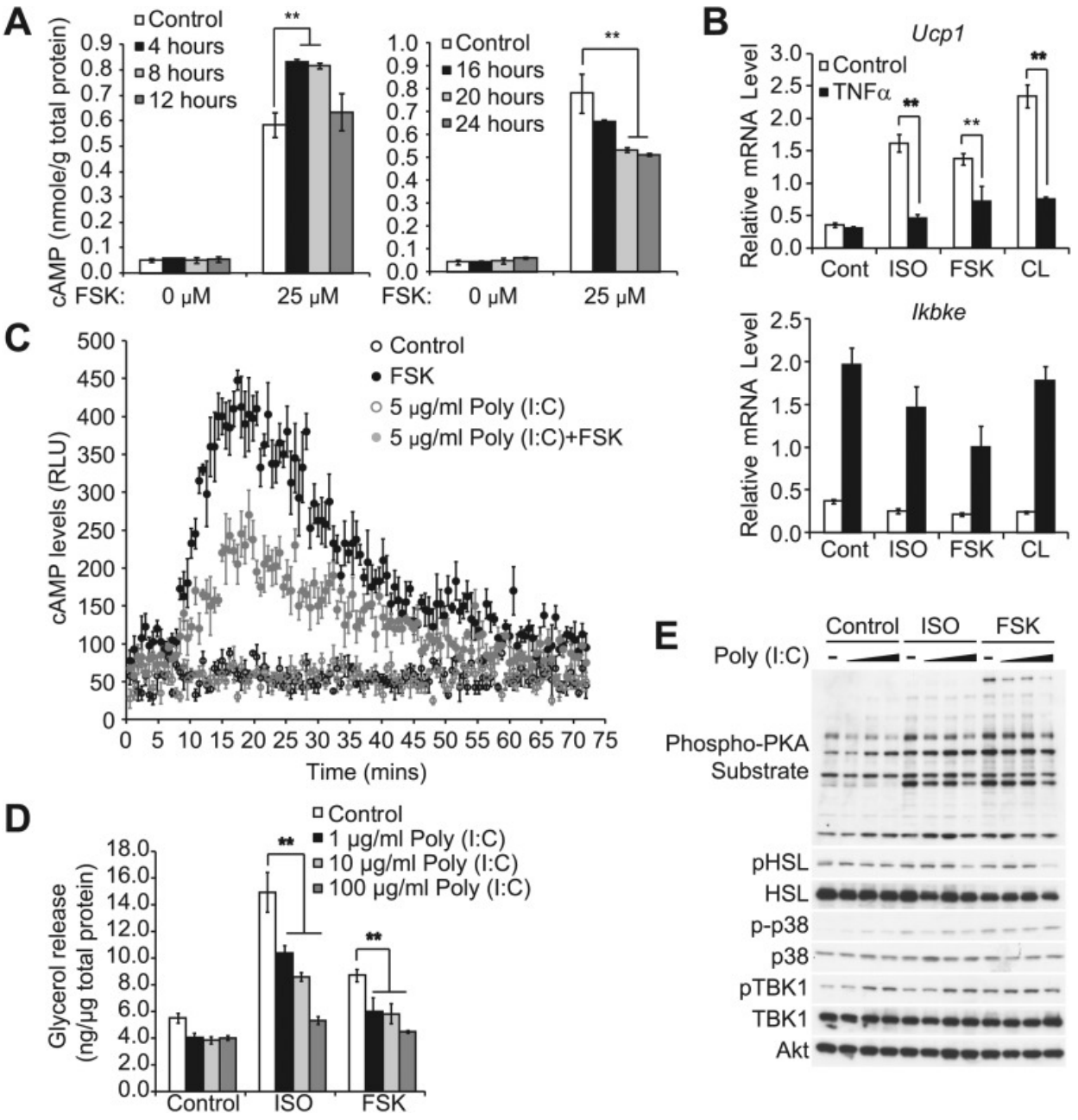

Supplemental Figure 3.2: Prolonged Treatment of inflammatory cytokines decreases the sensitivity of adipocytes to β-adrenergic stimulation

(A) cAMP levels from 3T3-L1 adipocytes treated with or without 100 ng/ml TNFα for the indicated amount of time (left panel: 0–12 hr, right panel: 0–24 hr) followed by treatment with or without 25 μM FSK. **p<0.01. Performed in duplicate. (B) Relative gene expression (top panel: Ucp1, bottom panel: Ikbke) in 3T3-L1 adipocytes treated with or without 100 ng/ml TNFα for 24 hr followed by treatment with or without 10 μM ISO or 50 μM FSK, or 10 μM CL-316,243 for 4 hrs. **P<0.01 and **p<0.0001. Performed in tripilicate. (C) cAMP levels as measured by Glosensor from 3T3-L1 adipocytes treated

with or without 5 μg/ml poly (I:C) for 24 hr followed by treatment with or without 50 μM FSK over the course of 75 min. Performed in triplicate. (D) Glycerol release from 3T3-L1 adipocytes treated with or without different concentrations of poly (I:C) as indicated for 24 hr followed by treatment with or without 10 μM ISO or 50 μM FSK. **p<0.0001. Performed in quadruplicate. (E) Immunoblots of whole cell lysates from 3T3-L1 adipocytes treated with or without different concentrations of poly (I:C) as same as Figure 3.2—figure supplement 1D for 24 hr followed by treatment with or without 10 μM ISO or 50 μM FSK. Results were replicated in multiple experiments.

IKKε and TBK1 Reduce cAMP Levels Through Activation of PDE3B

cAMP levels can also be regulated by phosphodiesterases, which cleave the second messenger and in the process dampen cAMP-dependent signals. Phosphodiesterase 3B (PDE3B) is the major PDE isoform expressed in adipocytes (130). Genetic ablation or pharmacological inhibition of PDE3B in cells and in vivo revealed an important role for the enzyme in lipid and glucose metabolism (121, 138, 139). Phosphorylation and activation of PDE3B by insulin in adipocytes is thought to be mediated by Akt, and cAMP itself acts as a negative feedback regulator of its own levels by promoting PKA-dependent phosphorylation and activation of PDE3B (121).

Since we observed that cAMP production was impaired in forskolin or isoproterenol-stimulated 3T3-L1 adipocytes overexpressing IKKε (Figure 3.1E), we examined whether noncanonical IKKs might desensitize adrenergic stimulation through increased activity of PDE3B in adipocytes. Pretreatment with a nonspecific phosphodiesterase inhibitor, IBMX, in 3T3-L1 adipocytes expressing IKKε or TBK1 rescued the full stimulation of cAMP production in response to forskolin (Figure 3.3A). Interestingly, the selective PDE3B and PDE4 inhibitor, Zardaverine (318), also blocked the inhibitory effects of IKKε and TBK1 overexpression on cAMP levels in response to isoproterenol and forskolin in 3T3-L1 adipocytes (Figure 3.3B), suggesting an important role for PDE3B as a target of the noncanonical IKKs.

We next examined whether IKKε and TBK1 directly phosphorylate PDE3B to regulate cAMP levels. Recombinant TBK1, Akt and PKA were incubated in vitro with [γ-32P]ATP and purified PDE3B as a substrate. Phosphorylation was assessed by SDS-

PAGE followed by autoradiography. TBK1 directly catalyzed the phosphorylation of PDE3B; phosphorylation was also produced by incubation with Akt and PKA, as previously reported (137, 319) (Figure 3.3C). IKKε also catalyzed this phosphorylation in vitro (data not shown). This increase in phosphorylation produced by in vitro incubation with TBK1, IKKε and PKA was also detected when PDE3B was blotted with antibodies that recognize the 14-3-3 binding motif (Figure 3.3—figure supplement 1A). When purified PDE3B was incubated with the same amount of recombinant TBK1 and canonical IKKβ kinases in vitro, phosphorylation of PDE3B by IKKβ was barely detectable, indicating a level of specificity in which PDE3B is a better target of the noncanonical IKKs (Figure 3.3—figure supplement 1B). This phosphorylation was dose-dependent with respect to ATP (Figure 3.3—figure supplement 1C).

To determine whether IKKε can phosphorylate PDE3B in cells, we co-expressed IKKε and its inactive mutant K38A with HA-tagged PDE3B in HEK293T cells, followed by immunoprecipitation (IP) with anti-HA antibodies. Expression of IKKε in cells caused a shift in electrophoretic mobility of PDE3B, and this shift was not detected when IKKε K38A was expressed (Figure 3.3—figure supplement 1D). Phosphorylation of PDE3B was also detected after expression of IKKε but not its kinase-inactive mutant K38A in cells, as detected by blotting with antibodies that recognize the 14-3-3 binding motif. To determine whether this molecular shift was dependent on phosphorylation of PDE3B, HA-PDE3B was co-expressed in Cos-1 cells along with IKKε, TBK1 or their kinase inactive mutants, and HA immunoprecipitates were treated with or without calf intestinal phosphatase (CIP). Expression of both of the wild-type kinases reduced the electrophoretic mobility of PDE3B, which could be reversed by treatment with the

phosphatase (Figure 3.3D, compare lane 3, 7 to lane 4, 8). Neither of the kinase-inactive mutants had an effect (Figure 3.3D, compare lane 5, 9 to lane 6, 10).

Previous studies suggested that IKKε and TBK1 bind to their respective substrates through a sequence that includes a ubiquitin-like domain (ULD) proximal to their kinase domain. This domain is highly conserved among the IKK family members, and is 49% identical between IKKε and TBK1 (320, 321). To confirm that PDE3B is a bona fide substrate of IKKε and TBK1, we prepared a GST-ULD domain fusion protein from TBK1 and incubated this fusion protein with 3T3-L1 adipocyte lysates. The fusion protein specifically precipitated endogenous PDE3B from these lysates (Figure 3.3—figure supplement 1E). To explore further the interaction of these two proteins, we co-expressed WT TBK1 and its K38A mutant with HA-tagged PDE3B in HEK293T cells, and immunoprecipitated the protein with anti-HA antibodies. Kinase-inactive TBK1 was preferentially co-immunoprecipitated with PDE3B, whereas the interaction of PDE3B with WT TBK1 was barely detectable (Figure 3.3—figure supplement 1F). These data suggest that TBK1 and IKKε associate with substrates such as PDE3B, and subsequently dissociate upon phosphorylation.

Next, to test further the role of PDE3B phosphorylation by IKKε and TBK1 in initiating its interaction with 14-3-3β, we prepared a GST-14-3-3β fusion protein which was incubated with lysates from HEK293T cells co-expressing TBK1 with PDE3B. PDE3B was preferentially pulled down by GST-14-3-3β after phosphorylation by TBK1 but not by its inactive K38A mutant, whereas GST beads alone enriched neither PDE3B nor its phosphorylated form (Figure 3.3E).

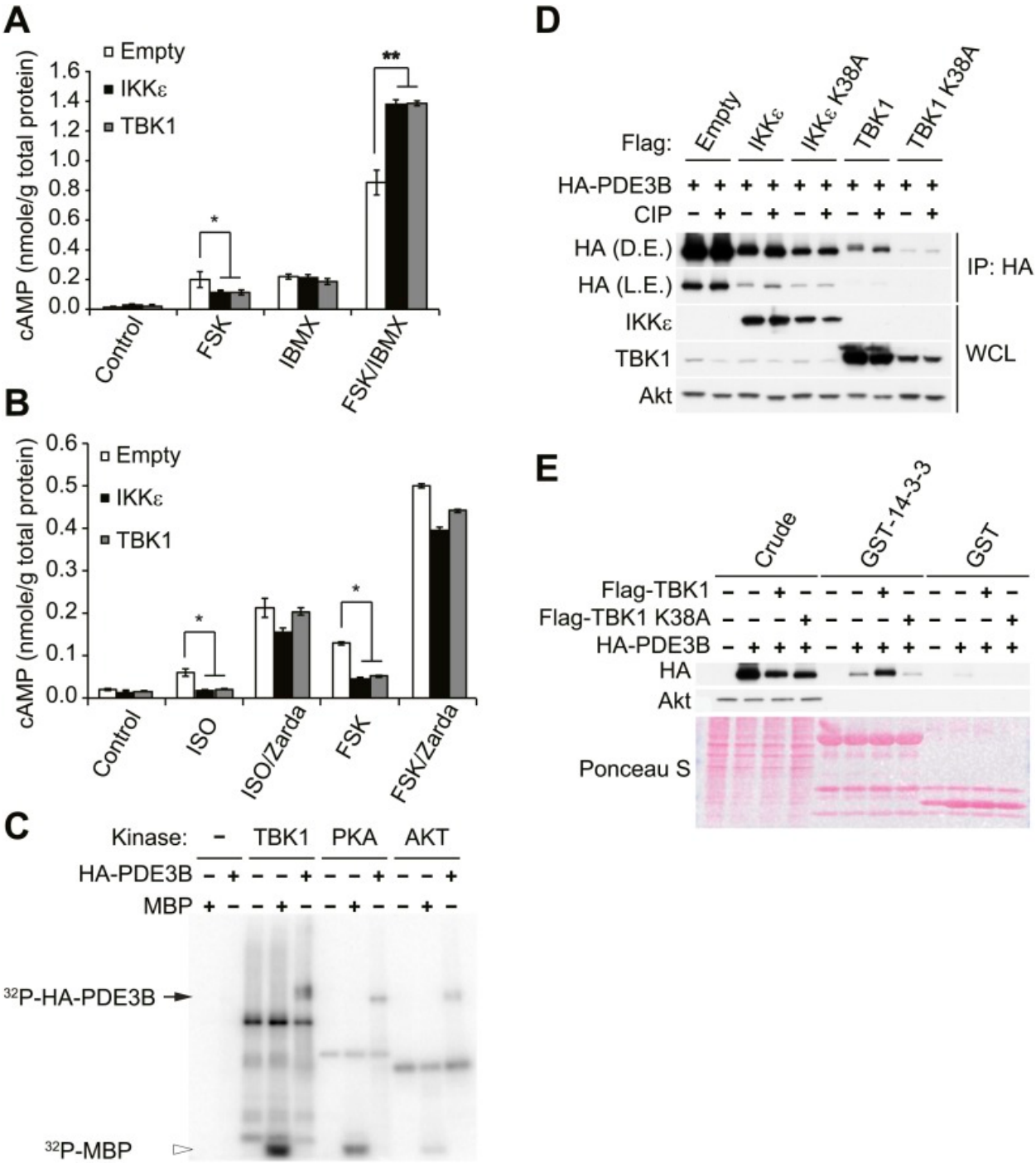

Figure 3.3: IKKε and TBK1 reduce cAMP through activation of PDE3B

(A) cAMP levels from 3T3-L1 adipocytes expressing empty vector, Flag-IKKε, or Flag-TBK1 treated with or without 50 μM FSK, 250 μM IBMX, or together for 15 min. *p<0.05 and **p<0.0001. Performed in duplicate. (B) cAMP levels from 3T3-L1 adipocytes expressing empty vector, Flag-IKKε, or Flag-TBK1 treated with or without 10 μM ISO or 50 μM FSK together with or without 10 μM Zardaverine (Zarda) for 15 min. *p<0.05.

Performed in duplicate. (C) 32P phospho-image of in vitro kinase reaction using either immunoprecipitated HA-PDE3B from HEK293T cells or 1 μg MBP (myelin basic protein) as a substrate with recombinant kinases as indicated. Results were replicated in multiple experiments. (D) Immunoblots of immunoprecipitation with anti-HA antibodies followed by treatment with or without CIP (top panel) and whole cell lysates (bottom panel) from Cos-1 cells co-expressing HA-PDE3B with Flag-IKKε/TBK1 or Flag-IKKε/TBK1 K38A. D.E. stands for dark exposure and L.E. stands for light exposure. Results were replicated in multiple experiments. (E) Immunoblots of GST-14-3-3 pulldown from HEK293T cells co-expressing HA-PDE3B with Flag-TBK1 or Flag-TBK1 K38A. Ponceau S staining shows the amount of beads used in GST-14-3-3 pulldown. Results were replicated in multiple experiments.

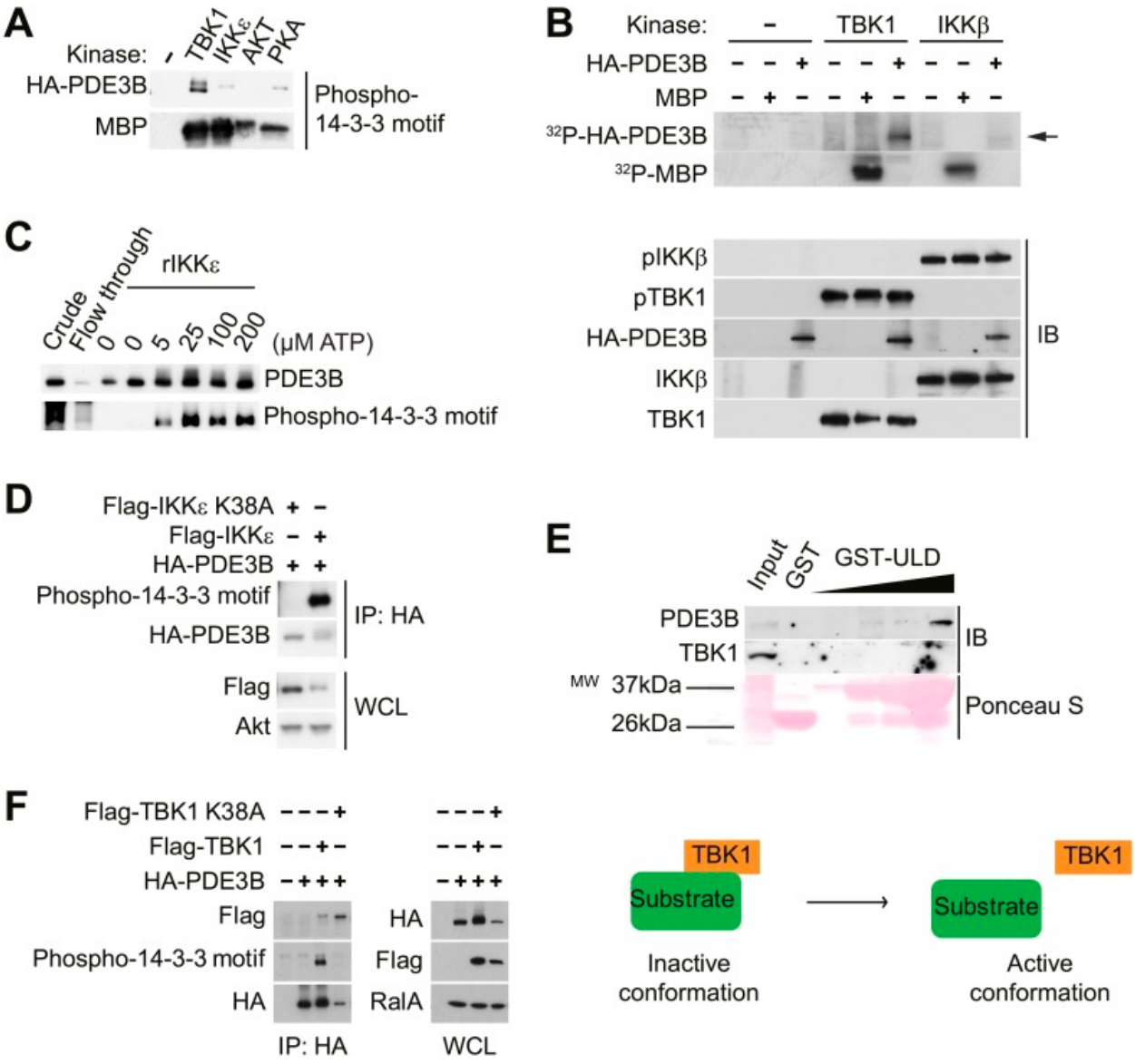

Supplemental Figure 3.3: IKKε and TBK1 interact with PDE3B in a manner dependent on the activity of IKKε and TBK1

(A) Immunoblots of in vitro kinase reaction using either immunoprecipitated HA-PDE3B from HEK293T cells or 1 μg MBP (myelin basic protein) as a substrate with recombinant kinases as indicated. Results were replicated in multiple experiments. (B) Top panel: 32P phospho-image of in vitro kinase reaction using either immunoprecipitated HA-PDE3B from HEK293T cells or 1 μg MBP as a substrate with recombinant kinases as indicated. Bottom panel: Immunoblots (IB) of in vitro kinase reaction. Results were replicated in multiple experiments. (C) Immunoblots of in vitro kinase reaction using immunoprecipitated HA-PDE3B from HEK293T cells as a substrate with recombinant MBP-IKKε kinase (rIKKε) using increasing amounts of ATP as indicated. Lane 1: Whole cell lysates from HEK293T cells expressing HA-PDE3B, Lane 2: IP flow-through, Lane

3: IP without rIKKε. Results were replicated in multiple experiments. (D) Immunoblots of immunoprecipitation with anti-HA antibodies (top panel) and whole cell lysates (WCL, bottom panel) from HEK293T cells co-expressing HA-PDE3B with Flag-IKKε or Flag-IKKε K38A. Results were replicated in multiple experiments. (E) Immunoblots of GST-TBK1 ULD pulldown from 3T3-L1 adipocytes. Ponceau S staining shows the amount of beads used in GST-TBK1 ULD pulldown. Results were replicated in multiple experiments. (F) Immunoblots of immunoprecipitation with anti-HA antibodies (left panel) and whole cell lysates (right panel) from HEK293T cells co-expressing HA-PDE3B with Flag-TBK1 or Flag-TBK1 K38A. Results were replicated in multiple experiments. The schematic model suggests that TBK1 associates with its substrates in an inactive conformation and subsequently dissociate upon phosphorylation in an active conformation.

IKKε and TBK1 Phosphorylate PDE3B at serine 318, Resulting in the Binding of 14-3-3β

To evaluate the regulatory role of PDE3B phosphorylation by IKKε and TBK1, we determined which sites are phosphorylated. HA-PDE3B was co-expressed in Cos-1 cells with IKKε and TBK1, and phosphorylated PDE3B was enriched by IP with anti-HA antibodies. Phosphorylation sites on human PDE3B were then determined by LC-MS/MS mass spectrometry. This analysis revealed that serines 22, 299, 318, 381, 463, 467, and 503 were phosphorylated by both kinases; there were no differences between the kinases (Figure 3.4A). Interestingly, the phosphorylation profile of PDE3B matched neither known Akt or PKA profiles (133). However, phosphorylation on serine 299 and serine 318 had previously been identified on mouse PDE3B (residues equivalent to Serine 277 and 296 in mouse PDE3B) in adipocytes and hepatocytes in response to both insulin and forskolin (133).

While several serine residues are known to be phosphorylated on PDE3B in response to stimuli, serine 318 (human) is the best characterized. This residue resides in a consensus phosphorylation sequence for both Akt and PKA, and also serves as a consensus 14-3-3 binding motif once phosphorylated (133, 137). We thus created a Ser318Ala (S318A) mutant of PDE3B, and examined its interaction with a GST-14-3-3β fusion protein or by GST-14-3-3 overlay assay. Interestingly, despite incubation with TBK1, the phospho-defective, S318A mutant of PDE3B, did not specifically interact with GST-14-3-3β, whereas the wild-type protein did (Figure 3.4B,C). In a GST pull-down assay, the molecular shift of PDE3B S318A was still detected by western blot (Figure 3.4B), indicating that phosphorylation of PDE3B by TBK1 on other sites still occurred, but were not crucial for 14-3-3β binding.

To examine the functional importance of the phosphorylation of PDE3B at Serine 318, we overexpressed WT PDE3B and its S318A mutant in 3T3-L1 adipocytes, and tested the response of the cells to TNFα. Overexpression of WT PDE3B in cells reduced the attenuation of forskolin-stimulated cAMP production and phosphorylation of HSL produced by TNFα, whereas PDE3B S318A was ineffective (Figure 3.4D, Figure 3.4—figure supplement 1A,B). These data suggest that although IKKε and TBK1 can phosphorylate PDE3B on several sites, serine 318 may be particularly important in the regulation of phosphodiesterase function by promoting the interaction between PDE3B and 14-3-3β. More importantly, this residue is the major site mediating the negative effects of IKKε and TBK1 on sensitivity of adipocytes to β-adrenergic stimulation.

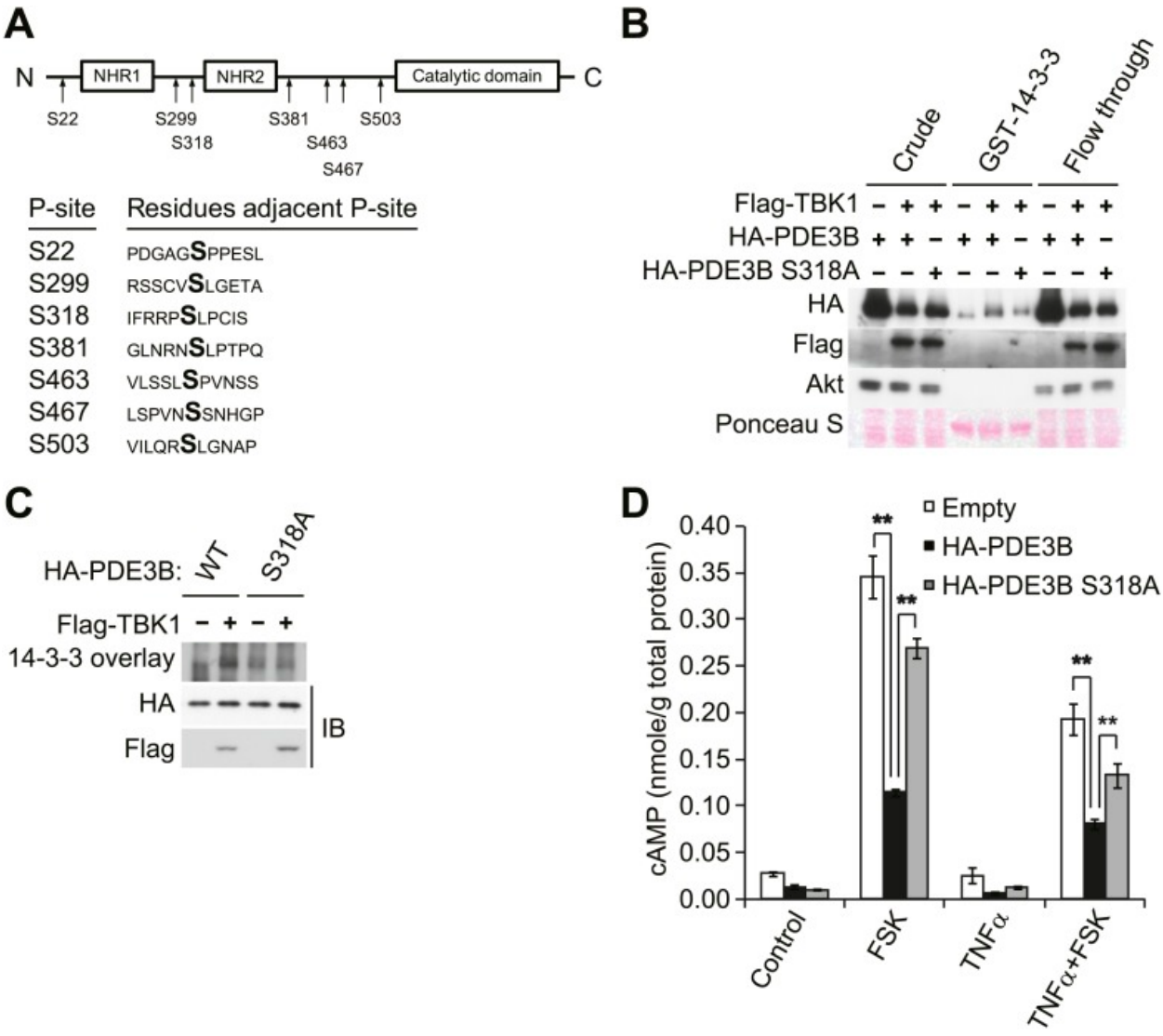

Figure 3.4: IKKε and TBK1 phosphorylate PDE3B at serine 318, resulting in the binding of 14-3-3β

(A) Summary of sites on PDE3B phosphorylated by IKKε or TBK1 (P-sites) from mass spectrometry experiments. (B) Immunoblots of GST-14-3-3 pulldown from HEK293T cells co-expressing HA-PDE3B or HA-PDE3B S318A with Flag-TBK1. Ponceau S staining shows the amount of beads used in GST-14-3-3 pulldown. Results were replicated in multiple experiments. (C) GST-14-3-3 overlay on nitrocellulose membrane (top blot) and an immunoblot (IB) of whole cell lysates from HEK293T cells co-expressing HA-PDE3B or HA-PDE3B S318A with Flag-TBK1 (bottom blot). Results were replicated in multiple experiments. (D) cAMP levels from 3T3-L1 adipocytes expressing empty vector, HA-PDE3B, or HA-PDE3B S318A treated with or without 100 ng/ml TNFα for 16 hr followed by treatment with or without 25 μM FSK for 15 min. **p<0.0001 and **p<0.01. Performed in duplicate.

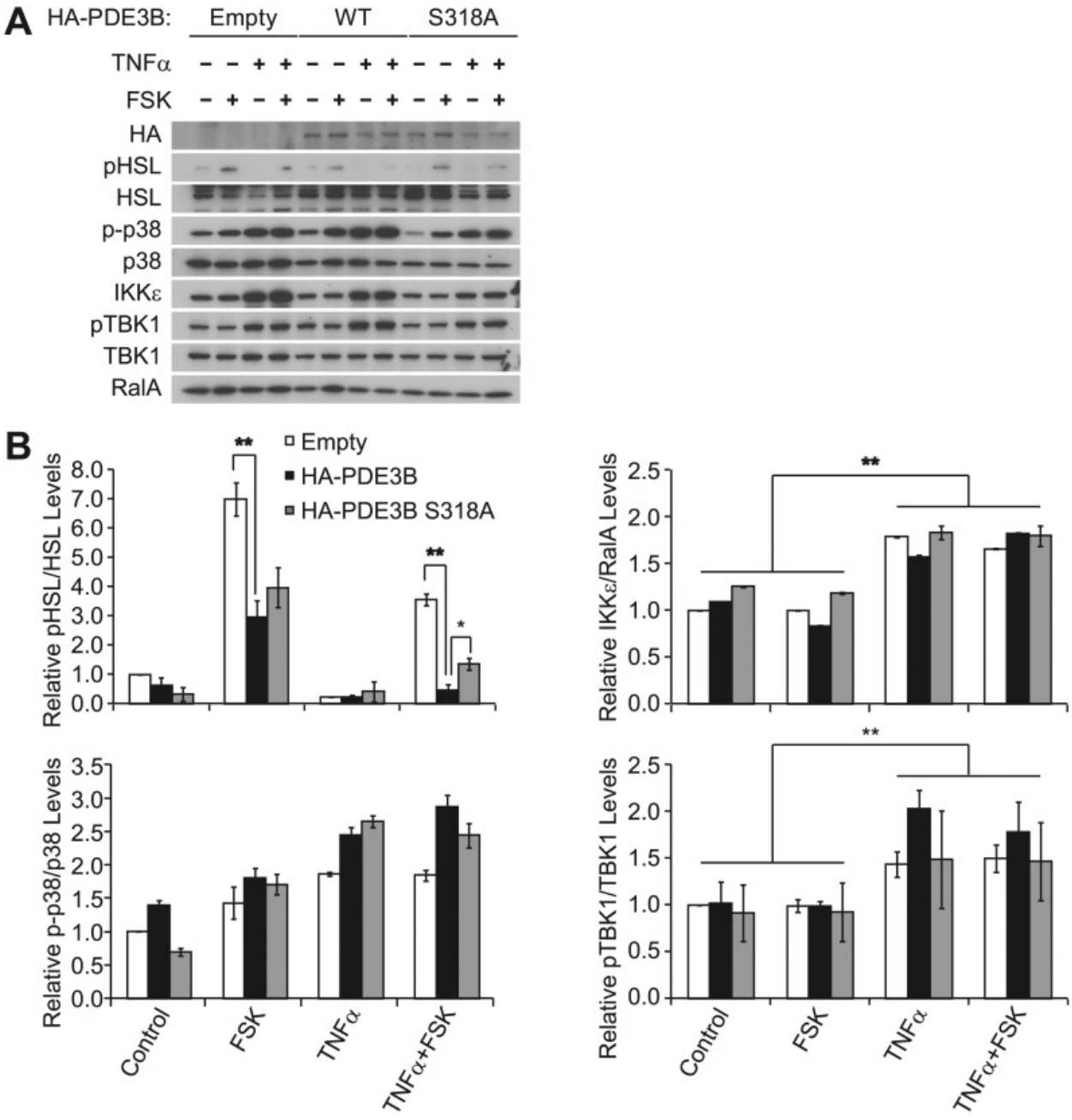

Figure 3.4: Overexpression of PDE3B in 3T3-L1 adipocytes reduces the attenuation of forskolin-stimulated β-adrenergic signaling produced by TNFα.

(A) Immunoblots of whole cell lysates from Figure 3.4D. (B) Top left panel, pHSL and total HSL signals in whole cell lysates were quantified and normalized to the basal signal (lane 1 in Figure 3.4—figure supplement 1A). The normalized pHSL/total HSL ratio is presented as the mean ± SEM of two independent experiments. **p<0.0001 and *p<0.05. Top right panel, quantification of total IKKε and RalA signals in whole cell lysates was performed as described above. **p<0.0001. Bottom left panel, quantification of phospho-p38 (p-p38) and total p38 signals in whole cell lysates was performed as

described above. Bottom right panel, quantification of pTBK1 and total TBK1 signals in whole cell lysated was performed as described above. **p<0.01.

IKKε and TBK1 Phosphorylate PDE3B at serine 318, Resulting in the Binding of 14-3-3β

Disruption of sympathetic activation of lipolysis and fat oxidation may play an important role in the development and maintenance of increased fat storage in obesity. Indeed, while numerous studies have demonstrated catecholamine resistance in obese adipose tissue (28, 36, 322-324), the underlying mechanisms remain unclear. To test the functional importance of the noncanonical IKKs in maintaining energy balance in vivo, we investigated whether the administration of a selective inhibitor of IKKε and TBK1, amlexanox, can reverse diet-induced catecholamine resistance in rodents. We fed mice a high fat or normal diet, treated them with amlexanox by oral gavage for 4 days (prior to the point when weight loss is seen), and then gave a single intraperitoneal (IP) injection of the β3-adrenergic agonist CL-316,243. Injection of CL-316,243 stimulated a threefold increase in serum FFA and glycerol levels in both vehicle and amlexanox-treated mice on normal diet (ND). The effect of CL-316,243 to increase serum FFAs was significantly attenuated in HFD-fed, vehicle-treated mice. However, HFD-fed mice treated with amlexanox responded like normal diet mice, despite the fact that they were weight matched with control HFD-fed mice (Figure 3.5A). The fold increase in serum glycerol levels was also significantly higher in amlexanox-treated HFD mice, as compared to vehicle-treated HFD-fed mice. In addition, ex vivo pretreatment of white adipose tissues from mice on a HFD with amlexanox enhanced glycerol release (Figure 3.5B). This effect was more pronounced in the inguinal fat depot, where amlexanox pretreatment increased phosphorylation of HSL, perilipin, and other proteins recognized by the PKA substrate motif antibody in response to CL-316,243 treatment compared to vehicle-pretreated tissues (Figure 3.5C). Amlexanox

also concurrently increased the phosphorylation of TBK1 at Ser172 due to the relief of feedback inhibition, as previously reported with other inhibitors (282, 292).

To examine whether inhibition of TBK1 and IKKε with amlexanox reverses resistance to catecholamine-induced lipolysis in vivo by increasing stimulation of cAMP production, we measured cAMP levels in epididymal adipose tissue from mice on HFD after CL-316,243 IP injection. Interestingly, levels of cAMP were increased after CL-316,243 IP injection in mice on HFD pretreated with amlexanox (Figure 3.5D). Consistent with this, HSL phosphorylation was also increased after CL-316,243 IP injection of HFD-fed mice pretreated with amlexanox (Figure 3.5E).

Our previous studies showed that increased expression of Ucp1 in white adipose depots resulted in increased energy expenditure in IKKε-deficient mice (288) and amlexanox-treated mice (292) while on a high fat diet but not on a normal diet. To examine whether inhibition of catecholamine resistance in obese adipose tissue by targeting noncanonical IKKs with amlexanox can lead to increase energy expenditure in diet-induced obese mice, we measured oxygen consumption rates of vehicle or amlexanox-treated HFD-fed mice after a single injection of CL-316,243 in metabolic cages. The effect of CL-316,243 to increase energy expenditure was more pronounced in amlexanox-treated HFD-fed mice, as compared to vehicle-treated HFD-fed mice (Figure 3.5F). These data suggest that targeting the noncanonical IKKs with the selective inhibitor amlexanox ameliorated catecholamine resistance in obese adipose tissue.

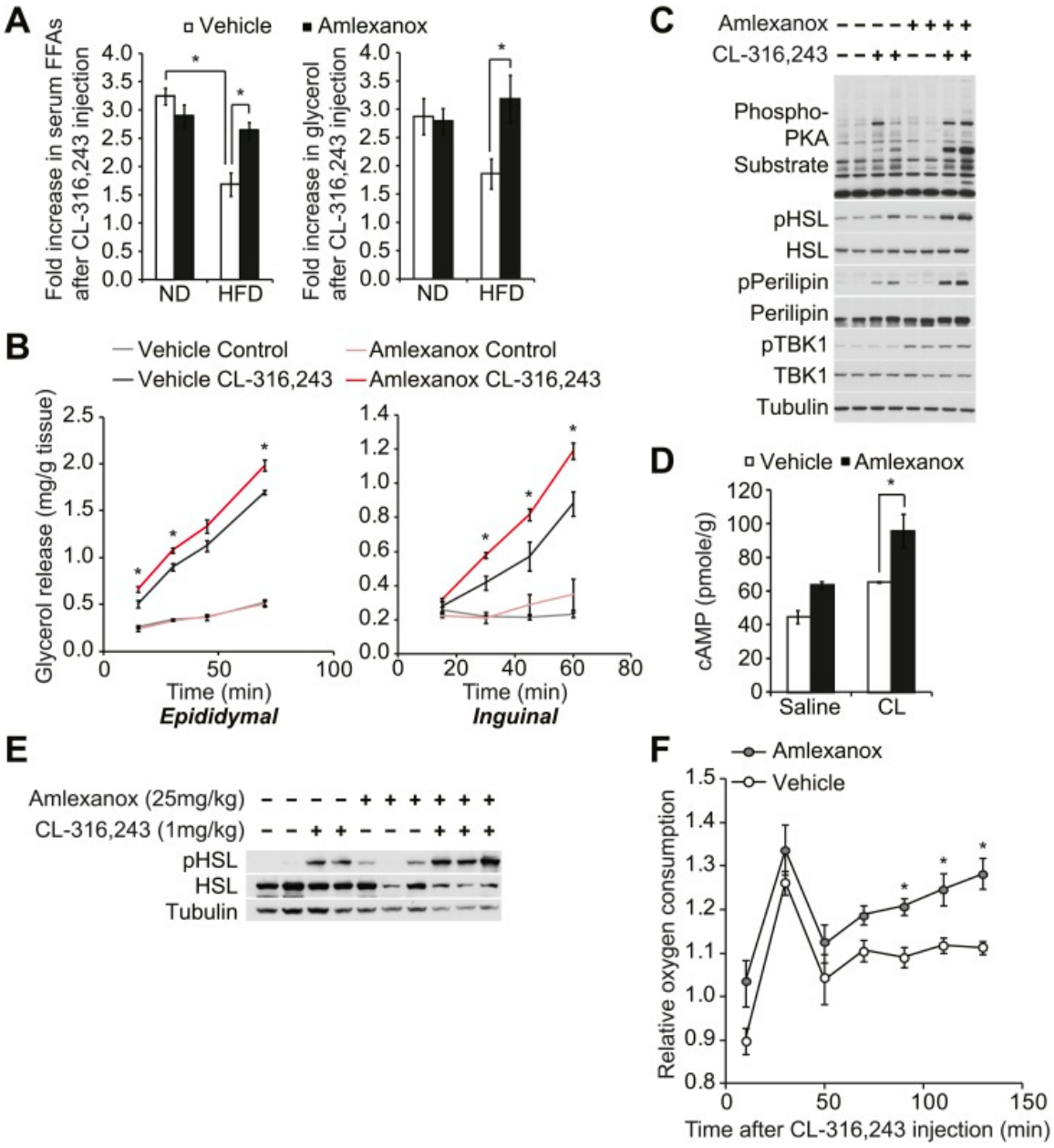

Figure 3.5: The IKKε/TBK1 inhibitor Amlexanox sensitizes β-adrenergic agonist-stimulated lipolysis in white adipose tissue in diet-induced obese mice.

(A) Fold increase in serum FFA (left panel) and glycerol (right panel) levels 15 min after CL-316,243 injection in ND- or HFD-fed mice treated with amlexanox or vehicle control for 4 days. n = 7 mice per group. *p<0.05. (B) Glycerol release from ex vivo epididymal (left panel) and inguinal (right panel) WATs after 1 hr pretreatment with amlexanox or vehicle. CL-316,243 treatment was started at time zero. n = 6, 3 WAT pieces × 2 mice.

*P<0.05. (C) Immunoblots in inguinal WAT lysates from Figure 5B after 60 min of CL-316,243 treatment. (D) cAMP levels in epididymal WAT 20 min after CL-316,243 (CL) or saline control injection in HFD-fed mice treated with amlexanox or vehicle control for 4 days. n = 2 mice per saline-treated group and n = 3 mice per CL-316,324-treated group. *p<0.05. (E) Immunoblots in epididymal WAT 5 min after CL-316,243 or saline control injection in HFD-fed mice treated with amlexanox or vehicle control for 4 days. (F) Relative oxygen comsumption of mice in each treatment group. n = 7 for the vehicle-treated group, n = 5 for the amlexanox-treated group. *P<0.05 (Student's t test).

Discussion

Decreased sympathetic activation of adipose tissue due to impaired catecholamine synthesis or sensitivity has been observed in obese patients (26, 36, 99, 304). Obesity is commonly associated with blunted whole-body catecholamine-induced lipolysis (99). This is thought to occur through a number of mechanisms, including leptin resistance (234), as well as the reduced expression of β-adrenergic receptors (36) or increased expression of α2-adrenergic receptors (295). White adipose tissue and cultured isolated adipocytes from obese human and mouse models exhibit decreased cAMP-stimulated lipolysis and fat oxidation, due to reduced energy expenditure from decreased mitochondrial uncoupling (294). This desensitization to adrenergic activation is also a feature of childhood onset obesity (28, 29), and has been observed in adipocytes from first-degree relatives of obese subjects (30).

We demonstrate here a novel link between obesity and reduced sympathetic activity and β-adrenergic sensitivity, through the inflammation-dependent induction of the noncanonical IκB kinases IKKε and TBK1. Obesity generates a state of low-grade inflammation in both humans and rodents, which involves activation of the NFκB pathway (1, 255, 256). Upon its prolonged activation, NFκB induces the expression of the noncanonical IκB kinases IKKε and TBK1. The induction of these kinases was blocked by administration of anti-inflammatory agents to mice without producing weight loss, suggesting that they are expressed in response to inflammation rather than obesity per se (292). Deletion of the IKKε gene rendered mice partially resistant to weight gain, insulin resistance, steatosis and the long-term inflammation produced by high fat diet (288), and administration of the dual specificity IKKε/TBK1 inhibitor amlexanox to diet-

induced obese or ob/ob mice produced even more profound effects (292). The blockade of these kinases in obese rodents with amlexanox results in increased phosphorylation of PKA substrates in adipose tissue, along with increased expression of Ucp1, and improved rates of lipolysis and fat oxidation (292). Amlexanox was shown to inhibit phosphodiesterase activity of rat peritoneal mast cells via an unknown mechanism (325). Together these data indicate that IKKε and TBK1 might exert their physiological effects in part by reducing the sensitivity of adipocytes to β-adrenergic stimulation via changes in cAMP.

Data presented here suggest that the molecular target of IKKε/TBK1 is the phosphodiesterase PDE3B. Upon increased expression in the obese state, these kinases can phosphorylate PDE3B, causing an increase in the activity of the enzyme that cleaves cAMP, reducing the stimulation of cAMP-dependent phosphorylation of proteins in response to sympathetic activation. These proteins include HSL and perilipin, responsible for β-adrenergic-stimulated lipolysis, and other proteins such as p38 that regulate expression of Ucp1. The reduced sensitivity to β-adrenergic activation can attenuate lipolysis and fatty acid oxidation, as well as adaptive thermogenesis.

Several issues deserve further attention. The first concerns the relative roles of the two noncanonical IKKs in this pathway. Both TBK1 and IKKε are induced in response to obesity-dependent inflammation, and appear to phosphorylate PDE3B on the same residues with equal efficiency. Although there are differences in expression of these kinases in other tissues (271), and perhaps differences in the upstream signals that lead to their regulation (306), their relative roles in controlling this pathway remain uncertain. Additionally, the mechanism by which PDE3B is regulated remains uncertain.

While phosphorylation correlates well with decreased levels of cAMP in cells, we have been unable to demonstrate increased catalytic activity of the enzyme due to phosphorylation by IKKε, TBK1 or the other kinases (137, 319) thought to regulate the phosphodiesterase. Perhaps the phosphorylation-dependent binding of the enzyme to 14-3-3 exerts changes in its localization and access to its substrate, thus explaining increased activity in cells.

How is it that insulin resistance produced by inflammation fails to block continued energy storage? One possible explanation may lie in the homeostatic response to inflammation itself, typified by the induction of TBK1 and IKKε. Our data confirm previous findings that TNFα and perhaps other inflammatory cytokines can promote lipolytic processes in cells after short-term treatment, but that after longer exposure elicit an inhibitory response that appears to be the result of TBK1 and IKKε induction. Thus, these kinases may be part of a 'counter-inflammatory' program that attenuates the extent to which inflammatory signals are effective, and also serves to conserve energy by repressing lipolysis and fatty acid oxidation through activation of PDE3B. Interestingly, PDE3B is also a target of insulin action in adipocytes (121). Thus, TBK1 and IKKε appear to co-opt insulin targets to conserve energy during obesity. These insights further suggest that the noncanonical IKKs might be interesting new therapeutic targets for the treatment of obesity and type 2 diabetes.

Materials and Methods

Reagents. All chemicals were obtained from Sigma-Aldrich (Saint Louis, MO) unless stated otherwise. Anti-Flag antibody was obtained from Sigma, and anti-HA antibody was obtained from Santa Cruz Biotechnology (Santa Cruz, CA). Anti-IKKε, anti-TBK1, anti-phospho-TBK1 (Ser172), anti-AKT, anti-phospho-AKT (Ser473), anti-HSL, anti-phospho-HSL (Ser660), anti-p38, anti-phospho-p38, anti-perilipin, anti-ATGL and anti-PPARγ antibodies were purchased from Cell Signaling Technology (Danvers, MA). Anti-phospho-perilipin (Ser522) was purchased from Vala Sciences Inc (San Diego, CA). Anti-CGI-58 was purchased from Novus Biologicals (Littleton, CO). Anti-RalA antibody was obtained from BD Bioscience (San Jose, CA). Anti-Ucp1 antibody was obtained from Alpha Diagnostics (San Antonio, TX). Anti-PDE3B was provided as a generous gift by the Dr Vince Manganiello (NHLBI, NIH). Enhanced chemiluminescence (ECL) reagents were purchased from Thermo Scientific (Rockford, IL). EDTA-free protease inhibitor tablet was purchased from Roche Diagnostics (Indianapolis, IN). Monoclonal anti-HA agarose (Sigma) was used for immunoprecipitations, performed using the manufacturer's protocol. The human PDE3B cDNA was kindly provided by Dr Morris Birnbaum (University of Pennsylvania). The human 14-3-3β cDNA was kindly provided by Dr Ken Inoki (University of Michigan) and subcloned into pKH3 (326) and pGEX-4T-1 vectors (GE Healthcare Life Sciences, MI). Amlexanox was purchased from Ontario Chemical Inc. (Guelph, Ontario, Canada). The TBK1/IKKε inhibitor CAY10576 was purchased from Cayman Chemical (Ann Arbor, MI).

Cell culture and transfection. 3T3-L1 fibroblasts (American Type Culture Collection, Manassas, VA) were cultured and differentiated as described previously (305). The cells

were routinely used within 7 days after completion of the differentiation process; only cultures in which >90% of cells displayed adipocyte morphology were used. 3T3-L1 adipocytes were transfected on the second day post FBS using Amaxa Cell Line Nucleofector Kit L (Lonza, Houston, TX) according to the manufacturer's protocol. 3T3-L1 adipocytes were serum starved for 12 hr with 0.5% fetal bovine serum (FBS) in Dulbecco's modified eagle medium (DMEM, Invitrogen, Grand Island, NY) prior to TNFα treatments (50 ng/ml unless otherwise noted). 3T3-L1 adipocytes were pre-treated for 1 hr with amlexanox at the given concentrations. Alternatively, 3T3-L1 adipocytes were treated with 50 μM forskolin or 10 μM isoproterenol for 15 min, after a 60 min amlexanox pretreatment. The cells were harvested for total RNA and analyzed by real-time PCR. Cell lysates were resolved on SDS-PAGE and analyzed by immunoblot using the indicated antibodies. HEK293T or Cos-1 cells were cultured to 90% confluence and transfected using Opti-MEM media (Invitrogen) and 3 μl Lipofectamine 2000 (Invitrogen) per μg DNA according to manufacturer's protocol. Coexpression of IKKε or TBK1 with HA-PDE3B was done using a 2 μg kinase: 1 μg PDE3B ratio of the expression constructs.

Western analyses. Tissues were homogenized in lysis buffer (50 mM Tris, pH 7.5, 5 mM EDTA, 250 mM sucrose, 1% NP40, 2 mM DTT, 1 mM sodium vanadate, 100 mM NaF, 10 mM Na4P2O7, and freshly added protease inhibitor tablet), then incubated for 1 hr at 4°C (288). Crude lysates were then centrifuged at 14,000 × g for 15 min twice and the protein concentration was determined using BioRad Protein Assay Reagent (Bio-Rad, Hercules, CA). Samples were diluted in sodium dodecyl sulfate (SDS) sample buffer and boiled for 5 min at 95°C. Proteins were resolved by SDS-polyacrylamide gel

electrophoresis and transferred to nitrocellulose membranes (Bio-Rad, Hercules, CA). Individual proteins were detected with the specific antibodies and visualized on film using horseradish peroxidase-conjugated secondary antibodies (Bio-Rad, Hercules, CA) and Western Lightning Enhanced Chemiluminescence (Perkin Elmer Life Sciences, Waltham, MA).

Animals and animal care. Wild-type male C57BL/6 mice were fed a high fat diet consisting of 45% of calories from fat (D12451 Research Diets Inc., New Brunswick, NJ) starting at 8 weeks of age for up to 6 months, while normal diet C57BL/6 controls were maintained on normal chow diet consisting of 4.5% fat (5002 Lab Diet, St. Louis, MO). Animals were housed in a specific pathogen-free facility with a 12-hr light/12-hr dark cycle and given free access to food and water. All animal use was in compliance with the Institute of Laboratory Animal Research Guide for the Care and Use of Laboratory Animals and approved by the University Committee on Use and Care of Animals at the University of Michigan.

Gene expression analysis. Total RNA was extracted from differentiated 3T3-L1 adipocytes using the RNeasy Kit (Qiagen, Valencia, CA) with a DNase step. The Superscript First-Strand Synthesis System for RT-PCR (Invitrogen, Grand Island, NY) was used with random primers for reverse transcription. Real-time PCR amplification of the cDNA was performed on samples in triplicate with Power SYBR Green PCR Master Mix (Applied Biosystems, Carlsbad, CA) using the Applied Biosystems 7900HT Fast Real-time PCR System. Adrp was chosen as the internal control for normalization as its expression was not significantly affected by experimental conditions. Sequences of Ucp1 primers used in this study are 5′ -AGGCTTCCAGTACCATTAGGT‐3′ and 5′

‐CTGAGTGAGGCAAAGCTGATTT‐3′. Sequences of Ikbke primers used in this study are 5′-ACAAGGCCCGAAACAAGAAAT-3′ and 5′-ACTGCGAATAGCTTCACGATG‐3′. Data were analyzed using the 2−ΔΔCT method (Livak and Schmittgen, 2001).

In vivo CL-316,243 treatment. Mice were placed on a high fat diet for 6 months, then after 1 week of daily gavage with vehicle, mice were gavaged with either vehicle or amlexanox (25 mg/kg) daily for 4 days. On the fourth day, mice were injected with CL-316,243 (1 mg/kg) or saline control. For analysis of blood metabolites, serum samples were collected before and 15 min after the injection, via a submandibular bleed. Mice were euthanized and WAT samples were collected for cAMP measurement and western blot analysis, 15 min or 20 min after injection. Analysis of oxygen consumption was performed in metabolic cages, as previously described (292), by the University of Michigan Metabolic Phenotyping Core. Relative oxygen consumption was obtained by normalization of oxygen consumption rates, after the CL-316,243 injection, to the oxygen consumption rates on day 3 in the same mouse after saline injection. Both injections were performed at 11 am.

Ex vivo glycerol release lipolysis assay in white adipose tissue. For experiments involving CL-316,243, pieces were pre-incubated for 30 min with amlexanox (100 μM) or DMSO vehicle control; then the tissue pieces were transferred to fresh media with and without 10 mM CL-316,243, and media samples were collected every 15 min for 1 hr. To measure glycerol release, 10 μl of supernatant was combined with 200 μl of Free Glycerol Reagent from the Free Glycerol Determination Kit (Sigma) and allowed to

incubate for 15 min at room temperature. Absorbance at 540 nm was measured to determine glycerol content and was normalized to determine glycerol production per mg of white adipose tissue.

Glycerol release lipolysis assay in 3T3-L1 adipocytes. 3T3-L1 adipocytes were incubated in DMEM (Invitrogen) without phenol red for 2 hr at 37°C. The cells then were incubated for 90 min at 37°C in HBSS-2% fatty acid-free BSA with 10 μM isoproterenol or 10 μM CL-316,243. Free glycerol concentration was measured by reacting 25 μl of conditioned media with 200 μl Free Glycerol Reagent (Sigma) and absorbance was measured at 540 nm using the manufacturer's protocol. Glycerol release was normalized to cellular protein content.

cAMP enzyme immunoassay. 3T3-L1 adipocytes were treated with β-agonists and/or phosphodiesterase inhibitors and allowed to incubate for the indicated amount of time at 37°C. The cells were lysed with 150 μl 0.1 M HCl, scraped and spun down. A cAMP Enzyme Immunoassay Kit (Sigma CA201) was used to quantify cAMP levels. 50 μl of cell lysates was combined with 50 μl Assay Buffer 2 in each well and cAMP levels were assayed according to the manufacturer's protocol. Tissue samples were homogenized in 5% TCA, then extracted with water-saturated ether, and dried before resuspension in Assay Buffer 2.

Glosensor cAMP assay in 3T3-L1 adipocytes. 80 μl of packed 3T3-L1 cells was electroporated with 3 μg of Glosensor 22-F using Amaxa Cell Line Nucleofector Kit L (Lonza) according to the manufacturer's protocol. Electroporated cells were resuspended in 10 ml of L1-FBS media and 200 μl per well was plated in six columns of

an opaque, white, 96-well tissue culture plate (BD Bioscience, San Jose, CA). After 20 hr, media were changed to 100 µl DMEM with 1.5 mg/ml luciferin and allowed to equilibrate for 1 hr. The cells were treated with 50 µM forskolin and luminescence was read every 30 s for 75 min.

In vitro kinase assays. In vitro kinase assays were performed by incubating purified kinase (IKKε, TBK1, IKKβ, PKA, or AKT) in kinase buffer containing 25 mM Tris (pH 7.5), 10 mM MgCl2, 1 mM DTT, and 10 µM ATP for 30 min at 30°C in the presence of 0.5 µCi γ-[32P]-ATP and 1 µg myelin basic protein (MBP) per sample as a substrate. IKKε and TBK1 were fused to MBP (maltose binding protein) and these fusion proteins were purified from insect SF9 cells by baculovirus expression system by Dr Stuart J Decker (Life Sciences Institute, University of Michigan). IKKβ, PKA, and AKT kinases were purchased from Millipore (Billerica, MA). The kinase reaction was stopped by adding 4X sodium dodecyl sulfate (SDS) sample buffer and boiling for 5 min at 95°C. Supernatants were resolved by SDS-polyacrylamide gel electrophoresis, transferred to nitrocellulose, and analyzed by autoradiography using a Typhoon 9410 phosphorimager (GE Life Sciences, Piscataway, NJ). The bands were quantified using ImageQuant.

Calf-intestinal phosphatase dephosphorylation. Calf intestinal phosphatase (CIP) was obtained from New England Biolabs (Ipswich, MA). Immunoprecipitated PDE3B was incubated for 1 hr at 37°C in a 100 µl reaction containing 50 mM Tris pH 7.5, 150 mM NaCl, 1% NP-40, EDTA-free protease, and 5 µl CIP.

Protein purification. For assays requiring soluble protein, purified GST-14-3-3β protein was eluted from glutathione beads by washing beads with 10 mM glutathione in PBS,

pH 8.0. The elution was monitored by A280 readings, and fractions containing protein were pooled and dialyzed overnight against 4 L of ice-cold PBS. The proteins were then concentrated using an Amicon centrifugal filtration unit (Millipore). Concentrated proteins were stored at −80°C in PBS containing 10% glycerol and 10 mM DTT.

GST-14-3-3 Pulldown. For GST-14-3-3 pulldowns, cells were washed twice with ice-cold PBS and then lysed in 1 ml of 14-3-3 pulldown buffer (PD buffer; 15 mM Tris, pH 7.5, 150 mM NaCl, 0.5% NP-40, 1 mM DTT) supplemented with a protease inhibitor tablet (Roche). Lysates were cleared by centrifuging at 13,000×g for 10 min and then were incubated with ~10 mg of GST or GST-14-3-3β bound to glutathione beads (GE Healthcare Life Sciences, MI) for 1.5 hr at 4°C. For samples treated with phosphatase, lysates were preincubated with 500 U of calf intestinal phosphatase (New England Biolabs, Inc.) at 37°C for 1 hr before adding GST-14-3-3 beads. The beads were washed three times with 1 ml of PD buffer and then resuspended in 2X SDS sample buffer.

Preparation of DIG-labeled proteins and overlay assay. GST or GST-14-3-3β was labeled with DIG by incubating 25 mg of protein with 2 ml of 5 mM Digoxigenin-3-O-methylcarbonyl-ε-aminocaproic acid-N-hydroxysuccinimide ester (DIG-NHS; Roche) in 350 ml of PBS for 15 min at room temperature. The labeling reaction was stopped by adding 100 ml of 1 M Tris-HCl, pH 7.4. Labeled protein was dialyzed against 1 L of 25 mM Tris-HCl, pH 7.4 for 1 hr at room temperature, then against 4 L of PBS, pH 7.4 for 4 hrs at 4°C, and finally against 4 L of fresh PBS, pH 7.4 for 16 hrs at 4°C. Labeled protein was then diluted in 25 ml of TBS (50 mM Tris-HCl, pH 7.4, 150 mM NaCl)

containing 2 mg/ml BSA (Sigma-Aldrich) and 0.01% sodium azide (Sigma-Aldrich). DIG-labeled proteins were stored at 4°C.

For overlay assays, PDE3B was immunoprecipitated from HEK293T cells and resolved by SDS-PAGE. Proteins were transferred to a nitrocellulose membrane. The membrane was blocked at room temperature overnight in blocking buffer (5% skim milk in TBS-T). The membrane was then incubated with DIG-labeled proteins for at least 4 hr at 4°C and then washed three times with TBS-T. The membrane was then incubated with blocking buffer containing anti-DIG HRP antibody (1:10,000; Roche) for 2 hr at room temperature, and washed three times with TBS-T. Overlays were visualized by reacting with ECL western blotting substrate (Perkin Elmer Life Sciences, Waltham, MA).

Mass spectrometry. In-gel digestion followed by LC-MS/MS analysis was carried out by the mass spectrometry-based proteomics resource in the Department of Pathology, University of Michigan. Briefly, tryptic peptides were resolved on a nano-C18 reverse phase column and sprayed directly onto Orbitrap mass spectrometer (LTQ-Orbitrap XL, Thermofisher). Orbitrap was operated in a data-dependent mode to acquire one full MS spectrum (resolution of 30,000@400 m/z) followed by MS/MS spectra on six most intense ions (top 6). Proteins were identified by searching data against human protein database (Uniprot, rel. 2010-9) using X!Tandem/TPP software suite. Oxidation of Met, carbamidomethylation of Cys and phosphorylation of Ser, Thr, and Tyr were considered as potential modifications (327).

Statistical analyses. Averaged values are presented as the mean ± SEM. When comparing two groups, we performed Student's t test to determine statistical

significance. When more than two groups and two factors were investigated, we first performed a two-way analysis of variance (ANOVA) to establish that not all groups were equal. After a statistically significant ANOVA result, we performed between-group comparisons using the Tukey post hoc analysis for comparisons of all means and Sidak for comparisons of within factor main effect means. ANOVA and Tukey/Sidak tests were performed using GraphPad Prism version 6.

Chapter IV:
Conclusion

To Every Metabolic Action, an Opposite Reaction

The persistence of insulin resistance with obesity creates a paradox. If obese animals are rendered insensitive to the anabolic effects of insulin, how is it that an anabolic state persists? Why does insulin resistance fail to reverse obesity? Energy balance consists of opposing anabolic and catabolic pressures. The body has evolved mechanisms to protect against wide fluctuations in body weight, by continually counterbalancing anabolic and catabolic processes. However, when faced with sustained overnutrition, the I conclude the resolution of these processes eventually favors the conserved evolutionary pressure to store energy.

Our lab studies the link between inflammation in adipose tissue and obesity. Through the studies detailed in this thesis, I hope to clarify the role of the IKK family of kinases as they relate to adipocyte metabolism. Whereas IKKβ has an established role in promoting inflammation in insulin resistance (255), the studies herein establish that the counterinflammatory IKK family members, IKKε and TBK1, promote obesity by activating PDE3B in adipose tissue. Below, I discuss the molecules that regulate the body's anabolic and catabolic processes and how these processes are altered in the development of obesity and insulin resistance, highlighting the contribution of IKKε and

TBK1. These ideas are also discussed in a review written by my mentor Dr. Alan Saltiel (316).

Insulin Action

Insulin is the most important regulator of anabolism (113). Insulin facilitates the storage of simple energy molecules, such as simple sugars, amino acids, and fatty acids, into complex storage molecules (113). Insulin is released from pancreatic β-cells in response to ingested carbohydrates. Protein or lipids stimulate insulin secretion by the action of incretins, such as glucagon like peptide 1 (328). Circulating insulin then acts on liver, muscle, and adipose tissue to promote the synthesis and storage of glycogen, protein, and triglycerides in these tissues (113). In adipose tissue, insulin stimulates adipocyte differentiation and adipose tissue expansion. Insulin's effects on adipose tissue expansion are attributed to its ability to stimulate uptake of free fatty acids and glucose, initiate *de novo* fatty acid synthesis, and inhibit lipolysis.

As mentioned previously, insulin decreases the lipolytic pathway through a variety of targets (see chapter 1). Insulin attenuates lipolysis partly by activating phosphodiesterase 3B (PDE3B) (121). Whereas activation of adenylyl cyclase produces cAMP, PDE3B is responsible for cleaving cAMP to AMP to terminate β-adrenergic pathway signaling in adipose tissue. Therefore, upregulation of PDE3B by hormonal cues, such as insulin, promotes anabolic processes and reduces catabolic processes in adipose tissue. This is important to highlight, because in chapter 3 I explored the regulation of PDE3B by IKKε and TBK1 in obesity.

Insulin Desensitization

A pathogenic model of counterbalancing homeostatic mechanisms in metabolic dysfunction is emerging. The progression of metabolic disease in adipose tissue begins with overnutrition, prolonged insulin action, and energy storage. As a consequence of sustained insulin receptor activation, insulin signaling is downregulated by reduced surface expression of the insulin receptor, increased phosphatase activity, and negative feedback by S6K through IRS phosphorylation (316). Therefore, acute desensitization events may serve as a homeostatic feedback mechanism to prevent insulin signaling, but these processes rapidly disappear so that animals can store energy in response to the next meal.

Leptin Action

Overnutrition leads to multiplication and expansion of adipocytes. Hypertrophied adipocytes secrete leptin which acts in the hypothalamus to reduce appetite and increase sympathetic activity to counter energy storage and adipose expansion (234). Upon leptin binding, the leptin receptor is phosphorylated at Tyr1138 and Tyr985, among other sites. Tyr1138 phosphorylation results in activation of STAT3, which increases satiety and energy expenditure, and leptin deficient animals have a thermogenic defect (235). UCP1 is required for leptin-stimulated reductions in white adipose tissue in pair fed mice (236). Therefore, leptin action, like insulin desensitization, serves as a catabolic counterbalance to increased adipocyte lipid accumulation.

Leptin Resistance

When elevated leptin levels are sustained for several days, STAT3 activation in the hypothalamus results in the upregulation of SOCS3 to cause leptin resistance (234) (329). SOCS3 is recruited to the leptin receptor by phosphorylation of Tyr985 to downregulate leptin receptor signaling. Tyr985 phosphorylation also recruits SHP-2 to the leptin receptor to downregulate receptor activity through a mechanism that is not fully understood. Phosphorylation of Tyr985 of the leptin receptor therefore serves as a mechanism by which the body counters the catabolic effects of leptin to favor a positive energy balance, despite the presence of insulin desensitization in the short-term.

Inflammatory Insulin Resistance and β-cell Dysfunction

Obesity produces a state of chronic, low-grade inflammation in liver and fat characterized by macrophage infiltration and the local secretion of inflammatory cytokines and chemokines (1, 255, 256). Prolonged adipose expansion leads to the release of chemokines, such as MCP-1, that recruit M1-polarized proinflammatory macrophages to adipose tissue. These macrophages secrete TNFα and other proinflammatory cytokines that trigger inflammatory receptors on adipocytes leading to JNK and IKKβ activation to mediate adipocyte resistance to insulin action (289). Many of these inflammatory signaling molecules work through IKKβ and NFκB. Circulating free fatty acids, interleukin 1, TNFα, advanced glycated end products, glucosamine, and ER stress have all been linked to NFκB in insulin resistance (257).

Resistance to insulin action in this inflammatory context occurs through some of the same insulin targets that non-inflammatory desensitization occurs. For example, decreased insulin receptor levels and increased inhibitory IRS serine phosphorylation is

facilitated by the action of JNK, IKKβ, and PKC isoforms in the obese state (330). Additionally, PPARγ is negatively regulated at the transcriptional and post-transcriptional level by the action of inflammatory kinases in adipocytes (289). The inability of adipose tissue to store fatty acids via PPARγ results in lipid overflow into circulation and the deposition of lipid in other tissues. Fatty acids are ectopically deposited in muscle and hepatic tissue, which further desensitizes the body to the action of insulin. Adipocytes can therefore regulate whole-body insulin sensitivity either directly in adipose tissue, or indirectly through the action of free fatty acids on muscle (289). In sum, Inflammation-induced insulin resistance serves as another homeostatic mechanism to protect the body against weight gain in the face of anabolic pressures, including sustained insulin action and leptin resistance.Another long-term mechanism leading to reduced insulin action is β-cell failure (331). At first, β cells compensate for chronic elevated glucose in the body by elevating insulin secretion in order to maintain near-normal blood glucose levels. However, prolonged elevated insulin secretion and the toxic effects of ectopic deposition of lipid in pancreatic β cells eventually reduce β-cell mass until insulin action can no longer maintain near-normal blood glucose levels, and decompensation occurs. This progresses to β-cell failure and unstable decompensation. When β cells fail, insulin secretion falls while blood glucose remains high. β-cell dysfunction results in decreased insulin production and secretion, providing another mechanism by which insulin's anabolic effects are limited during obesity.

Counterinflammation by IKKε and TBK1

With chronic insulin desensitization, insulin resistance, and β-cell dysfunction on the rise, how does the body persist in effectively storing calories? We propose that

chronic NFκB activity associated with insulin resistance in adipose tissue induces negative feedback mediators, such as IKKε and TBK1, to the counter inflammatory effects of NFκB-related insulin resistance. Therefore, inflammatory insulin resistance may be held in check by the action of counterinflammatory processes by IKKε and TBK1 to promote anabolism.

In chapter 2, we demonstrate that high-fat diet induces adipocyte expression of IKKε and TBK1 (288), which counter the action of IKKβ—NFκB signaling (276). In the IKKε knockout mice, we saw decreased diet-induced obesity, which was attributed to increased energy expenditure. Furthermore, mice lacking IKKε had higher core body temperatures and increased adipose UCP1 levels (288). A similar phenotype was observed in mice that were administered amlexanox, a selective inhibitor of IKKε and TBK1 activity. Mice fed a high-fat diet or leptin-deficient mice had decreased weight gain and increased energy expenditure when given amlexanox. Similar to mice lacking IKKε, amlexanox administered animals had higher core body temperatures, and higher adipose UCP1 levels (292). Inhibitors of IKKε and TBK1 substituted for IBMX in 3T3-L1 differentiation, which paralleled adipocyte hyperplasia in the IKKε knockout mouse and suggested that IKKε and TBK1 may suppress cAMP.

Interestingly, insulin resistance remains high throughout the pathogenesis of obesity, suggesting that counterinflammatory processes may play an anabolic role independent of the response to circulating insulin. Through my work, I have established an anabolic mechanism that works through a target of insulin signaling, PDE3B, without the requirement of circulating insulin or signaling through the insulin receptor. IKKε and TBK1 co-opts a target of insulin signaling to promote an anabolic state, despite the

absence of insulin's action. In chapter three, I demonstrate that IKKε and TBK1 phosphorylates and activates PDE3B to decrease cAMP and regulate adipocyte metabolism.

If IKKε and TBK1 desensitize adipose tissue to adrenergic signaling in mouse adipose tissue, then their action in human adipose tissue may be the same. Whereas humans lose large brown adipose tissue depots early in life, UCP1-laden adipocytes with a distinct developmental origin from brown adipose tissue are found in adult white adipose depots. It would be interesting to measure IKKε and TBK1 activity in human adipose tissue and quantify the amount of brown adipocyte activity is present using PET scans. Potentially, these brown-like adipocytes emerge through increased adrenergic signaling and increased cAMP load in cells. If IKKε and TBK1 decrease cAMP levels in human adipose tissue similar to mouse adipose tissue, then these kinases would prevent the emergence of UCP1-laden adipocytes in human adipose tissue and decrease energy expenditure. These and other experiments described in this thesis collectively suggest that IKKε and TBK1 act outside the central nervous system in adipose tissue to downregulate catabolic processes and further the obese state.

Appendix

Feedback control of upstream kinases by IKK family members

Abstract

The regulation of inflammatory pathways is essential to a coordinated immune response. In this study, we reveal a role for IKK family members in downregulating their own activity by feedback control on upstream kinases. Inhibition of IKKβ upregulates phosphorylation of its own activation loop Ser177/181, indicating negative feedback control, and inhibition of IKKε/TBK1 upregulates activation loop Ser172 phosphorylation on TBK1 indicating negative feedback control. Both inhibitor-induced activation loop phosphorylation events are augmented by treatment with TLR agonists, LPS and poly(I:C). TAK1 is required for activation loop phosphorylation of IKKβ in response to inflammatory stimuli or IKKβ inhibitor treatment, while another upstream kinase is responsible for TBK1 activation loop phosphorylation in response to inflammatory stimuli or the IKKε/TBK1 inhibitor. IKKβ phosphorylates TAB1 Thr431 in response to inflammatory stimuli. We therefore propose that feedback control of TAK1 by IKKβ occurs through phosphorylation of TAB1, and that the IKK family has a conserved pattern of negative feedback control of upstream kinases.

All experiments were performed with the expert assistance of Dr. Louise Chang

Introduction

The NFκB family of transcription factors regulate inflammation, along with a variety of stress-oriented cellular responses (259). NFκB activity is an important effector of inflammatory cell surface receptors, such as Toll-like receptors (TLRs) (260), and receptors of proinflammatory cytokines, including TNFα (261). TLRs recognize pathogen-associated molecular patterns, such as lipopolysaccharide (LPS) and double stranded RNA (dsRNA), which trigger inflammatory signals that orchestrate immune cell action to clear microbes from the body (260). Both TLRs and TNFα receptors (TNFRs) initiate inflammatory signaling cascades using protein adaptors and polyubiquitin ligases that colocalize with these receptors (259). TGFβ activated protein kinase (TAK1) is bound by TAK1-binding proteins (TABs), which are phosphorylated in response to inflammatory stimuli, and are necessary for TAK1 stability and activity (262-265). TAK1 activity simultaneously leads to parallel MAPK (p38, JNK) and IKK pathway phosphorylation and activation (266). A selective inhibitor, oxozeaenol, was able to prevent activation of MAPK and IKK pathways (332). With respect to IKKs, TLR and TNFα receptor stimulation leads to receptor interacting protein 1 (RIP1) polyubiquitination, which recruits the IKK complex regulatory scaffolding protein NEMO to TAB-TAK1, so that TAK1 phosphorylates and activates the IKKβ (267) (268). Active IKKβ phosphorylates the inhibitor of κB (IκB), which results in IκB polyubiquitination and subsequent degradation through the 26S proteosome (269). The degradation of IκB exposes the nuclear translocation sequence of NFκB family members allowing these transcription factors to translocate to the nucleus and control the expression of inflammatory target genes.

The IKK family of proteins is composed of four members: IKKα, IKKβ, IKKε, and TANK-binding kinase (TBK1). Similarities and differences have emerged in IKK family member function. Whereas IKKα and IKKβ complex with their regulatory subunit NEMO to make the canonical heterotrimeric IKK complex, IKKε and TBK1 complex with their regulatory subunit TANK to form the noncanonical IKK-related kinase complex (259). IKKβ is essential for mediating innate immune responses, including TLR and TNFα signaling, while IKKα is more important for regulating adaptive immunity (270). IKKε and TBK1, also known as IKK-related kinases, phosphorylate interferon regulatory factors (IRFs), which are essential for the expression of type I interferon genes mainly in coordinating antiviral responses (272-274).

The IKK family regulates many facets of immune responses, but kinase activation of IKK family members occurs through a conserved mechanism. Phosphorylation of activation loop serine residues is important for IKK family kinase activation (281). TAK1 phosphorylates IKKβ on activation loop serine 177/181 between kinase subdomains VII and VIII leading to IKKβ activation (279). Substitution of alanine for serine 177/181 dramatically reduces IKKβ activity, while substitution for phosphomimetic glutamate generates a constituitively active kinase (280, 281). Phosphorylation of serine 172 on TBK1 and IKKε has been associated with increased activity, and serine 172 is required for IKKε/TBK1 activity (282, 283). Therefore, regulation of activation loop phosphorylation is indicative of IKK family member activity. Several phosphatases are important for the dephosphorylation of the activation loop to terminate IKK family member activity (284, 285). However, the mechanisms by which IKK family member phosphorylation and activity are downregulated remain unclear.

p38 phosphorylates TAB1 at Ser423 and Thr431 to downregulate TAK1 activity as a mechanism of feedback control to terminate TAK1-dependent p38 signaling (333). Since p38 negatively feeds back to downregulate TAK1 activity, we explored the possibility that IKK family kinases negatively regulate upstream kinase activity in a similar manner. In this study, we reveal a role for IKK family members in downregulating their own activity by feedback control on upstream kinases. Inhibition of IKKβ upregulates activation loop Ser177/181 phosphorylation indicating negative feedback control, and inhibition of IKKε/TBK1 upregulates activation loop Ser172 phosphorylation on TBK1 indicating negative feedback control. Both inhibitor-induced activation loop phosphorylation events are augmented by treatment with TNFα or TLR agonists, LPS and poly(I:C); however, phosphorylation of substrates downstream of IKK family members are predictably eliminated. We show that TAK1 is required for activation loop phosphorylation of IKKβ in response to inflammatory stimuli and IKKβ inhibitor treatment, while an upstream kinase other than TAK1, inhibited by small molecule PKC412, is responsible for TBK1 activation loop phosphorylation in response to inflammatory stimuli and IKKε/TBK1 inhibitor. Furthermore, we show IKKβ phosphorylates TAB1 Thr431 in response to inflammatory stimuli. We therefore propose that feedback control of TAK1 by IKKβ occurs through phosphorylation of TAB1, similar to negative feedback control of TAK1 by p38, and that the IKK family has a conserved pattern of negative feedback control of upstream kinases.

Results

Inhibition of IKK Family Members Upregulates Activation Loop Phosphorylation

Phosphorylation of the IKKβ activation loop was increased by LPS (Figure A.1A) and Poly(I:C) (Figure A.1B) in RAW264.7 macrophages. Inhibitors of IKKβ (Compounds IV, VII, VIII, PS1145, and BAY) also increased phosphorylation of the IKKβ activation loop in the basal state (Figure A.1A,B). Additionally, pretreatment of RAW264.7 cells with IKKβ inhibitors followed by stimulation with LPS or Poly(I:C) resulted in augmented phosphorylation of IKKβ. IKKβ and IKKα knockout MEFs demonstrate that IKKβ, not IKKα, is responsible for phosphorylation of the IKKβ activation loop in response to compound VIII (Figure A.1C). IKKε/TBK1 double knockout MEFs treated with TNFα had increased IKKβ phosphorylation compared to wild type MEFs, which is consistent with IKKε/TBK1 downregulating NFκB activity (data not shown) (276). Phosphorylation of the TBK1 activation loop was slightly decreased in response to compound VIII in RAW264.7 macrophages (data not shown). Phosphorylation of IRF3, a downstream effector of IKKε and TBK1, was mildly affected by compound VIII. However, phosphorylation of JNK, a downstream effector of TAK1 activity, was augmented by compound VIII when treated with LPS and Poly(I:C) (data not shown). The MEK inhibitor, U0126, was able to decrease Erk1/2 phosphorylation as previously reported (334); however, U0126 was not able to reduce IKKβ phosphorylation (data not shown).

Phosphorylation of the IKKε and TBK1 activation loops, and activity, were previously reported to be induced by LPS and Poly(I:C) (282). In that study, an inhibitor of IKKε and TBK1, known as BX795, augmented activation loop phosphorylation in response to LPS and Poly(I:C), which suggested that IKKε and TBK1 negatively

regulate their own activity after stimulation. Treatment of RAW264.7 cells with another inhibitor of IKKε and TBK1 that is structurally unrelated to BX795, known as CAY 10576, resulted in increased phosphorylation of the TBK1 activation loop (Figure A.3A), which suggested negative feedback by IKKε and TBK1 even in the basal state. TBK1 activation loop phosphorylation was augmented by LPS and Poly(I:C) after pretreatment by CAY10576. Therefore activation loop phosphorylation of both canonical IKKβ and noncanonical TBK1 are negatively regulated by their own activity in both the basal and stimulated states.

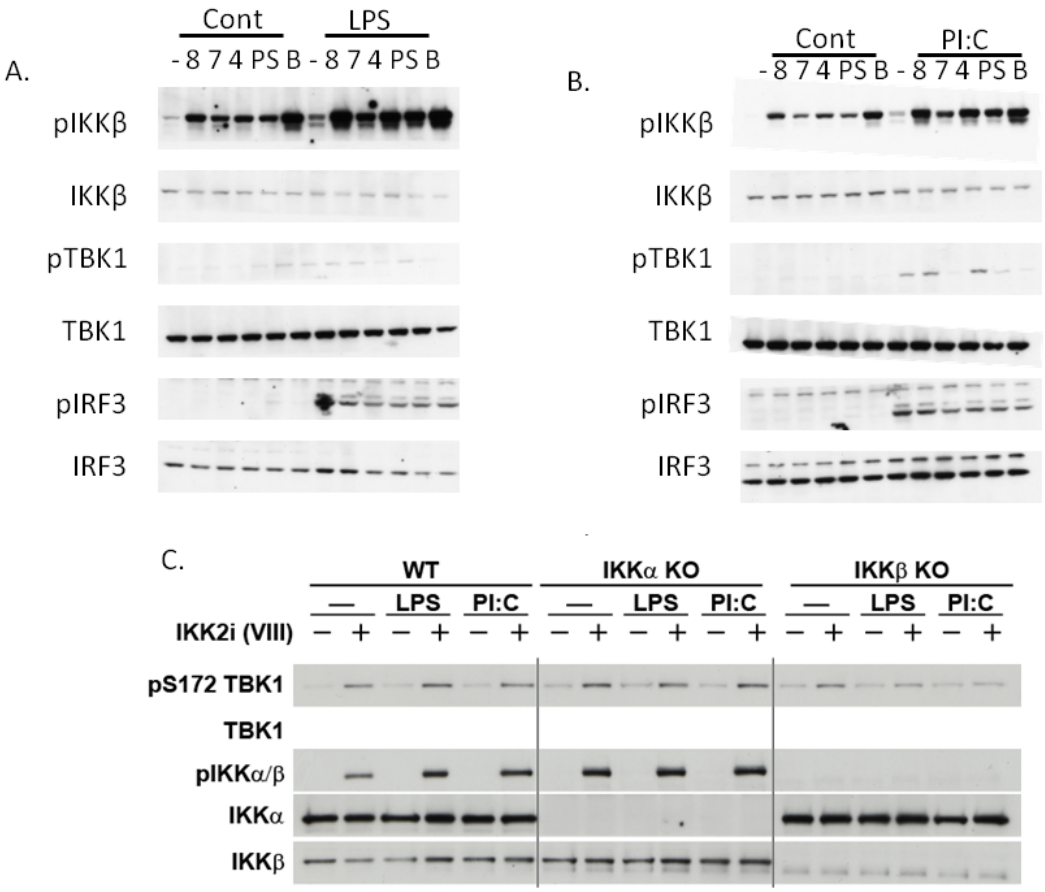

Figure A.1 Inhibition of IKKβ upregulates activation loop phosphorylation and is augmented by treatment with the TLR agonists A) Western blot of RAW264.7 cells treated with IKKβ inhibitors and LPS B) Western blot of RAW264.7 cells treated with IKKβ inhibitors and LPS C) Western blot of MEFs treated with compound VIII and LPS or Poly(I:C).

TAK1 is required for the upregulation of IKKβ activation loop phosphorylation

Next, we examined the mechanism by which IKKβ negatively regulates its own activation loop phosphorylation. Pretreatment of RAW264.7 cells with the TAK1 inhibitor, oxozeaenol (332), dramatically reduced the phosphorylation of the IKKβ activation loop in response to LPS and Poly(I:C) (Figure A.2A), similar to earlier reports (332, 335). When oxozeaenol was cotreated with an inhibitor of IKKβ, compound VIII, the inhibitor-induced IKKβ activation loop phosphorylation was dramatically reduced (Figure A.2B). Therefore, TAK1 was required for increased IKKβ activation loop phosphorylation in response to inhibitors of IKKβ, which prevent IKKβ negative feedback, as well as inflammatory stimuli. Oxozeaenol treatment also demonstrated that TAK1 was required for compound VIII-augmented IKKβ activation loop phosphorylation in response to LPS and Poly(I:C) (Figure A.2A).

TAK1 knockout MEFs were employed to examine the IKKβ negative feedback pathway in a TAK1 genetic loss-of-function context (336). The phosphorylation of the IKKβ activation loop in response to TNFα and IKKβ inhibitors was reduced in TAK knockout MEFs compared to wild-type MEFs, further indicating that TAK1 is required for the IKKβ negative feedback pathway (Figure A.2C).

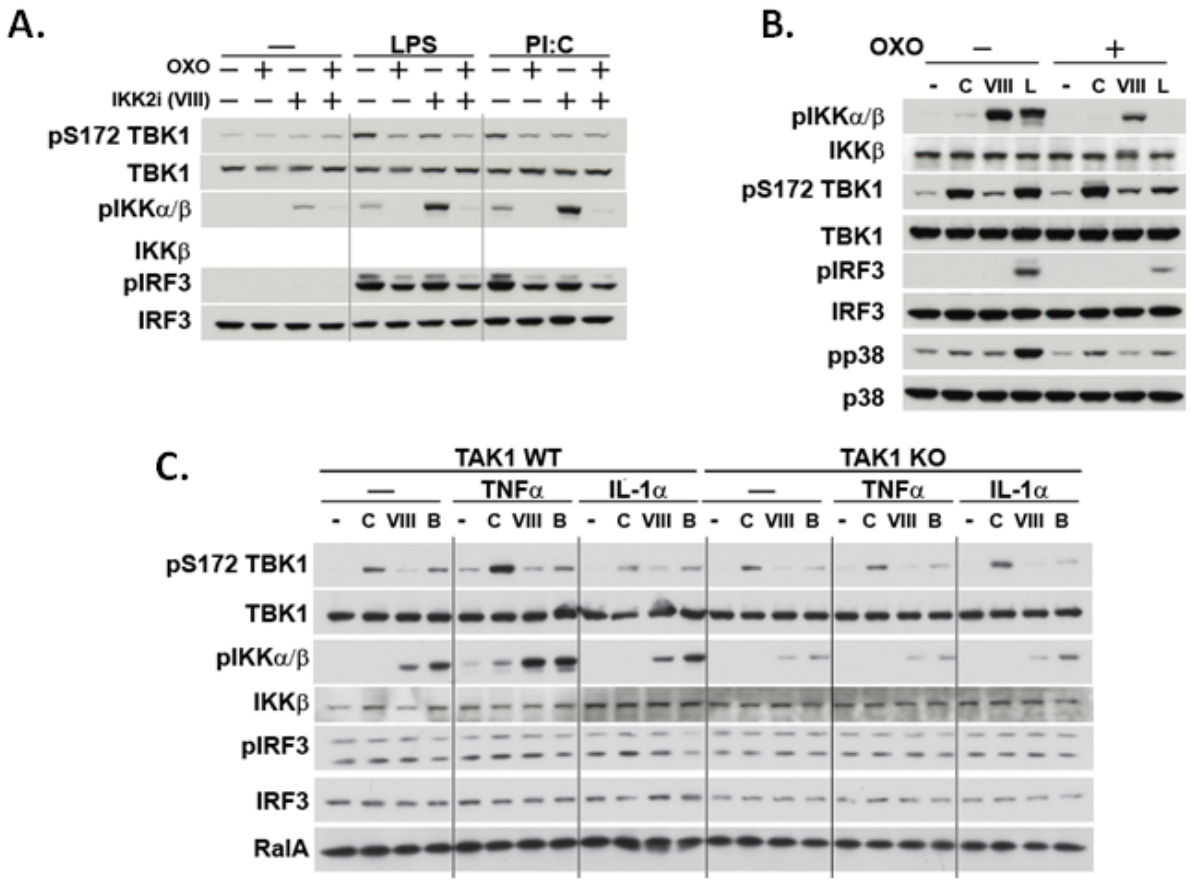

Figure A.2: TAK1 is required (oxozeaenol or TAK1 -/-) for the upregulation of IKKβ activation loop phosphorylation in response to agonists and IKKβ inhibitors A) Western blot of RAW264.7 cells treated with oxozeaenol, compound VIII, LPS and Poly(I:C) B) Western blot of RAW264.7 cells treated with compound VIII, CAY10576, oxozeaenol, and LPS C) Western blot of MEFs treated with CAY10576, compound VIII, TNFα and IL-1α.

An Upstream Kinase, not IKKβ nor TAK1, is Required for Upregulation of TBK1 Activation Loop Phosphorylation

Previous reports have shown that IKKβ is required for IKKε and TBK1 activation loop phosphorylation (276). The CAY10576-induced phosphorylation of the TBK1 activation loop was not eliminated by pretreatment with the IKKβ inhibitors PS1145, compound VIII, or BAY (Figure A.3A). TBK1 phosphorylation was not eliminated by oxozeaenol in RAW264.7 cells. Therefore, we performed a kinase inhibitor screen to see if any other kinases were required for IKKε/TBK1 negative feedback. Out of 80 kinase inhibitors used in this screen, PKC412 was the only inhibitor that could dramatically reduce CAY10576-induced TBK1 activation loop phosphorylation (data not shown).

Further studies demonstrated that PKC412 could inhibit TBK1 phosphorylation in response to CAY10576 and PKC412 could partially inhibit LPS and Poly(I:C) stimulated TBK1 activation loop phosphorylation (Figure A.3B). IRF3 phosphorylation in response to LPS and Poly(I:C) was eliminated by PKC412, indicating that PKC412 reduces downstream effectors of IKK-related kinase TLR signaling as well. The IC50 of PKC412 on CAY10576-induced TBK1 phosphorylation was measured at ~300nM (data not shown).

Interestingly, IKKβ activation loop phosphorylation in response to LPS and Poly(I:C) was decreased by PKC412 as well, suggesting that PKC412 inhibits a kinase upstream of IKKβ as well. PKC412 was not able to inhibit IKKβ inhibitor-induced phosphorylation of the IKKβ activation loop. In fact, PKC412 actually augmented phosphorylation of the activation loop of IKKβ in response to IKKβ inhibitor treatment,

suggesting that PKC412 inhibits kinases other than TAK1. Therefore, it is likely that both the canonical IKKβ and the noncanonical TBK1 pathways are activated by the same upstream kinases in response to agonists; however, the negative feedback observed by IKKβ and TBK1 is mediated by different upstream kinase pathways.

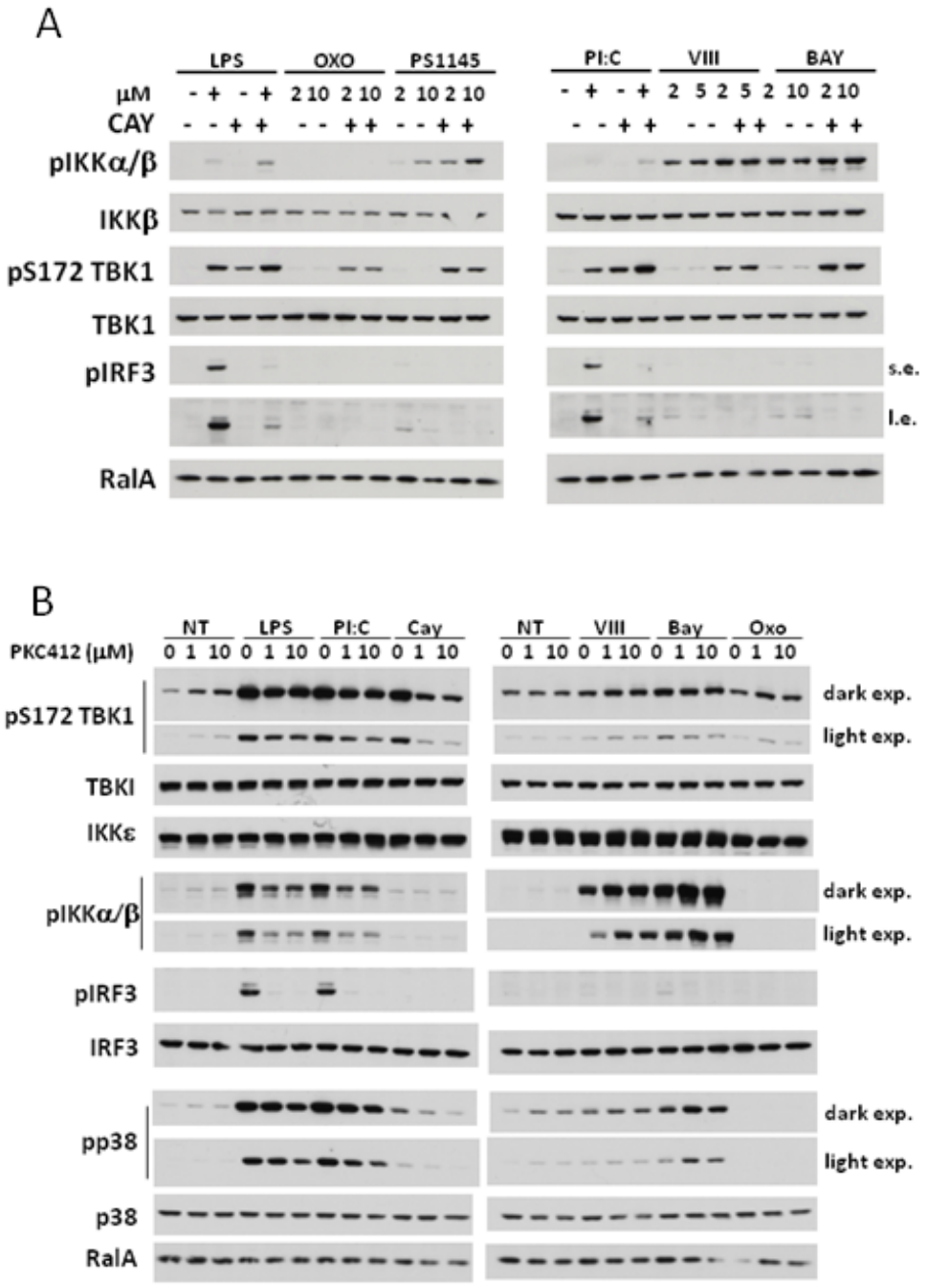

Figure A.3 An Upstream Kinase, not IKKβ nor TAK1, is Required for Upregulation of TBK1 Activation Loop Phosphorylation in Response to Inflammatory Stimuli and the IKKε/TBK1 inhibitor CAY10576 A) Western blot of RAW264.7 cells treated with CAY10576 pretreated with oxozeaenol, IKKβ inhibitors, LPS, or PolyIC B) Western blot of RAW264.7 cells pretreated with PKC412 followed by oxozeaenol, IKKβ inhibitors, LPS, or PolyIC.

IKKβ Phosphorylates TAB1 and Reduces Kinase Activity of TAK1

Feedback control of TAK1 by p38 has been previously reported (333). In that study, p38 phosphorylated TAB1 on Thr431, a site that downregulated TAK1 activity. We examined whether IKKβ regulates TAK1 through the same mechanism as p38 through phosphorylation of TAB1 Thr431. Coexpression of IKKβ with the TAB1-TAK1 complex in Cos cells resulted in a band shift in TAB1 and increased phosphorylation of TAB1 Thr431 (Figure A.4). Interestingly, coexpression of IKKβ with TAB1 and wild type TAK1 resulted in a band shift of TAK1, and the TAK1 band shift was not observed when the TAK1 dead kinase was used, suggesting TAK1 kinase activity is required for further phosphorylation by IKKβ. Phosphorylation of TAB1 Thr431 in response to TLR stimulation was reduced in RAW264.7 macrophages pretreated with the compound VIII. The inhibition of IKKβ decreased phosphorylation of a higher molecular weight version of TAB1 (data not shown).

Coexpression of IKKβ with the TAB1-TAK1 complex resulted in decreased phosphorylation of TAK1 on its activation loop Thr184/187 (Figure A.4). These sites were previously reported to be autophosphorylated and responsible for TAK1 activity (337). Therefore, IKKβ downregulates phosphorylation of the TAK1 activation loop and TAK1 activity.

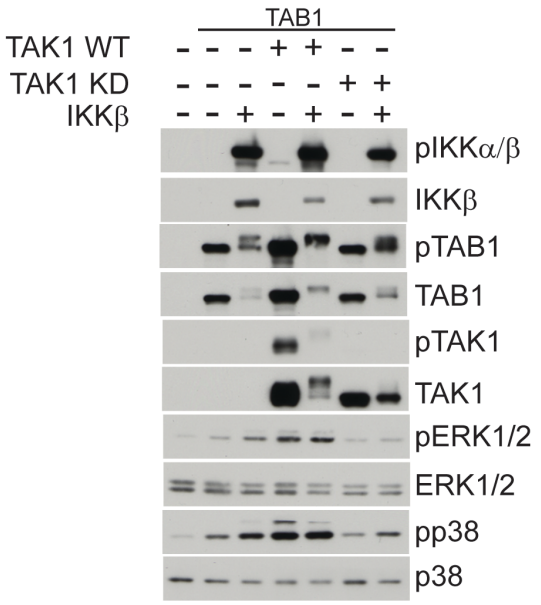

Figure A.4 IKKβ Phosphorylates TAB1 and Reduces Kinase Activity of TAK1. Western blot of Cos cells expressing TAB1, TAK1 WT, TAK1 kinase dead, and IKKβ.

Discussion

The experiments performed in this study suggest that IKK family members negatively feedback upon upstream kinases of their own activating pathways. IKKε and TBK1 have been reported to negatively feedback upon their upstream pathway to reduce their own activation loop phosphorylation (282). In that study, macrophages treated with an inhibitor of IKK-related kinases augmented activation loop phosphorylation when stimulated with LPS or poly(I:C). It has also been reported that IKKβ phosphorylates and activates IKKε and TBK1 (276). The mechanism for IKK-related kinase negative feedback was proposed to occur by IKKε and TBK1 phosphorylating and inhibiting the canonical IKKβ complex.

In this study, we show that the IKK-related kinase inhibitor, CAY10576, increases TBK1 activation loop phosphorylation both with and without the augmentation of TLR agonists LPS and Poly(I:C). Interestingly, we do not see the elimination of TBK1 phosphorylation in response to CAY10576 after inhibiting IKKβ or TAK1, suggesting that IKK-related kinases feedback is mediated by a separate kinase than IKKβ in a separate pathway from TAK1. A screen of 80 kinase inhibitors identified PKC412 as a potent inhibitor of TBK1 activation loop phosphorylation in response to IKK-related kinase inhibitor CAY10576. Studies with PKC412 reveal that it is likely that both the canonical IKKβ and the noncanonical TBK1 pathways are activated by similar upstream kinases in response to TLR agonists; however, the negative feedback observed by IKKβ and TBK1 is mediated by different upstream kinase pathways. Previous studies have suggested that the identity of this upstream kinase for IKKε and TBK1 may be a member of MAPK pathways (282).

Moreover, no group had previously described negative feedback of IKKβ upon its own pathway. In the present study, we show that inhibitors of IKKβ increase IKKβ activation loop phosphorylation both with and without the augmentation of inflammatory stimuli, LPS or poly(I:C), similar to IKK-related kinases (282). IKKβ inhibitor-induced activation loop phosphorylation was eliminated in TAK1 loss-of-function studies using the TAK1 inhibitor, oxozeaenol, or TAK1 knockout MEFs. Finally, we demonstrate that IKKβ phosphorylates TAB1 on the same site as previously reported for p38 to exert negative feedback control on TAK1 autophosphorylation.

It is important to recognize that several phosphatases are known to dephosphorylate IKK family activation loops. Ser/Thr phosphatases are grouped into two distinct subfamilies, both of which are important for dephosphorylating Ser177/181. From the phosphoprotein phosphatase (PPP) family, PP1 and PP2A have been implicated in downregulating IKKβ activity. From the phosphoprotein phosphatase M (PPM) family, which require Mn^{2+}/Mg^{2+} metal ions, PPM1A and PPM1B have been implicated in downregulating IKKβ activity (284), and PPM1B negatively regulates antiviral response by dephosphorylating TBK1 (285). TAB1, is a pseudophosphatase that has close structural similarity to PPM family phosphatases (286).

While our studies do not preclude the involvement of phosphatases in regulating phosphorylation state, we believe that modulation of upstream inflammatory kinase activity serves as an additional feedback mechanism of regulation by IKK family members on inflammatory pathways.

Bibliography

1. Hotamisligil GS (2006) Inflammation and metabolic disorders. *Nature* 444(7121):860-867.
2. Finucane MM*, et al.* (2011) National, regional, and global trends in body-mass index since 1980: systematic analysis of health examination surveys and epidemiological studies with 960 country-years and 9.1 million participants. *Lancet* 377(9765):557-567.
3. Anonymous (1998) Executive summary of the clinical guidelines on the identification, evaluation, and treatment of overweight and obesity in adults. *Arch Intern Med* 158(17):1855-1867.
4. Flegal KM, Carroll MD, Kit BK, & Ogden CL (2012) Prevalence of obesity and trends in the distribution of body mass index among US adults, 1999-2010. *JAMA* 307(5):491-497.
5. Power C & Jefferis BJ (2002) Fetal environment and subsequent obesity: a study of maternal smoking. *Int J Epidemiol* 31(2):413-419.
6. Dabelea D*, et al.* (2000) Intrauterine exposure to diabetes conveys risks for type 2 diabetes and obesity: a study of discordant sibships. *Diabetes* 49(12):2208-2211.
7. Hediger ML, Overpeck MD, Kuczmarski RJ, & Ruan WJ (2001) Association between infant breastfeeding and overweight in young children. *JAMA* 285(19):2453-2460.
8. Harder T, Bergmann R, Kallischnigg G, & Plagemann A (2005) Duration of breastfeeding and risk of overweight: a meta-analysis. *Am J Epidemiol* 162(5):397-403.
9. Guo SS, Wu W, Chumlea WC, & Roche AF (2002) Predicting overweight and obesity in adulthood from body mass index values in childhood and adolescence. *Am J Clin Nutr* 76(3):653-658.
10. Prentice AM & Jebb SA (1995) Obesity in Britain: gluttony or sloth? *BMJ* 311(7002):437-439.
11. Swinburn BA*, et al.* (2011) The global obesity pandemic: shaped by global drivers and local environments. *Lancet* 378(9793):804-814.
12. Lowell BB & Bachman ES (2003) Beta-Adrenergic receptors, diet-induced thermogenesis, and obesity. *J Biol Chem* 278(32):29385-29388.
13. Cannon B & Nedergaard J (2004) Brown adipose tissue: function and physiological significance. *Physiol Rev* 84(1):277-359.
14. Landsberg L (2006) Feast or famine: the sympathetic nervous system response to nutrient intake. *Cell Mol Neurobiol* 26(4-6):497-508.
15. Morrison SF (2004) Activation of 5-HT1A receptors in raphe pallidus inhibits leptin-evoked increases in brown adipose tissue thermogenesis. *Am J Physiol Regul Integr Comp Physiol* 286(5):R832-837.
16. Sell H, Deshaies Y, & Richard D (2004) The brown adipocyte: update on its metabolic role. *Int J Biochem Cell Biol* 36(11):2098-2104.
17. Davies BS, Beigneux AP, Fong LG, & Young SG (2012) New wrinkles in lipoprotein lipase biology. *Curr Opin Lipidol* 23(1):35-42.
18. Greenberg AS*, et al.* (2001) Stimulation of lipolysis and hormone-sensitive lipase via the extracellular signal-regulated kinase pathway. *J Biol Chem* 276(48):45456-45461.
19. Robidoux J*, et al.* (2006) Maximal beta3-adrenergic regulation of lipolysis involves Src and epidermal growth factor receptor-dependent ERK1/2 activation. *J Biol Chem* 281(49):37794-37802.
20. Kolditz CI & Langin D (2010) Adipose tissue lipolysis. *Curr Opin Clin Nutr Metab Care* 13(4):377-381.
21. Moro C, Berlan M, & Lafontan M (2006) [Physiological and pathophysiological features of the control of lipolysis and lipid mobilization by natriuretic peptides]. *J Soc Biol* 200(1):67-76.

22. Connacher AA*, et al.* (1991) Effect of adrenaline infusion on fatty acid and glucose turnover in lean and obese human subjects in the post-absorptive and fed states. *Clin Sci (Lond)* 81(5):635-644.
23. Blaak EE*, et al.* (1994) beta-Adrenergic stimulation of skeletal muscle metabolism in relation to weight reduction in obese men. *Am J Physiol* 267(2 Pt 1):E316-322.
24. Blaak EE*, et al.* (1994) Beta-adrenergic stimulation of energy expenditure and forearm skeletal muscle metabolism in lean and obese men. *Am J Physiol* 267(2 Pt 1):E306-315.
25. Webber J*, et al.* (1994) A comparison of the thermogenic, metabolic and haemodynamic responses to infused adrenaline in lean and obese subjects. *Int J Obes Relat Metab Disord* 18(11):717-724.
26. Jocken JW*, et al.* (2008) Effect of beta-adrenergic stimulation on whole-body and abdominal subcutaneous adipose tissue lipolysis in lean and obese men. *Diabetologia* 51(2):320-327.
27. Langin D*, et al.* (2005) Adipocyte lipases and defect of lipolysis in human obesity. *Diabetes* 54(11):3190-3197.
28. Bougneres P*, et al.* (1997) In vivo resistance of lipolysis to epinephrine. A new feature of childhood onset obesity. *J Clin Invest* 99(11):2568-2573.
29. Enoksson S*, et al.* (2000) Impaired in vivo stimulation of lipolysis in adipose tissue by selective beta2-adrenergic agonist in obese adolescent girls. *Diabetes* 49(12):2149-2153.
30. Hellstrom L, Langin D, Reynisdottir S, Dauzats M, & Arner P (1996) Adipocyte lipolysis in normal weight subjects with obesity among first-degree relatives. *Diabetologia* 39(8):921-928.
31. Barbe P, Millet L, Galitzky J, Lafontan M, & Berlan M (1996) In situ assessment of the role of the beta 1-, beta 2- and beta 3-adrenoceptors in the control of lipolysis and nutritive blood flow in human subcutaneous adipose tissue. *Br J Pharmacol* 117(5):907-913.
32. Lonnqvist F, Thome A, Nilsell K, Hoffstedt J, & Arner P (1995) A pathogenic role of visceral fat beta 3-adrenoceptors in obesity. *J Clin Invest* 95(3):1109-1116.
33. Stich V*, et al.* (2003) Activation of alpha2-adrenergic receptors blunts epinephrine-induced lipolysis in subcutaneous adipose tissue during a hyperinsulinemic euglycemic clamp in men. *Am J Physiol Endocrinol Metab* 285(3):E599-607.
34. Taussig R, Tang WJ, Hepler JR, & Gilman AG (1994) Distinct patterns of bidirectional regulation of mammalian adenylyl cyclases. *J Biol Chem* 269(8):6093-6100.
35. Serazin-Leroy V, Morot M, de Mazancourt P, & Giudicelli Y (2001) Differences in type II, IV, V and VI adenylyl cyclase isoform expression between rat preadipocytes and adipocytes. *Biochim Biophys Acta* 1550(1):37-51.
36. Reynisdottir S, Wahrenberg H, Carlstrom K, Rossner S, & Arner P (1994) Catecholamine resistance in fat cells of women with upper-body obesity due to decreased expression of beta 2-adrenoceptors. *Diabetologia* 37(4):428-435.
37. McGraw DW, Forbes SL, Kramer LA, & Liggett SB (1998) Polymorphisms of the 5' leader cistron of the human beta2-adrenergic receptor regulate receptor expression. *J Clin Invest* 102(11):1927-1932.
38. Green SA, Turki J, Bejarano P, Hall IP, & Liggett SB (1995) Influence of beta 2-adrenergic receptor genotypes on signal transduction in human airway smooth muscle cells. *Am J Respir Cell Mol Biol* 13(1):25-33.
39. Large V*, et al.* (1997) Human beta-2 adrenoceptor gene polymorphisms are highly frequent in obesity and associate with altered adipocyte beta-2 adrenoceptor function. *J Clin Invest* 100(12):3005-3013.
40. Jocken JW*, et al.* (2007) Association of a beta-2 adrenoceptor (ADRB2) gene variant with a blunted in vivo lipolysis and fat oxidation. *Int J Obes (Lond)* 31(5):813-819.

41. Jimenez M*, et al.* (2002) Beta(1)/beta(2)/beta(3)-adrenoceptor knockout mice are obese and cold-sensitive but have normal lipolytic responses to fasting. *FEBS Lett* 530(1-3):37-40.
42. Cheng X, Ji Z, Tsalkova T, & Mei F (2008) Epac and PKA: a tale of two intracellular cAMP receptors. *Acta Biochim Biophys Sin (Shanghai)* 40(7):651-662.
43. Park SJ*, et al.* (2012) Resveratrol ameliorates aging-related metabolic phenotypes by inhibiting cAMP phosphodiesterases. *Cell* 148(3):421-433.
44. Petersen RK*, et al.* (2008) Cyclic AMP (cAMP)-mediated stimulation of adipocyte differentiation requires the synergistic action of Epac- and cAMP-dependent protein kinase-dependent processes. *Mol Cell Biol* 28(11):3804-3816.
45. Omar B, Zmuda-Trzebiatowska E, Manganiello V, Goransson O, & Degerman E (2009) Regulation of AMP-activated protein kinase by cAMP in adipocytes: roles for phosphodiesterases, protein kinase B, protein kinase A, Epac and lipolysis. *Cell Signal* 21(5):760-766.
46. Zimmermann R*, et al.* (2004) Fat mobilization in adipose tissue is promoted by adipose triglyceride lipase. *Science* 306(5700):1383-1386.
47. Lass A*, et al.* (2006) Adipose triglyceride lipase-mediated lipolysis of cellular fat stores is activated by CGI-58 and defective in Chanarin-Dorfman Syndrome. *Cell Metab* 3(5):309-319.
48. Subramanian V*, et al.* (2004) Perilipin A mediates the reversible binding of CGI-58 to lipid droplets in 3T3-L1 adipocytes. *J Biol Chem* 279(40):42062-42071.
49. Yamaguchi T, Omatsu N, Matsushita S, & Osumi T (2004) CGI-58 interacts with perilipin and is localized to lipid droplets. Possible involvement of CGI-58 mislocalization in Chanarin-Dorfman syndrome. *J Biol Chem* 279(29):30490-30497.
50. Haemmerle G*, et al.* (2006) Defective lipolysis and altered energy metabolism in mice lacking adipose triglyceride lipase. *Science* 312(5774):734-737.
51. Fischer J*, et al.* (2007) The gene encoding adipose triglyceride lipase (PNPLA2) is mutated in neutral lipid storage disease with myopathy. *Nat Genet* 39(1):28-30.
52. Schoenborn V*, et al.* (2006) The ATGL gene is associated with free fatty acids, triglycerides, and type 2 diabetes. *Diabetes* 55(5):1270-1275.
53. Ryden M*, et al.* (2007) Comparative studies of the role of hormone-sensitive lipase and adipose triglyceride lipase in human fat cell lipolysis. *Am J Physiol Endocrinol Metab* 292(6):E1847-1855.
54. Schweiger M*, et al.* (2006) Adipose triglyceride lipase and hormone-sensitive lipase are the major enzymes in adipose tissue triacylglycerol catabolism. *J Biol Chem* 281(52):40236-40241.
55. Miyoshi H*, et al.* (2006) Perilipin promotes hormone-sensitive lipase-mediated adipocyte lipolysis via phosphorylation-dependent and -independent mechanisms. *J Biol Chem* 281(23):15837-15844.
56. Moore HP, Silver RB, Mottillo EP, Bernlohr DA, & Granneman JG (2005) Perilipin targets a novel pool of lipid droplets for lipolytic attack by hormone-sensitive lipase. *J Biol Chem* 280(52):43109-43120.
57. Granneman JG*, et al.* (2007) Analysis of lipolytic protein trafficking and interactions in adipocytes. *J Biol Chem* 282(8):5726-5735.
58. Marcinkiewicz A, Gauthier D, Garcia A, & Brasaemle DL (2006) The phosphorylation of serine 492 of perilipin a directs lipid droplet fragmentation and dispersion. *J Biol Chem* 281(17):11901-11909.
59. Anthonsen MW, Ronnstrand L, Wernstedt C, Degerman E, & Holm C (1998) Identification of novel phosphorylation sites in hormone-sensitive lipase that are phosphorylated in response to isoproterenol and govern activation properties in vitro. *J Biol Chem* 273(1):215-221.
60. Egan JJ*, et al.* (1992) Mechanism of hormone-stimulated lipolysis in adipocytes: translocation of hormone-sensitive lipase to the lipid storage droplet. *Proc Natl Acad Sci U S A* 89(18):8537-8541.

61. Syu LJ & Saltiel AR (1999) Lipotransin: a novel docking protein for hormone-sensitive lipase. *Mol Cell* 4(1):109-115.
62. Large V*, et al.* (1999) Decreased expression and function of adipocyte hormone-sensitive lipase in subcutaneous fat cells of obese subjects. *J Lipid Res* 40(11):2059-2066.
63. Lofgren P*, et al.* (2002) Major gender differences in the lipolytic capacity of abdominal subcutaneous fat cells in obesity observed before and after long-term weight reduction. *J Clin Endocrinol Metab* 87(2):764-771.
64. Ray H*, et al.* (2003) The presence of a catalytically inactive form of hormone-sensitive lipase is associated with decreased lipolysis in abdominal subcutaneous adipose tissue of obese subjects. *Diabetes* 52(6):1417-1422.
65. Roduit R*, et al.* (2001) A role for hormone-sensitive lipase in glucose-stimulated insulin secretion: a study in hormone-sensitive lipase-deficient mice. *Diabetes* 50(9):1970-1975.
66. Voshol PJ*, et al.* (2003) Increased hepatic insulin sensitivity together with decreased hepatic triglyceride stores in hormone-sensitive lipase-deficient mice. *Endocrinology* 144(8):3456-3462.
67. Peyot ML*, et al.* (2004) Hormone-sensitive lipase has a role in lipid signaling for insulin secretion but is nonessential for the incretin action of glucagon-like peptide 1. *Diabetes* 53(7):1733-1742.
68. Park SY*, et al.* (2005) Hormone-sensitive lipase knockout mice have increased hepatic insulin sensitivity and are protected from short-term diet-induced insulin resistance in skeletal muscle and heart. *Am J Physiol Endocrinol Metab* 289(1):E30-39.
69. Talmud PJ, Palmen J, & Walker M (1998) Identification of genetic variation in the human hormone-sensitive lipase gene and 5' sequences: homology of 5' sequences with mouse promoter and identification of potential regulatory elements. *Biochem Biophys Res Commun* 252(3):661-668.
70. Garenc C*, et al.* (2002) The hormone-sensitive lipase gene and body composition: the HERITAGE Family Study. *Int J Obes Relat Metab Disord* 26(2):220-227.
71. Hoffstedt J*, et al.* (2001) A common hormone-sensitive lipase i6 gene polymorphism is associated with decreased human adipocyte lipolytic function. *Diabetes* 50(10):2410-2413.
72. Magre J*, et al.* (1998) Human hormone-sensitive lipase: genetic mapping, identification of a new dinucleotide repeat, and association with obesity and NIDDM. *Diabetes* 47(2):284-286.
73. Lavebratt C*, et al.* (2002) The hormone-sensitive lipase i6 gene polymorphism and body fat accumulation. *Eur J Clin Invest* 32(12):938-942.
74. Mottagui-Tabar S*, et al.* (2003) Evidence for an important role of perilipin in the regulation of human adipocyte lipolysis. *Diabetologia* 46(6):789-797.
75. Qi L*, et al.* (2004) Genetic variation at the perilipin (PLIN) locus is associated with obesity-related phenotypes in White women. *Clin Genet* 66(4):299-310.
76. Martinez-Botas J*, et al.* (2000) Absence of perilipin results in leanness and reverses obesity in Lepr(db/db) mice. *Nat Genet* 26(4):474-479.
77. Tansey JT*, et al.* (2001) Perilipin ablation results in a lean mouse with aberrant adipocyte lipolysis, enhanced leptin production, and resistance to diet-induced obesity. *Proc Natl Acad Sci U S A* 98(11):6494-6499.
78. Fredrikson G, Tornqvist H, & Belfrage P (1986) Hormone-sensitive lipase and monoacylglycerol lipase are both required for complete degradation of adipocyte triacylglycerol. *Biochim Biophys Acta* 876(2):288-293.
79. Taschler U*, et al.* (2011) Monoglyceride lipase deficiency in mice impairs lipolysis and attenuates diet-induced insulin resistance. *J Biol Chem* 286(20):17467-17477.
80. Jung KM*, et al.* (2012) 2-arachidonoylglycerol signaling in forebrain regulates systemic energy metabolism. *Cell Metab* 15(3):299-310.

81. Hamilton JA & Kamp F (1999) How are free fatty acids transported in membranes? Is it by proteins or by free diffusion through the lipids? *Diabetes* 48(12):2255-2269.
82. Abumrad NA, el-Maghrabi MR, Amri EZ, Lopez E, & Grimaldi PA (1993) Cloning of a rat adipocyte membrane protein implicated in binding or transport of long-chain fatty acids that is induced during preadipocyte differentiation. Homology with human CD36. *J Biol Chem* 268(24):17665-17668.
83. Zhou SL, Stump D, Sorrentino D, Potter BJ, & Berk PD (1992) Adipocyte differentiation of 3T3-L1 cells involves augmented expression of a 43-kDa plasma membrane fatty acid-binding protein. *J Biol Chem* 267(20):14456-14461.
84. Schaffer JE & Lodish HF (1994) Expression cloning and characterization of a novel adipocyte long chain fatty acid transport protein. *Cell* 79(3):427-436.
85. Trigatti BL, Anderson RG, & Gerber GE (1999) Identification of caveolin-1 as a fatty acid binding protein. *Biochem Biophys Res Commun* 255(1):34-39.
86. Shen WJ, Sridhar K, Bernlohr DA, & Kraemer FB (1999) Interaction of rat hormone-sensitive lipase with adipocyte lipid-binding protein. *Proc Natl Acad Sci U S A* 96(10):5528-5532.
87. Jenkins-Kruchten AE*, et al.* (2003) Fatty acid-binding protein-hormone-sensitive lipase interaction. Fatty acid dependence on binding. *J Biol Chem* 278(48):47636-47643.
88. Coe NR, Simpson MA, & Bernlohr DA (1999) Targeted disruption of the adipocyte lipid-binding protein (aP2 protein) gene impairs fat cell lipolysis and increases cellular fatty acid levels. *J Lipid Res* 40(5):967-972.
89. Kampf JP, Parmley D, & Kleinfeld AM (2007) Free fatty acid transport across adipocytes is mediated by an unknown membrane protein pump. *Am J Physiol Endocrinol Metab* 293(5):E1207-1214.
90. Hibuse T*, et al.* (2005) Aquaporin 7 deficiency is associated with development of obesity through activation of adipose glycerol kinase. *Proc Natl Acad Sci U S A* 102(31):10993-10998.
91. Prudente S*, et al.* (2007) A functional variant of the adipocyte glycerol channel aquaporin 7 gene is associated with obesity and related metabolic abnormalities. *Diabetes* 56(5):1468-1474.
92. MacDougald OA & Burant CF (2005) Obesity and metabolic perturbations after loss of aquaporin 7, the adipose glycerol transporter. *Proc Natl Acad Sci U S A* 102(31):10759-10760.
93. Marrades MP, Milagro FI, Martinez JA, & Moreno-Aliaga MJ (2006) Differential expression of aquaporin 7 in adipose tissue of lean and obese high fat consumers. *Biochem Biophys Res Commun* 339(3):785-789.
94. Summers LK, Samra JS, Humphreys SM, Morris RJ, & Frayn KN (1996) Subcutaneous abdominal adipose tissue blood flow: variation within and between subjects and relationship to obesity. *Clin Sci (Lond)* 91(6):679-683.
95. Blaak EE*, et al.* (1995) Beta-adrenergic stimulation and abdominal subcutaneous fat blood flow in lean, obese, and reduced-obese subjects. *Metabolism* 44(2):183-187.
96. Bulow J & Madsen J (1981) Influence of blood flow on fatty acid mobilization form lipolytically active adipose tissue. *Pflugers Arch* 390(2):169-174.
97. Borsheim E, Lonnroth P, Knardahl S, & Jansson PA (2000) No difference in the lipolytic response to beta-adrenoceptor stimulation in situ but a delayed increase in adipose tissue blood flow in moderately obese compared with lean men in the postexercise period. *Metabolism* 49(5):579-587.
98. Mauriege P*, et al.* (1991) Regional variation in adipose tissue lipolysis in lean and obese men. *J Lipid Res* 32(10):1625-1633.
99. Horowitz JF & Klein S (2000) Whole body and abdominal lipolytic sensitivity to epinephrine is suppressed in upper body obese women. *Am J Physiol Endocrinol Metab* 278(6):E1144-1152.

100. Tchernof A*, et al.* (2006) Regional differences in adipose tissue metabolism in women: minor effect of obesity and body fat distribution. *Diabetes* 55(5):1353-1360.
101. Arner P, Hellstrom L, Wahrenberg H, & Bronnegard M (1990) Beta-adrenoceptor expression in human fat cells from different regions. *J Clin Invest* 86(5):1595-1600.
102. Reynisdottir S, Dauzats M, Thorne A, & Langin D (1997) Comparison of hormone-sensitive lipase activity in visceral and subcutaneous human adipose tissue. *J Clin Endocrinol Metab* 82(12):4162-4166.
103. Fisher RM*, et al.* (2001) Fatty acid binding protein expression in different adipose tissue depots from lean and obese individuals. *Diabetologia* 44(10):1268-1273.
104. Bolinder J, Kager L, Ostman J, & Arner P (1983) Differences at the receptor and postreceptor levels between human omental and subcutaneous adipose tissue in the action of insulin on lipolysis. *Diabetes* 32(2):117-123.
105. Zierath JR*, et al.* (1998) Regional difference in insulin inhibition of non-esterified fatty acid release from human adipocytes: relation to insulin receptor phosphorylation and intracellular signalling through the insulin receptor substrate-1 pathway. *Diabetologia* 41(11):1343-1354.
106. Wu X*, et al.* (2001) Depot-specific variation in protein-tyrosine phosphatase activities in human omental and subcutaneous adipose tissue: a potential contribution to differential insulin sensitivity. *J Clin Endocrinol Metab* 86(12):5973-5980.
107. Richelsen B (1992) Release and effects of prostaglandins in adipose tissue. *Prostaglandins Leukot Essent Fatty Acids* 47(3):171-182.
108. Carlson LA (1963) Studies on the effect of nicotinic acid on catecholamine stimulated lipolysis in adipose tissue in vitro. *Acta Med Scand* 173:719-722.
109. Dole VP (1961) Effect of nucleic acid metabolites on lipolysis in adipose tissue. *J Biol Chem* 236:3125-3130.
110. Valet P*, et al.* (1990) Neuropeptide Y and peptide YY inhibit lipolysis in human and dog fat cells through a pertussis toxin-sensitive G protein. *J Clin Invest* 85(1):291-295.
111. Bradley RL, Mansfield JP, & Maratos-Flier E (2005) Neuropeptides, including neuropeptide Y and melanocortins, mediate lipolysis in murine adipocytes. *Obes Res* 13(4):653-661.
112. Harmancey R*, et al.* (2005) The vasoactive peptide adrenomedullin is secreted by adipocytes and inhibits lipolysis through NO-mediated beta-adrenergic agonist oxidation. *FASEB J* 19(8):1045-1047.
113. Saltiel AR & Kahn CR (2001) Insulin signalling and the regulation of glucose and lipid metabolism. *Nature* 414(6865):799-806.
114. Abel ED*, et al.* (2001) Adipose-selective targeting of the GLUT4 gene impairs insulin action in muscle and liver. *Nature* 409(6821):729-733.
115. Carvalho E, Kotani K, Peroni OD, & Kahn BB (2005) Adipose-specific overexpression of GLUT4 reverses insulin resistance and diabetes in mice lacking GLUT4 selectively in muscle. *Am J Physiol Endocrinol Metab* 289(4):E551-561.
116. Bluher M*, et al.* (2002) Adipose tissue selective insulin receptor knockout protects against obesity and obesity-related glucose intolerance. *Dev Cell* 3(1):25-38.
117. Engfeldt P, Hellmer J, Wahrenberg H, & Arner P (1988) Effects of insulin on adrenoceptor binding and the rate of catecholamine-induced lipolysis in isolated human fat cells. *J Biol Chem* 263(30):15553-15560.
118. Illiano G & Cuatrecasas P (1972) Modulation of adenylate cyclase activity in liver and fat cell membranes by insulin. *Science* 175(4024):906-908.
119. Zhang J, Hupfeld CJ, Taylor SS, Olefsky JM, & Tsien RY (2005) Insulin disrupts beta-adrenergic signalling to protein kinase A in adipocytes. *Nature* 437(7058):569-573.

120. Stralfors P & Honnor RC (1989) Insulin-induced dephosphorylation of hormone-sensitive lipase. Correlation with lipolysis and cAMP-dependent protein kinase activity. *Eur J Biochem* 182(2):379-385.
121. Degerman E*, et al.* (2011) From PDE3B to the regulation of energy homeostasis. *Curr Opin Pharmacol* 11(6):676-682.
122. Bender AT & Beavo JA (2006) Cyclic nucleotide phosphodiesterases: molecular regulation to clinical use. *Pharmacol Rev* 58(3):488-520.
123. Armani A, Marzolla V, Rosano GM, Fabbri A, & Caprio M (2011) Phosphodiesterase type 5 (PDE5) in the adipocyte: a novel player in fat metabolism? *Trends Endocrinol Metab* 22(10):404-411.
124. Snyder PB, Esselstyn JM, Loughney K, Wolda SL, & Florio VA (2005) The role of cyclic nucleotide phosphodiesterases in the regulation of adipocyte lipolysis. *J Lipid Res* 46(3):494-503.
125. Thompson PE, Manganiello V, & Degerman E (2007) Re-discovering PDE3 inhibitors--new opportunities for a long neglected target. *Curr Top Med Chem* 7(4):421-436.
126. Kenan Y, Murata T, Shakur Y, Degerman E, & Manganiello VC (2000) Functions of the N-terminal region of cyclic nucleotide phosphodiesterase 3 (PDE 3) isoforms. *J Biol Chem* 275(16):12331-12338.
127. Shakur Y*, et al.* (2000) Membrane localization of cyclic nucleotide phosphodiesterase 3 (PDE3). Two N-terminal domains are required for the efficient targeting to, and association of, PDE3 with endoplasmic reticulum. *J Biol Chem* 275(49):38749-38761.
128. Thorn H*, et al.* (2003) Cell surface orifices of caveolae and localization of caveolin to the necks of caveolae in adipocytes. *Mol Biol Cell* 14(10):3967-3976.
129. Eriksson JW, Wesslau C, & Smith U (1994) The cGMP-inhibitable phosphodiesterase modulates glucose transport activation by insulin. *Biochim Biophys Acta* 1189(2):163-167.
130. Zmuda-Trzebiatowska E, Oknianska A, Manganiello V, & Degerman E (2006) Role of PDE3B in insulin-induced glucose uptake, GLUT-4 translocation and lipogenesis in primary rat adipocytes. *Cell Signal* 18(3):382-390.
131. Hardie DG (2011) Sensing of energy and nutrients by AMP-activated protein kinase. *Am J Clin Nutr* 93(4):891S-896.
132. Sette C & Conti M (1996) Phosphorylation and activation of a cAMP-specific phosphodiesterase by the cAMP-dependent protein kinase. Involvement of serine 54 in the enzyme activation. *J Biol Chem* 271(28):16526-16534.
133. Lindh R*, et al.* (2007) Multisite phosphorylation of adipocyte and hepatocyte phosphodiesterase 3B. *Biochim Biophys Acta* 1773(4):584-592.
134. Ahmad F*, et al.* (2007) Insulin-induced formation of macromolecular complexes involved in activation of cyclic nucleotide phosphodiesterase 3B (PDE3B) and its interaction with PKB. *Biochem J* 404(2):257-268.
135. Ahmad F*, et al.* (2009) Differential regulation of adipocyte PDE3B in distinct membrane compartments by insulin and the beta3-adrenergic receptor agonist CL316243: effects of caveolin-1 knockdown on formation/maintenance of macromolecular signalling complexes. *Biochem J* 424(3):399-410.
136. Rahn T*, et al.* (1996) Identification of the site in the cGMP-inhibited phosphodiesterase phosphorylated in adipocytes in response to insulin and isoproterenol. *J Biol Chem* 271(19):11575-11580.
137. Palmer D*, et al.* (2007) Protein kinase A phosphorylation of human phosphodiesterase 3B promotes 14-3-3 protein binding and inhibits phosphatase-catalyzed inactivation. *J Biol Chem* 282(13):9411-9419.
138. Choi YH*, et al.* (2006) Alterations in regulation of energy homeostasis in cyclic nucleotide phosphodiesterase 3B-null mice. *J Clin Invest* 116(12):3240-3251.

139. Berger K*, et al.* (2009) Phosphodiesterase 3B is localized in caveolae and smooth ER in mouse hepatocytes and is important in the regulation of glucose and lipid metabolism. *PLoS One* 4(3):e4671.
140. Engfeldt P, Arner P, Bolinder J, & Ostman J (1982) Phosphodiesterase activity in human subcutaneous adipose tissue in insulin- and noninsulin-dependent diabetes mellitus. *J Clin Endocrinol Metab* 55(5):983-988.
141. Johnson JA, Fried SK, Pi-Sunyer FX, & Albu JB (2001) Impaired insulin action in subcutaneous adipocytes from women with visceral obesity. *Am J Physiol Endocrinol Metab* 280(1):E40-49.
142. Tzanavari T, Giannogonas P, & Karalis KP (2010) TNF-alpha and obesity. *Curr Dir Autoimmun* 11:145-156.
143. Ryden M & Arner P (2007) Tumour necrosis factor-alpha in human adipose tissue -- from signalling mechanisms to clinical implications. *J Intern Med* 262(4):431-438.
144. Matthias A*, et al.* (2000) Thermogenic responses in brown fat cells are fully UCP1-dependent. UCP2 or UCP3 do not substitute for UCP1 in adrenergically or fatty scid-induced thermogenesis. *J Biol Chem* 275(33):25073-25081.
145. Fredriksson JM*, et al.* (2001) Analysis of inhibition by H89 of UCP1 gene expression and thermogenesis indicates protein kinase A mediation of beta(3)-adrenergic signalling rather than beta(3)-adrenoceptor antagonism by H89. *Biochim Biophys Acta* 1538(2-3):206-217.
146. Seale P (2010) Transcriptional control of brown adipocyte development and thermogenesis. *Int J Obes (Lond)* 34 Suppl 1:S17-22.
147. Rosen ED & MacDougald OA (2006) Adipocyte differentiation from the inside out. *Nat Rev Mol Cell Biol* 7(12):885-896.
148. Cao Z, Umek RM, & McKnight SL (1991) Regulated expression of three C/EBP isoforms during adipose conversion of 3T3-L1 cells. *Genes Dev* 5(9):1538-1552.
149. Yeh WC, Cao Z, Classon M, & McKnight SL (1995) Cascade regulation of terminal adipocyte differentiation by three members of the C/EBP family of leucine zipper proteins. *Genes Dev* 9(2):168-181.
150. Freytag SO, Paielli DL, & Gilbert JD (1994) Ectopic expression of the CCAAT/enhancer-binding protein alpha promotes the adipogenic program in a variety of mouse fibroblastic cells. *Genes Dev* 8(14):1654-1663.
151. Lin FT & Lane MD (1992) Antisense CCAAT/enhancer-binding protein RNA suppresses coordinate gene expression and triglyceride accumulation during differentiation of 3T3-L1 preadipocytes. *Genes Dev* 6(4):533-544.
152. Tontonoz P, Hu E, & Spiegelman BM (1994) Stimulation of adipogenesis in fibroblasts by PPAR gamma 2, a lipid-activated transcription factor. *Cell* 79(7):1147-1156.
153. Farmer SR (2006) Transcriptional control of adipocyte formation. *Cell Metab* 4(4):263-273.
154. Zhang JW, Klemm DJ, Vinson C, & Lane MD (2004) Role of CREB in transcriptional regulation of CCAAT/enhancer-binding protein beta gene during adipogenesis. *J Biol Chem* 279(6):4471-4478.
155. Fox KE*, et al.* (2008) Regulation of cyclin D1 and Wnt10b gene expression by cAMP-responsive element-binding protein during early adipogenesis involves differential promoter methylation. *J Biol Chem* 283(50):35096-35105.
156. Seale P*, et al.* (2008) PRDM16 controls a brown fat/skeletal muscle switch. *Nature* 454(7207):961-967.
157. Atit R*, et al.* (2006) Beta-catenin activation is necessary and sufficient to specify the dorsal dermal fate in the mouse. *Dev Biol* 296(1):164-176.
158. Seale P, Kajimura S, & Spiegelman BM (2009) Transcriptional control of brown adipocyte development and physiological function--of mice and men. *Genes Dev* 23(7):788-797.

159. Kajimura S*, et al.* (2009) Initiation of myoblast to brown fat switch by a PRDM16-C/EBP-beta transcriptional complex. *Nature* 460(7259):1154-1158.
160. Wang P, Mariman E, Renes J, & Keijer J (2008) The secretory function of adipocytes in the physiology of white adipose tissue. *J Cell Physiol* 216(1):3-13.
161. Tiraby C*, et al.* (2003) Acquirement of brown fat cell features by human white adipocytes. *J Biol Chem* 278(35):33370-33376.
162. Wu J*, et al.* (2012) Beige adipocytes are a distinct type of thermogenic fat cell in mouse and human. *Cell* 150(2):366-376.
163. Bartness TJ & Bamshad M (1998) Innervation of mammalian white adipose tissue: implications for the regulation of total body fat. *Am J Physiol* 275(5 Pt 2):R1399-1411.
164. Bartness TJ & Song CK (2007) Brain-adipose tissue neural crosstalk. *Physiol Behav* 91(4):343-351.
165. Himms-Hagen J*, et al.* (2000) Multilocular fat cells in WAT of CL-316243-treated rats derive directly from white adipocytes. *Am J Physiol Cell Physiol* 279(3):C670-681.
166. Cinti S (2002) Adipocyte differentiation and transdifferentiation: plasticity of the adipose organ. *J Endocrinol Invest* 25(10):823-835.
167. Petrovic N*, et al.* (2010) Chronic peroxisome proliferator-activated receptor gamma (PPARgamma) activation of epididymally derived white adipocyte cultures reveals a population of thermogenically competent, UCP1-containing adipocytes molecularly distinct from classic brown adipocytes. *J Biol Chem* 285(10):7153-7164.
168. Xue B*, et al.* (2007) Genetic variability affects the development of brown adipocytes in white fat but not in interscapular brown fat. *J Lipid Res* 48(1):41-51.
169. Cummings DE*, et al.* (1996) Genetically lean mice result from targeted disruption of the RII beta subunit of protein kinase A. *Nature* 382(6592):622-626.
170. Dahle MK*, et al.* (2002) Mechanisms of FOXC2- and FOXD1-mediated regulation of the RI alpha subunit of cAMP-dependent protein kinase include release of transcriptional repression and activation by protein kinase B alpha and cAMP. *J Biol Chem* 277(25):22902-22908.
171. Cederberg A*, et al.* (2001) FOXC2 is a winged helix gene that counteracts obesity, hypertriglyceridemia, and diet-induced insulin resistance. *Cell* 106(5):563-573.
172. Hansen JB*, et al.* (2004) Retinoblastoma protein functions as a molecular switch determining white versus brown adipocyte differentiation. *Proc Natl Acad Sci U S A* 101(12):4112-4117.
173. Kozak UC*, et al.* (1994) An upstream enhancer regulating brown-fat-specific expression of the mitochondrial uncoupling protein gene. *Mol Cell Biol* 14(1):59-67.
174. Shaywitz AJ & Greenberg ME (1999) CREB: a stimulus-induced transcription factor activated by a diverse array of extracellular signals. *Annu Rev Biochem* 68:821-861.
175. Cao W, Medvedev AV, Daniel KW, & Collins S (2001) beta-Adrenergic activation of p38 MAP kinase in adipocytes: cAMP induction of the uncoupling protein 1 (UCP1) gene requires p38 MAP kinase. *J Biol Chem* 276(29):27077-27082.
176. Robidoux J*, et al.* (2005) Selective activation of mitogen-activated protein (MAP) kinase kinase 3 and p38alpha MAP kinase is essential for cyclic AMP-dependent UCP1 expression in adipocytes. *Mol Cell Biol* 25(13):5466-5479.
177. Cao W*, et al.* (2004) p38 mitogen-activated protein kinase is the central regulator of cyclic AMP-dependent transcription of the brown fat uncoupling protein 1 gene. *Mol Cell Biol* 24(7):3057-3067.
178. Xue B, Coulter A, Rim JS, Koza RA, & Kozak LP (2005) Transcriptional synergy and the regulation of Ucp1 during brown adipocyte induction in white fat depots. *Mol Cell Biol* 25(18):8311-8322.
179. Carmona MC*, et al.* (2005) Defective thermoregulation, impaired lipid metabolism, but preserved adrenergic induction of gene expression in brown fat of mice lacking C/EBPbeta. *Biochem J* 389(Pt 1):47-56.

180. Karamanlidis G, Karamitri A, Docherty K, Hazlerigg DG, & Lomax MA (2007) C/EBPbeta reprograms white 3T3-L1 preadipocytes to a Brown adipocyte pattern of gene expression. *J Biol Chem* 282(34):24660-24669.
181. Yubero P*, et al.* (1994) CCAAT/enhancer binding proteins alpha and beta are transcriptional activators of the brown fat uncoupling protein gene promoter. *Biochem Biophys Res Commun* 198(2):653-659.
182. Bennett CE*, et al.* (2010) CCAAT/enhancer binding protein alpha, beta and delta gene variants: associations with obesity related phenotypes in the Leeds Family Study. *Diab Vasc Dis Res* 7(3):195-203.
183. de Jesus LA*, et al.* (2001) The type 2 iodothyronine deiodinase is essential for adaptive thermogenesis in brown adipose tissue. *J Clin Invest* 108(9):1379-1385.
184. Ribeiro MO*, et al.* (2010) Expression of uncoupling protein 1 in mouse brown adipose tissue is thyroid hormone receptor-beta isoform specific and required for adaptive thermogenesis. *Endocrinology* 151(1):432-440.
185. Bianco AC, Sheng XY, & Silva JE (1988) Triiodothyronine amplifies norepinephrine stimulation of uncoupling protein gene transcription by a mechanism not requiring protein synthesis. *J Biol Chem* 263(34):18168-18175.
186. Silva JE & Rabelo R (1997) Regulation of the uncoupling protein gene expression. *Eur J Endocrinol* 136(3):251-264.
187. Okuno A*, et al.* (1998) Troglitazone increases the number of small adipocytes without the change of white adipose tissue mass in obese Zucker rats. *J Clin Invest* 101(6):1354-1361.
188. Wilson-Fritch L*, et al.* (2003) Mitochondrial biogenesis and remodeling during adipogenesis and in response to the insulin sensitizer rosiglitazone. *Mol Cell Biol* 23(3):1085-1094.
189. Wilson-Fritch L*, et al.* (2004) Mitochondrial remodeling in adipose tissue associated with obesity and treatment with rosiglitazone. *J Clin Invest* 114(9):1281-1289.
190. Steppan CM*, et al.* (2001) The hormone resistin links obesity to diabetes. *Nature* 409(6818):307-312.
191. Vernochet C*, et al.* (2009) C/EBPalpha and the corepressors CtBP1 and CtBP2 regulate repression of select visceral white adipose genes during induction of the brown phenotype in white adipocytes by peroxisome proliferator-activated receptor gamma agonists. *Mol Cell Biol* 29(17):4714-4728.
192. Fukui Y, Masui S, Osada S, Umesono K, & Motojima K (2000) A new thiazolidinedione, NC-2100, which is a weak PPAR-gamma activator, exhibits potent antidiabetic effects and induces uncoupling protein 1 in white adipose tissue of KKAy obese mice. *Diabetes* 49(5):759-767.
193. Guan HP, Ishizuka T, Chui PC, Lehrke M, & Lazar MA (2005) Corepressors selectively control the transcriptional activity of PPARgamma in adipocytes. *Genes Dev* 19(4):453-461.
194. Puri V*, et al.* (2008) Cidea is associated with lipid droplets and insulin sensitivity in humans. *Proc Natl Acad Sci U S A* 105(22):7833-7838.
195. Barbera MJ*, et al.* (2001) Peroxisome proliferator-activated receptor alpha activates transcription of the brown fat uncoupling protein-1 gene. A link between regulation of the thermogenic and lipid oxidation pathways in the brown fat cell. *J Biol Chem* 276(2):1486-1493.
196. Puigserver P*, et al.* (1998) A cold-inducible coactivator of nuclear receptors linked to adaptive thermogenesis. *Cell* 92(6):829-839.
197. Uldry M*, et al.* (2006) Complementary action of the PGC-1 coactivators in mitochondrial biogenesis and brown fat differentiation. *Cell Metab* 3(5):333-341.
198. Leone TC*, et al.* (2005) PGC-1alpha deficiency causes multi-system energy metabolic derangements: muscle dysfunction, abnormal weight control and hepatic steatosis. *PLoS Biol* 3(4):e101.

199. Lin J*, et al.* (2004) Defects in adaptive energy metabolism with CNS-linked hyperactivity in PGC-1alpha null mice. *Cell* 119(1):121-135.
200. Ek J*, et al.* (2001) Mutation analysis of peroxisome proliferator-activated receptor-gamma coactivator-1 (PGC-1) and relationships of identified amino acid polymorphisms to Type II diabetes mellitus. *Diabetologia* 44(12):2220-2226.
201. Scime A*, et al.* (2005) Rb and p107 regulate preadipocyte differentiation into white versus brown fat through repression of PGC-1alpha. *Cell Metab* 2(5):283-295.
202. Hallberg M*, et al.* (2008) A functional interaction between RIP140 and PGC-1alpha regulates the expression of the lipid droplet protein CIDEA. *Mol Cell Biol* 28(22):6785-6795.
203. Leonardsson G*, et al.* (2004) Nuclear receptor corepressor RIP140 regulates fat accumulation. *Proc Natl Acad Sci U S A* 101(22):8437-8442.
204. Powelka AM*, et al.* (2006) Suppression of oxidative metabolism and mitochondrial biogenesis by the transcriptional corepressor RIP140 in mouse adipocytes. *J Clin Invest* 116(1):125-136.
205. Pan D, Fujimoto M, Lopes A, & Wang YX (2009) Twist-1 is a PPARdelta-inducible, negative-feedback regulator of PGC-1alpha in brown fat metabolism. *Cell* 137(1):73-86.
206. Wang H*, et al.* (2008) Liver X receptor alpha is a transcriptional repressor of the uncoupling protein 1 gene and the brown fat phenotype. *Mol Cell Biol* 28(7):2187-2200.
207. Seale P*, et al.* (2007) Transcriptional control of brown fat determination by PRDM16. *Cell Metab* 6(1):38-54.
208. Nedergaard J, Bengtsson T, & Cannon B (2007) Unexpected evidence for active brown adipose tissue in adult humans. *Am J Physiol Endocrinol Metab* 293(2):E444-452.
209. Cypess AM*, et al.* (2009) Identification and importance of brown adipose tissue in adult humans. *N Engl J Med* 360(15):1509-1517.
210. Saito M*, et al.* (2009) High incidence of metabolically active brown adipose tissue in healthy adult humans: effects of cold exposure and adiposity. *Diabetes* 58(7):1526-1531.
211. van Marken Lichtenbelt WD*, et al.* (2009) Cold-activated brown adipose tissue in healthy men. *N Engl J Med* 360(15):1500-1508.
212. Virtanen KA*, et al.* (2009) Functional brown adipose tissue in healthy adults. *N Engl J Med* 360(15):1518-1525.
213. Zingaretti MC*, et al.* (2009) The presence of UCP1 demonstrates that metabolically active adipose tissue in the neck of adult humans truly represents brown adipose tissue. *FASEB J* 23(9):3113-3120.
214. Rossmeisl M*, et al.* (2005) Triglyceride-lowering effect of respiratory uncoupling in white adipose tissue. *Obes Res* 13(5):835-844.
215. Cannon B & Nedergaard J (2010) Metabolic consequences of the presence or absence of the thermogenic capacity of brown adipose tissue in mice (and probably in humans). *Int J Obes (Lond)* 34 Suppl 1:S7-16.
216. Golozoubova V, Cannon B, & Nedergaard J (2006) UCP1 is essential for adaptive adrenergic nonshivering thermogenesis. *Am J Physiol Endocrinol Metab* 291(2):E350-357.
217. Feldmann HM, Golozoubova V, Cannon B, & Nedergaard J (2009) UCP1 ablation induces obesity and abolishes diet-induced thermogenesis in mice exempt from thermal stress by living at thermoneutrality. *Cell Metab* 9(2):203-209.
218. Gong DW*, et al.* (2000) Lack of obesity and normal response to fasting and thyroid hormone in mice lacking uncoupling protein-3. *J Biol Chem* 275(21):16251-16257.
219. Golozoubova V*, et al.* (2001) Only UCP1 can mediate adaptive nonshivering thermogenesis in the cold. *FASEB J* 15(11):2048-2050.
220. Griggio MA (1982) The participation of shivering and nonshivering thermogenesis in warm and cold-acclimated rats. *Comp Biochem Physiol A Comp Physiol* 73(3):481-484.

221. Ocloo A, Shabalina IG, Nedergaard J, & Brand MD (2007) Cold-induced alterations of phospholipid fatty acyl composition in brown adipose tissue mitochondria are independent of uncoupling protein-1. *Am J Physiol Regul Integr Comp Physiol* 293(3):R1086-1093.
222. Fredriksson JM, Lindquist JM, Bronnikov GE, & Nedergaard J (2000) Norepinephrine induces vascular endothelial growth factor gene expression in brown adipocytes through a beta -adrenoreceptor/cAMP/protein kinase A pathway involving Src but independently of Erk1/2. *J Biol Chem* 275(18):13802-13811.
223. Xue Y*, et al.* (2009) Hypoxia-independent angiogenesis in adipose tissues during cold acclimation. *Cell Metab* 9(1):99-109.
224. Enerback S*, et al.* (1997) Mice lacking mitochondrial uncoupling protein are cold-sensitive but not obese. *Nature* 387(6628):90-94.
225. Locke RM, Rial E, & Nicholls DG (1982) The acute regulation of mitochondrial proton conductance in cells and mitochondria from the brown fat of cold-adapted and warm-adapted guinea pigs. *Eur J Biochem* 129(2):381-387.
226. Mohell N, Connolly E, & Nedergaard J (1987) Distinction between mechanisms underlying alpha 1- and beta-adrenergic respiratory stimulation in brown fat cells. *Am J Physiol* 253(2 Pt 1):C301-308.
227. Wilcke M & Nedergaard J (1989) Alpha 1- and beta-adrenergic regulation of intracellular Ca2+ levels in brown adipocytes. *Biochem Biophys Res Commun* 163(1):292-300.
228. Cunningham SA & Nicholls DG (1987) Induction of functional uncoupling protein in guinea pigs infused with noradrenaline. Studies with isolated brown adipocytes. *Biochem J* 245(2):485-491.
229. Zhao J, Cannon B, & Nedergaard J (1997) alpha1-Adrenergic stimulation potentiates the thermogenic action of beta3-adrenoreceptor-generated cAMP in brown fat cells. *J Biol Chem* 272(52):32847-32856.
230. Zhao J, Cannon B, & Nedergaard J (1998) Thermogenesis is beta3- but not beta1-adrenergically mediated in rat brown fat cells, even after cold acclimation. *Am J Physiol* 275(6 Pt 2):R2002-2011.
231. Nedergaard J*, et al.* (2001) UCP1: the only protein able to mediate adaptive non-shivering thermogenesis and metabolic inefficiency. *Biochim Biophys Acta* 1504(1):82-106.
232. Vaanholt LM, Daan S, Schubert KA, & Visser GH (2009) Metabolism and aging: effects of cold exposure on metabolic rate, body composition, and longevity in mice. *Physiol Biochem Zool* 82(4):314-324.
233. Kozak LP (2010) Brown fat and the myth of diet-induced thermogenesis. *Cell Metab* 11(4):263-267.
234. Myers MG, Jr., Leibel RL, Seeley RJ, & Schwartz MW (2010) Obesity and leptin resistance: distinguishing cause from effect. *Trends Endocrinol Metab* 21(11):643-651.
235. Trayhurn P, Thurlby PL, & James WP (1977) Thermogenic defect in pre-obese ob/ob mice. *Nature* 266(5597):60-62.
236. Commins SP, Watson PM, Frampton IC, & Gettys TW (2001) Leptin selectively reduces white adipose tissue in mice via a UCP1-dependent mechanism in brown adipose tissue. *Am J Physiol Endocrinol Metab* 280(2):E372-377.
237. Glick Z & Raum WJ (1986) Norepinephrine turnover in brown adipose tissue is stimulated by a single meal. *Am J Physiol* 251(1 Pt 2):R13-17.
238. Esterbauer H*, et al.* (1998) Uncoupling protein-1 mRNA expression in obese human subjects: the role of sequence variations at the uncoupling protein-1 gene locus. *J Lipid Res* 39(4):834-844.
239. Clement K*, et al.* (1996) Additive effect of A-->G (-3826) variant of the uncoupling protein gene and the Trp64Arg mutation of the beta 3-adrenergic receptor gene on weight gain in morbid obesity. *Int J Obes Relat Metab Disord* 20(12):1062-1066.

240. Sramkova D*, et al.* (2007) The UCP1 gene polymorphism A-3826G in relation to DM2 and body composition in Czech population. *Exp Clin Endocrinol Diabetes* 115(5):303-307.
241. Lee H, Iida T, Mizuno A, Suzuki M, & Caterina MJ (2005) Altered thermal selection behavior in mice lacking transient receptor potential vanilloid 4. *J Neurosci* 25(5):1304-1310.
242. Liu X*, et al.* (2003) Paradoxical resistance to diet-induced obesity in UCP1-deficient mice. *J Clin Invest* 111(3):399-407.
243. Inokuma K*, et al.* (2006) Indispensable role of mitochondrial UCP1 for antiobesity effect of beta3-adrenergic stimulation. *Am J Physiol Endocrinol Metab* 290(5):E1014-1021.
244. Kontani Y*, et al.* (2005) UCP1 deficiency increases susceptibility to diet-induced obesity with age. *Aging Cell* 4(3):147-155.
245. Granneman JG, Burnazi M, Zhu Z, & Schwamb LA (2003) White adipose tissue contributes to UCP1-independent thermogenesis. *Am J Physiol Endocrinol Metab* 285(6):E1230-1236.
246. Ursino MG, Vasina V, Raschi E, Crema F, & De Ponti F (2009) The beta3-adrenoceptor as a therapeutic target: current perspectives. *Pharmacol Res* 59(4):221-234.
247. Geloen A, Collet AJ, Guay G, & Bukowiecki LJ (1988) Beta-adrenergic stimulation of brown adipocyte proliferation. *Am J Physiol* 254(1 Pt 1):C175-182.
248. Bronnikov G, Houstek J, & Nedergaard J (1992) Beta-adrenergic, cAMP-mediated stimulation of proliferation of brown fat cells in primary culture. Mediation via beta 1 but not via beta 3 adrenoceptors. *J Biol Chem* 267(3):2006-2013.
249. Himms-Hagen J*, et al.* (1994) Effect of CL-316,243, a thermogenic beta 3-agonist, on energy balance and brown and white adipose tissues in rats. *Am J Physiol* 266(4 Pt 2):R1371-1382.
250. Bronnikov G*, et al.* (1999) beta1 to beta3 switch in control of cyclic adenosine monophosphate during brown adipocyte development explains distinct beta-adrenoceptor subtype mediation of proliferation and differentiation. *Endocrinology* 140(9):4185-4197.
251. Hoffmann C, Leitz MR, Oberdorf-Maass S, Lohse MJ, & Klotz KN (2004) Comparative pharmacology of human beta-adrenergic receptor subtypes--characterization of stably transfected receptors in CHO cells. *Naunyn Schmiedebergs Arch Pharmacol* 369(2):151-159.
252. Mattsson CL*, et al.* (2011) beta(1)-Adrenergic receptors increase UCP1 in human MADS brown adipocytes and rescue cold-acclimated beta(3)-adrenergic receptor-knockout mice via nonshivering thermogenesis. *Am J Physiol Endocrinol Metab* 301(6):E1108-1118.
253. Vallerand AL, Perusse F, & Bukowiecki LJ (1990) Stimulatory effects of cold exposure and cold acclimation on glucose uptake in rat peripheral tissues. *Am J Physiol* 259(5 Pt 2):R1043-1049.
254. Inokuma K*, et al.* (2005) Uncoupling protein 1 is necessary for norepinephrine-induced glucose utilization in brown adipose tissue. *Diabetes* 54(5):1385-1391.
255. Shoelson SE, Herrero L, & Naaz A (2007) Obesity, inflammation, and insulin resistance. *Gastroenterology* 132(6):2169-2180.
256. Wellen KE & Hotamisligil GS (2005) Inflammation, stress, and diabetes. *J Clin Invest* 115(5):1111-1119.
257. Solinas G & Karin M (2010) JNK1 and IKKbeta: molecular links between obesity and metabolic dysfunction. *FASEB J* 24(8):2596-2611.
258. Zhang X*, et al.* (2008) Hypothalamic IKKbeta/NF-kappaB and ER stress link overnutrition to energy imbalance and obesity. *Cell* 135(1):61-73.
259. Hacker H & Karin M (2006) Regulation and function of IKK and IKK-related kinases. *Sci STKE* 2006(357):re13.
260. Kawai T & Akira S (2007) Signaling to NF-kappaB by Toll-like receptors. *Trends Mol Med* 13(11):460-469.

261. Zhou A, Scoggin S, Gaynor RB, & Williams NS (2003) Identification of NF-kappa B-regulated genes induced by TNFalpha utilizing expression profiling and RNA interference. *Oncogene* 22(13):2054-2064.
262. Shibuya H*, et al.* (1996) TAB1: an activator of the TAK1 MAPKKK in TGF-beta signal transduction. *Science* 272(5265):1179-1182.
263. Takaesu G*, et al.* (2000) TAB2, a novel adaptor protein, mediates activation of TAK1 MAPKKK by linking TAK1 to TRAF6 in the IL-1 signal transduction pathway. *Mol Cell* 5(4):649-658.
264. Cheung PC, Nebreda AR, & Cohen P (2004) TAB3, a new binding partner of the protein kinase TAK1. *Biochem J* 378(Pt 1):27-34.
265. Prickett TD*, et al.* (2008) TAB4 stimulates TAK1-TAB1 phosphorylation and binds polyubiquitin to direct signaling to NF-kappaB. *J Biol Chem* 283(28):19245-19254.
266. Sato S*, et al.* (2005) Essential function for the kinase TAK1 in innate and adaptive immune responses. *Nat Immunol* 6(11):1087-1095.
267. Meylan E*, et al.* (2004) RIP1 is an essential mediator of Toll-like receptor 3-induced NF-kappa B activation. *Nat Immunol* 5(5):503-507.
268. Ea CK, Deng L, Xia ZP, Pineda G, & Chen ZJ (2006) Activation of IKK by TNFalpha requires site-specific ubiquitination of RIP1 and polyubiquitin binding by NEMO. *Mol Cell* 22(2):245-257.
269. Karin M & Ben-Neriah Y (2000) Phosphorylation meets ubiquitination: the control of NF-[kappa]B activity. *Annu Rev Immunol* 18:621-663.
270. Bonizzi G & Karin M (2004) The two NF-kappaB activation pathways and their role in innate and adaptive immunity. *Trends Immunol* 25(6):280-288.
271. Shimada T*, et al.* (1999) IKK-i, a novel lipopolysaccharide-inducible kinase that is related to IkappaB kinases. *Int Immunol* 11(8):1357-1362.
272. Sharma S*, et al.* (2003) Triggering the interferon antiviral response through an IKK-related pathway. *Science* 300(5622):1148-1151.
273. Fitzgerald KA*, et al.* (2003) IKKepsilon and TBK1 are essential components of the IRF3 signaling pathway. *Nat Immunol* 4(5):491-496.
274. Hemmi H*, et al.* (2004) The roles of two IkappaB kinase-related kinases in lipopolysaccharide and double stranded RNA signaling and viral infection. *J Exp Med* 199(12):1641-1650.
275. Wang N, Ahmed S, & Haqqi TM (2005) Genomic structure and functional characterization of the promoter region of human IkappaB kinase-related kinase IKKi/IKKvarepsilon gene. *Gene* 353(1):118-133.
276. Clark K*, et al.* (2011) Novel cross-talk within the IKK family controls innate immunity. *Biochem J* 434(1):93-104.
277. Clark K, Takeuchi O, Akira S, & Cohen P (2011) The TRAF-associated protein TANK facilitates cross-talk within the IkappaB kinase family during Toll-like receptor signaling. *Proc Natl Acad Sci U S A* 108(41):17093-17098.
278. Chau TL*, et al.* (2008) Are the IKKs and IKK-related kinases TBK1 and IKK-epsilon similarly activated? *Trends Biochem Sci* 33(4):171-180.
279. Wang C*, et al.* (2001) TAK1 is a ubiquitin-dependent kinase of MKK and IKK. *Nature* 412(6844):346-351.
280. Zandi E & Karin M (1999) Bridging the gap: composition, regulation, and physiological function of the IkappaB kinase complex. *Mol Cell Biol* 19(7):4547-4551.
281. Delhase M, Hayakawa M, Chen Y, & Karin M (1999) Positive and negative regulation of IkappaB kinase activity through IKKbeta subunit phosphorylation. *Science* 284(5412):309-313.
282. Clark K, Plater L, Peggie M, & Cohen P (2009) Use of the pharmacological inhibitor BX795 to study the regulation and physiological roles of TBK1 and IkappaB kinase epsilon: a distinct

upstream kinase mediates Ser-172 phosphorylation and activation. *J Biol Chem* 284(21):14136-14146.
283. Kishore N*, et al.* (2002) IKK-i and TBK-1 are enzymatically distinct from the homologous enzyme IKK-2: comparative analysis of recombinant human IKK-i, TBK-1, and IKK-2. *J Biol Chem* 277(16):13840-13847.
284. Sun W*, et al.* (2009) PPM1A and PPM1B act as IKKbeta phosphatases to terminate TNFalpha-induced IKKbeta-NF-kappaB activation. *Cell Signal* 21(1):95-102.
285. Zhao Y*, et al.* (2012) PPM1B negatively regulates antiviral response via dephosphorylating TBK1. *Cell Signal*.
286. Conner SH*, et al.* (2006) TAK1-binding protein 1 is a pseudophosphatase. *Biochem J* 399(3):427-434.
287. Tenoever BR*, et al.* (2007) Multiple functions of the IKK-related kinase IKKepsilon in interferon-mediated antiviral immunity. *Science* 315(5816):1274-1278.
288. Chiang SH*, et al.* (2009) The protein kinase IKKepsilon regulates energy balance in obese mice. *Cell* 138(5):961-975.
289. Guilherme A, Virbasius JV, Puri V, & Czech MP (2008) Adipocyte dysfunctions linking obesity to insulin resistance and type 2 diabetes. *Nat Rev Mol Cell Biol* 9(5):367-377.
290. Peters RT, Liao SM, & Maniatis T (2000) IKKepsilon is part of a novel PMA-inducible IkappaB kinase complex. *Mol Cell* 5(3):513-522.
291. Shen RR & Hahn WC (2011) Emerging roles for the non-canonical IKKs in cancer. *Oncogene* 30(6):631-641.
292. Reilly SM*, et al.* (2013) An inhibitor of the protein kinases TBK1 and IKK-varepsilon improves obesity-related metabolic dysfunctions in mice. *Nat Med* 19(3):313-321.
293. Ellis AC, Hyatt TC, Hunter GR, & Gower BA (2010) Respiratory quotient predicts fat mass gain in premenopausal women. *Obesity (Silver Spring)* 18(12):2255-2259.
294. Yehuda-Shnaidman E, Buehrer B, Pi J, Kumar N, & Collins S (2010) Acute stimulation of white adipocyte respiration by PKA-induced lipolysis. *Diabetes* 59(10):2474-2483.
295. Stich V*, et al.* (2002) Hypocaloric diet reduces exercise-induced alpha 2-adrenergic antilipolytic effect and alpha 2-adrenergic receptor mRNA levels in adipose tissue of obese women. *J Clin Endocrinol Metab* 87(3):1274-1281.
296. Bell J (2005) Amlexanox for the treatment of recurrent aphthous ulcers. *Clin Drug Investig* 25(9):555-566.
297. Bamborough P*, et al.* (2006) 5-(1H-Benzimidazol-1-yl)-3-alkoxy-2-thiophenecarbonitriles as potent, selective, inhibitors of IKK-epsilon kinase. *Bioorg Med Chem Lett* 16(24):6236-6240.
298. Hausman DB, DiGirolamo M, Bartness TJ, Hausman GJ, & Martin RJ (2001) The biology of white adipocyte proliferation. *Obes Rev* 2(4):239-254.
299. Lumeng CN, Deyoung SM, & Saltiel AR (2007) Macrophages block insulin action in adipocytes by altering expression of signaling and glucose transport proteins. *Am J Physiol Endocrinol Metab* 292(1):E166-174.
300. Arkan MC*, et al.* (2005) IKK-beta links inflammation to obesity-induced insulin resistance. *Nat Med* 11(2):191-198.
301. Jiao P*, et al.* (2012) Constitutive activation of IKKbeta in adipose tissue prevents diet-induced obesity in mice. *Endocrinology* 153(1):154-165.
302. Tang T*, et al.* (2010) Uncoupling of inflammation and insulin resistance by NF-kappaB in transgenic mice through elevated energy expenditure. *J Biol Chem* 285(7):4637-4644.
303. Murray B, Biagioni PA, & Lamey PJ (2006) The efficacy of amlexanox OraDisc on the prevention of recurrent minor aphthous ulceration. *J Oral Pathol Med* 35(2):117-122.

304. Stallknecht B, Bulow J, Frandsen E, & Galbo H (1997) Desensitization of human adipose tissue to adrenaline stimulation studied by microdialysis. *J Physiol* 500 (Pt 1):271-282.
305. Liu J, DeYoung SM, Zhang M, Cheng A, & Saltiel AR (2005) Changes in integrin expression during adipocyte differentiation. *Cell Metab* 2(3):165-177.
306. Wunderlich FT*, et al.* (2008) Hepatic NF-kappa B essential modulator deficiency prevents obesity-induced insulin resistance but synergizes with high-fat feeding in tumorigenesis. *Proc Natl Acad Sci U S A* 105(4):1297-1302.
307. Yuan M*, et al.* (2001) Reversal of obesity- and diet-induced insulin resistance with salicylates or targeted disruption of Ikkbeta. *Science* 293(5535):1673-1677.
308. Kravchenko VV, Mathison JC, Schwamborn K, Mercurio F, & Ulevitch RJ (2003) IKKi/IKKepsilon plays a key role in integrating signals induced by pro-inflammatory stimuli. *J Biol Chem* 278(29):26612-26619.
309. Larabi A*, et al.* (2013) Crystal structure and mechanism of activation of TANK-binding kinase 1. *Cell Rep* 3(3):734-746.
310. Klein J, Fasshauer M, Benito M, & Kahn CR (2000) Insulin and the beta3-adrenoceptor differentially regulate uncoupling protein-1 expression. *Mol Endocrinol* 14(6):764-773.
311. Zhang HH, Halbleib M, Ahmad F, Manganiello VC, & Greenberg AS (2002) Tumor necrosis factor-alpha stimulates lipolysis in differentiated human adipocytes through activation of extracellular signal-related kinase and elevation of intracellular cAMP. *Diabetes* 51(10):2929-2935.
312. Souza SC*, et al.* (2003) TNF-alpha induction of lipolysis is mediated through activation of the extracellular signal related kinase pathway in 3T3-L1 adipocytes. *J Cell Biochem* 89(6):1077-1086.
313. Green A, Rumberger JM, Stuart CA, & Ruhoff MS (2004) Stimulation of lipolysis by tumor necrosis factor-alpha in 3T3-L1 adipocytes is glucose dependent: implications for long-term regulation of lipolysis. *Diabetes* 53(1):74-81.
314. Plomgaard P, Fischer CP, Ibfelt T, Pedersen BK, & van Hall G (2008) Tumor necrosis factor-alpha modulates human in vivo lipolysis. *J Clin Endocrinol Metab* 93(2):543-549.
315. Gregor MF & Hotamisligil GS (2011) Inflammatory mechanisms in obesity. *Annu Rev Immunol* 29:415-445.
316. Saltiel AR (2012) Insulin resistance in the defense against obesity. *Cell Metab* 15(6):798-804.
317. Calay ES & Hotamisligil GS (2013) Turning off the inflammatory, but not the metabolic, flames. *Nat Med* 19(3):265-267.
318. Schudt C, Winder S, Eltze M, Kilian U, & Beume R (1991) Zardaverine: a cyclic AMP specific PDE III/IV inhibitor. *Agents Actions Suppl* 34:379-402.
319. Kitamura T*, et al.* (1999) Insulin-induced phosphorylation and activation of cyclic nucleotide phosphodiesterase 3B by the serine-threonine kinase Akt. *Mol Cell Biol* 19(9):6286-6296.
320. Ikeda F*, et al.* (2007) Involvement of the ubiquitin-like domain of TBK1/IKK-i kinases in regulation of IFN-inducible genes. *EMBO J* 26(14):3451-3462.
321. May MJ, Larsen SE, Shim JH, Madge LA, & Ghosh S (2004) A novel ubiquitin-like domain in IkappaB kinase beta is required for functional activity of the kinase. *J Biol Chem* 279(44):45528-45539.
322. Jensen MD, Haymond MW, Rizza RA, Cryer PE, & Miles JM (1989) Influence of body fat distribution on free fatty acid metabolism in obesity. *J Clin Invest* 83(4):1168-1173.
323. Arner P (1999) Catecholamine-induced lipolysis in obesity. *Int J Obes Relat Metab Disord* 23 Suppl 1:10-13.
324. Jocken JW & Blaak EE (2008) Catecholamine-induced lipolysis in adipose tissue and skeletal muscle in obesity. *Physiol Behav* 94(2):219-230.
325. Makino H, Saijo T, Ashida Y, Kuriki H, & Maki Y (1987) Mechanism of action of an antiallergic agent, amlexanox (AA-673), in inhibiting histamine release from mast cells. Acceleration of

cAMP generation and inhibition of phosphodiesterase. *Int Arch Allergy Appl Immunol* 82(1):66-71.
326. Chen XW, Leto D, Chiang SH, Wang Q, & Saltiel AR (2007) Activation of RalA is required for insulin-stimulated Glut4 trafficking to the plasma membrane via the exocyst and the motor protein Myo1c. *Dev Cell* 13(3):391-404.
327. Maine GN*, et al.* (2010) A bimolecular affinity purification method under denaturing conditions for rapid isolation of a ubiquitinated protein for mass spectrometry analysis. *Nat Protoc* 5(8):1447-1459.
328. Kim W & Egan JM (2008) The role of incretins in glucose homeostasis and diabetes treatment. *Pharmacol Rev* 60(4):470-512.
329. Munzberg H, Flier JS, & Bjorbaek C (2004) Region-specific leptin resistance within the hypothalamus of diet-induced obese mice. *Endocrinology* 145(11):4880-4889.
330. Gao Z*, et al.* (2004) Inhibition of insulin sensitivity by free fatty acids requires activation of multiple serine kinases in 3T3-L1 adipocytes. *Mol Endocrinol* 18(8):2024-2034.
331. Weir GC & Bonner-Weir S (2004) Five stages of evolving beta-cell dysfunction during progression to diabetes. *Diabetes* 53 Suppl 3:S16-21.
332. Ninomiya-Tsuji J*, et al.* (2003) A resorcylic acid lactone, 5Z-7-oxozeaenol, prevents inflammation by inhibiting the catalytic activity of TAK1 MAPK kinase kinase. *J Biol Chem* 278(20):18485-18490.
333. Cheung PC, Campbell DG, Nebreda AR, & Cohen P (2003) Feedback control of the protein kinase TAK1 by SAPK2a/p38alpha. *EMBO J* 22(21):5793-5805.
334. Favata MF*, et al.* (1998) Identification of a novel inhibitor of mitogen-activated protein kinase kinase. *J Biol Chem* 273(29):18623-18632.
335. Ear T, Fortin CF, Simard FA, & McDonald PP (2010) Constitutive association of TGF-beta-activated kinase 1 with the IkappaB kinase complex in the nucleus and cytoplasm of human neutrophils and its impact on downstream processes. *J Immunol* 184(7):3897-3906.
336. Shim JH*, et al.* (2005) TAK1, but not TAB1 or TAB2, plays an essential role in multiple signaling pathways in vivo. *Genes Dev* 19(22):2668-2681.
337. Sakurai H, Miyoshi H, Mizukami J, & Sugita T (2000) Phosphorylation-dependent activation of TAK1 mitogen-activated protein kinase kinase kinase by TAB1. *FEBS Lett* 474(2-3):141-145.